

Stony Brook University



OFFICIAL COPY

The official electronic file of this thesis or dissertation is maintained by the University Libraries on behalf of The Graduate School at Stony Brook University.

© All Rights Reserved by Author.

Annual sedimentary extracellular enzyme activities in Great Peconic Bay

-- From a two dimensional perspective

A Dissertation Presented

by

Zhenrui Cao

to

The Graduate School

in Partial Fulfillment of the

Requirements

for the Degree of

Doctor of Philosophy

in

Marine and Atmospheric Science

Stony Brook University

December 2013

Copyright by
Zhenrui Cao
2013

Stony Brook University

The Graduate School

Zhenrui Cao

We, the dissertation committee for the above candidate for the
Doctor of Philosophy degree, hereby recommend
acceptance of this dissertation.

Robert C. Aller, Distinguished Professor and Dissertation Advisor
School of Marine and Atmospheric Sciences

Cindy Lee, Distinguished Professor and Chair of Defense
School of Marine and Atmospheric Sciences

Josephine Y. Aller, Professor and Co-Advisor
School of Marine and Atmospheric Sciences

Qingzhi Zhu, Assistant Professor
School of Marine and Atmospheric Sciences

Carol Arnosti, Professor
Department of Marine Sciences
University of North Carolina at Chapel Hill

This dissertation is accepted by the Graduate School

Charles Taber
Dean of the Graduate School

Abstract of the Dissertation

Annual sedimentary extracellular enzyme activities in Great Peconic Bay

-- From a two dimensional perspective

by

Zhenrui Cao

Doctor of Philosophy

in

Marine and Atmospheric Science

Stony Brook University

2013

Extracellular enzymes (EE) initiate heterotrophic remineralization by hydrolyzing high-molecular-weight organic matter to substrates sufficiently small (~600 Da) to be transported across cell membranes. An accurate understanding of EE associated remineralization processes in sedimentary deposits requires measuring patterns of extracellular enzyme activity (EEA) with minimal disturbance. Traditional methods for measuring EEA typically involve sectioning of sediment cores and incubation. This approach at best results in an averaged one-dimensional profile with low resolution. Any natural heterogeneity in enzyme activity is obscured and the possible association of activity patterns with sedimentary structure minimized.

My dissertation work focused on the development of a planar sensor system to measure two-dimensional EEA in marine sediments. The underlying principle of this new system is the incorporation of a fluorogenic enzyme substrate (Leu-MCA in this application) into a polymer carrier and the controlled release of that substrate into a contacting medium while transport and reactions are continuously monitored. The sensor foils reveal real-time proteolytic enzyme (Leucine-aminopeptidase) activity patterns across the planar surfaces at high spatial resolution (~50-100 μ m). This 2-D methodology provides a unique means to directly and independently

measure the complex, unsteady processes affecting reactive organic matter substrate distributions in both oxic and anoxic zones of sedimentary deposits.

This new sensor system was used to study seasonal EEA distributions in Great Peconic Bay sediments. Results showed that EEA varies seasonally: highest during the spring bloom and summer, and lowest during the fall and early winter. Seasonal variation is determined by both temperature and the availability of reactive organic substrates. Spatial heterogeneity was less obvious in cold seasons mainly due to low bio-activities. In warm seasons, however, a higher degree of horizontal heterogeneity was observed as the result of increased organic deposits and active macrobenthos. Degradation hot spots with sizes ranging from millimeters to one centimeter were observed in some seasons and were found to be associated with burrow structures and phytoplankton aggregates. The deposition of phyto-detritus from an early spring bloom greatly enhanced surface sediment EEA, and at this time high EEA closely coincided with regions of elevated metabolite production. However, EEA and solute build up patterns are decoupled during much of the year because of the different transport mechanisms and rates of transport affecting reactive particle substrates and solutes in bioturbated deposits. EEA correlates directly with depth integrated remineralization rates (ΣCO_2 , NH_4^+ production) but because EEA is a potential measurement (saturated rate) the correlation is not necessarily stoichiometrically exact.

An incubation experiment was conducted to study the EEA change as a response of bacteria communities to rapid variation in temperature. The results showed that bacteria responded quickly to temperature changes. Bacteria tend to synthesize a higher portion of LAP at low temperatures and a greater portion of Glucosidase and Phosphatase at temperatures higher than the *in situ* temperature they live. Temperature sensitivity curves showed that the initial response of the bacteria community to temperature change is always to alter their yield of EE. With longer exposure to a temperature change, community structure may alter or a succession of isoenzymes may occur shortly after a temperature shift.

Table of Contents

List of Figures	ix
List of Tables	xiii
Acknowledgments.....	xiv
Chapter 1: Introduction.....	1
1. What are Extracellular Enzymes (EE) and their ecological significance	2
2. The ecological role and significance of extracellular enzymes(EE).....	2
3. Major groups of extracellular enzymes.....	3
4. Enzyme reaction kinetics	5
5. Factors that control extracellular enzyme(EE) performance	6
5.1.The quantity of substrates	6
5.2.The quality of substrates	6
5.3.The location of enzymes	7
5.4.Temperature	8
5.5.Other factors.....	9
6. Mechanisms that control EE stocks in environments	9
6.1.The decay rate of EE.....	9
6.2.Regulation of EE production	10
6.2.1. Species level regulation.....	10
6.2.2. Community level regulation.....	11
7. EEA in marine sediments.....	13
8. Current techniques for EEA measurements	15
9. The necessity of observing surface sediments in multiple dimensions and new appeared techniques designed for this need.....	18

10. Major objectives of this dissertation	19
Chapter 2: Development of fluorosensor for two-dimensional measurements of extracellular enzyme activity in marine sediments	20
1. Introduction	21
2. Materials and Methods	23
2.1. <i>Reagents</i>	23
2.2. Controlled-release sensor membrane fabrication.....	23
2.3. Instrumentation	24
2.4. Membrane characterization and optimization.....	25
2.5. Transport and adsorption of the fluorophore in sediment.....	26
2.6. Experimental applications.....	27
3. Results	28
3.1. Diffusive release properties of the Leu-MCA carrier foil	28
3.2. Adsorption behavior of MCA on sediment particles	28
3.3. Sensor response.....	31
3.4. Membrane uniformity	32
4. Discussion	32
4.1. Leu-Aminopeptidase foil system design.....	32
4.2. Determination of optimized Leu-MCA load.....	33
4.3. Enzyme activities calculation and correction for diffusion and adsorption.....	34
4.4. Vertical enzyme activity profile in microcosm and comparison with traditional incubations	35
4.5. Spatial heterogeneity of Leu-AP activity distribution in marine sediments	36
5. Summary and conclusions	38
Chapter 3: Temperature dependence of extracellular enzyme activities in temperate coastal sediments.....	46

1. Introduction	47
2. Methods	48
3. Results	50
3.1. Behavior of LAP standard in pre-deactivated sediments.....	50
3.2. Laboratory incubation.....	50
3.3. Seasonal temperature dependence of field sample EEA in great Peconic Bay	51
4. Discussion	52
4.1. Temperature optimum.....	52
4.2. EEA change during short-term incubation at varied temperatures	52
4.3. Activation energy change during short period incubation.....	54
4.4. A simplified model to estimate the cost for EE production at different temperatures	55
4.5. Seasonal EEA patterns from field sample measurements.....	56
5. Conclusion	57
Chapter 4: Seasonal, 2-D sedimentary extracellular enzyme activities and controlling processes in Great Peconic Bay, Long Island	69
1. Introduction	70
2. Materials and Methods	72
2.1. Study site and sampling	72
2.2. Pore water analyses and bacteria counts	72
2.3. EEA measured by traditional incubation methods.....	73
2.4. EEA Controlled-release foil sensing system.....	74
2.5. Instrumentation and deployment.....	75
3. Results	76
3.1. Nutrients and Environmental parameters.....	76
3.2. Seasonal patterns of EEA.....	76

3.3. Bacterial abundance	77
3.4. 2-D Enzyme activity distribution patterns	77
4. Discussion	78
4.1. Comparison of enzyme activity profiles determined by fluorosensor and traditional incubations	78
4.2. Annual pattern of EEA in Great Peconic Bay	79
4.3. Surface sediment heterogeneity and decomposition “hot spots” discriminated by EEA imaging	80
4.4. Hot spots associated with burrow structures	82
4.5. Impacts of algal blooms and pulse deposition of detritus	83
4.6. Factors controlling EEA in Great Peconic Bay sediments	84
5. Conclusions	87
Chapter 5: Summary and future perspectives	102
1. Summary of major findings	103
2. Future perspectives	104
References	106

List of Figures

- Fig.2.1. Imaging instrumentation used for two-dimensional Leucine-Aminopeptidase measurements (after Zhu et al., 2005)..... 39
- Fig. 2.2. (A) Release behavior of MCA membranes with different D4 loads. (B) Variation of unit time release rate of linear release period (represented as % total MCA/min) versus different D4 loads. Insert: relationship between D4 load and layer thickness..... 40
- Fig. 2.3. (A) Adsorption behavior of MCA with time at 4 °C and room temperature 22 °C. MCA concentration: 10.5 µM. (B) Adsorption isotherms of MCA fitted to Freundlich equations (lines). 1: after 1 hr incubation (△); 2: after 22 hrs incubation (◆), (C) Desorption behavior of MCA in sediment shown as the percentage of adsorbed MCA released at a particular time after adsorption : (○) MCA adsorption behavior if the adsorption were completely reversible; (●) measured adsorption behavior of MCA in sediment..... 41
- Fig. 2.4. (A) The response of the enzyme fluorosensor in the presence of various extracellular enzyme activities in marine sediments. The surface sediment (0 – 5 cm) collected from Long Island Sound was homogenized and sieved through a 1 mm mesh sieve before use. The relative fluorescence intensity increases with the incubation time. (B) Correlation between the rate of increase of fluorescence intensity and extracellular enzyme activity added into each sample. Substrate loaded: 0.5 µmol Leu-MCA/cm². Extracellular enzyme activity: (◆) natural sediment; then added (■) 0.10, (▲) 0.19, (×) 0.29, and (*) 0.38 µmol sub/hr/g standard Leu-AP enzyme into the natural sediment..... 42
- Fig. 2.5. The effect of substrate Leu-MCA load in the foil on sensor response. The homogenized surface marine sediment (0 – 5 cm) was obtained from Long Island Sound. The Leu-MCA amounts in each sensor foil are: (□) 0.12, (◇) 0.16, (▲) 0.20, (+) 0.24 and (○) 0.32 µmol/cm² 43
- Fig. 2.6. (A) Visible and pseudo-color (red) fluorescence images of marine sediment at 6, 10 28 min after sensor foil deployment. The intact microcosm core was collected from Flax Pond, Long Island. (B) The comparison of enzyme activity profiles obtained from traditional methods and the fluorosensor technique. The fluorescence increase of the sensor during the

first 10 – 40 minutes of incubation was used to calculate enzyme activities. The solid dots are horizontally averaged data extracted from 2-dimensional enzyme distribution 44

Fig. 2.7. Left: 2-dimensional extracellular enzyme distribution pattern in an intact marine sediment microcosm core collected from the Great Peconic Bay, Long Island. Right: Horizontally averaged enzyme activity vertical profile (black line) and its comparison with results from traditional incubations (gray dots) 45

Fig. 3.1. Temperature dependence of activities of LAP(Leucine-Aminopeptidase) standards added in deactivated sediments 61

Fig. 3.2. The Ln(EEA) vs 1/T curve of standard LAP added in deactivated sediments. Activation energy (E_a) and Q10 were calculated from the slope of the regression line..... 62

Fig. 3.3. Change of activities of three EEs (LAP, PA and BGA) and Total CO₂ during 4 days incubation..... 63

Fig. 3.4. Temperature sensitivity curves of three EEs on Day 1 64

Fig. 3.5. Temperature sensitivity curves of three EEs on Day 3 65

Fig. 3.6. Temperature sensitivity curves of three EEs on Day 5 66

Fig. 3.7. Percentage new produced ($\% \cdot d^{-1}$) of three EEs at different temperatures compared to the respective activities on day 1 during incubation 67

Fig. 3.8. Temperature sensitivity curves of three EEs of Peconic Bay sediments. EEAs were 0-12 cm integrated activities. Temperatures are *in situ* temperatures 68

Fig. 4.1. Location of sampling sites in Great Peconic Bay, at the eastern end of Long Island, New York, USA 90

Fig. 4.2. Imaging instrumentation used for two-dimensional Leucine-aminopeptidase measurements (modified after (Zhu et al. 2005) showing position of enzyme substrate (green) against the sediment..... 91

Fig. 4.3. Vertically integrated activities (as bars) over the top 12 cm of A: leucine aminopeptidase (LAP) B: phosphatase (PA), and C: β -glucosidase (BG) in different sampling seasons overlain by the percentage of EEA in the top 2 cm for depth integrated values. While LAP activity overall was greater than PA activity followed by BG activity all

three enzymes showed similar seasonal patterns activities lowest in winter, highest in the summer and Site 1 more active than Site 2	92
Fig. 4.4. Comparison of bacterial abundances during fall and winter 2009 at Sites 1 and 2. Overall higher concentrations and elevated concentrations at the surface during winter are consistent with lower grazing rates	93
Fig. 4.5. 2-Dimensional extracellular leucine aminopeptidase (LAP) distribution patterns plotted as pseudo-color images in cores collected in different seasons of Site 1. From left to right: April 2009, July 2009, Oct.2009, Feb. 2010, May 2010. X and Y axes are actual length scale within the sediment. Point 0 on the Y axis indicates the position of the water-sediment interface. Because the sediment surface is seldom level, the exact position of the interface is estimated. Color bar reflects EEA. The average EEA over the image area is indicated at the lower left in each panel	94
Fig. 4.6. 2-Dimensional extracellular leucine aminopeptidase (LAP) distribution patterns plotted as pseudo-color images in cores collected in different seasons of Site 2. From left to right: July 2009, Nov.2009, Mar. 2010, May 2010. X and Y axes are actual length scale within the sediment. Point 0 on the Y axis indicates the position of the water-sediment interface. Color bar reflects EEA. The average EEA over the image area is indicated at the lower left of each panel	95
Fig. 4.7. Vertical profiles of horizontally averaged enzyme activity obtained from 2-D sensor images (black line) compared with results from traditional incubations (black dots)	96
Fig. 4.8. Histograms showing surface sediment (0-2 cm) EEA distributions without (top) and with (bottom) hot spots. The x axis is the range of EEA and the y axis represents the number of pixels that are within each EEA interval. Red lines in each figure are normal distribution simulations based on sample mean and variance	97
Fig. 4.9. Aminopeptidase activity (LAP) (Image B) and $p\text{CO}_2$ (Image D) in vertical sections from two cores taken during the spring bloom (late Feb – Mar 2010) in Great Peconic Bay at Site 1. Image A and C are raw visible images under green light corresponding to each sensor image respectively (black color in visible images is Fe-sulfide). Note that the vertical and horizontal scales are in cm. The depositional focusing of reactive particles and the relative	

lack of bioirrigation results in the close correspondence of reactive particle and metabolite distributions near the sediment-water interface (red rectangle outlines) 98

Fig. 4.10. Natural log of the depth integrated EEAs plotted against 1/T. T is absolute temperature. The hollow circle is the Feb 10 EEA while the filled circles are EEAs from the other 5 seasons as shown in Fig. 4.3. The solid line is a linear regression of the solid circles. The dashed line is the regression of all points 99

Fig. 4.11. Comparison of the activities of the three classes of enzymes with each other during all sampling seasons demonstrating correlations and suggesting coupled controlling factors . 100

Fig. 4.12. EEAs versus their respective end member nutrient production rates : The relationship between BG and $\sum\text{CO}_2$ production (integrated as equivalent flux) (A) and between LAP and NH_4 production (B) show clear correlations, whereas there is no clear relationship between N/P and LAP/PA (C) although the N/P is lower during the warmer seasons compared with that in colder seasons. The lines plotted in (A) and (B) are the type 2 (geometric mean) regressions ($\sum\text{CO}_2$ flux = $0.87(\text{BG}) - 36.2$; $r^2 = 0.79$; NH_4^+ flux = $0.0068(\text{LAP}) - 1.76$; $r^2 = 0.73$) 101

List of tables

Table 3.1. pH and percentage activity changes of three EEs during incubation. The initial pH on day 1 is 7.10	59
Table 3.2. Activation energies (Ea) of three EEs at different days. The Ea values at day 5 were calculated for all temperatures and two temperature stages (as shown in Fig. 3.6) respectively	60
Table 4.1. Integrated (0-15cm) nutrient inventories and depth integrated (0 – 15 cm) production rates in different seasons	89

Acknowledgments

This dissertation concludes my PhD study, a long journey I could not have completed on my own. My advisor Dr. Robert Aller has been my resource of knowledge, insight, as well as critical comments. My co-advisor Dr. Josie Aller has been encouraging and considerate all the time. Her care and love is what I will never be able to return. I am also grateful to my committee members, Dr. Qingzhi Zhu, Dr. Cindy Lee, Dr. Carol Arnosti, for their suggestions and advices to the completion of this dissertation. Qing guided me a lot in the sensor system development. Cindy and Carol spent enormous time in helping me improve the written document. This work could not have been done without their scientific support, moral encouragement and kind consideration.

I am grateful to Christina Heilbrun, the best research scientist and technician. She is so warm hearted and always ready to help others. I also want to thank all my lab mates: Stuart Waugh, Shaily Rahman, Jaime Soto-Neira, Isaac Klingensmith. To finish a PhD is never easy. For years, we have been working together, encouraging each other, and making fun of each other. I am fortunate enough to have worked in such a great lab. I will never forget those shared experiences.

I am also grateful to all SoMAS faculty, staff and fellow students, particularly Dr. Mary Scranton, Carol Dove, and Mark Lang. I would not have been able to finish my study without your helps. I also want to thank all my friends that have been around to share all the excitement, joy and disappointment with me.

Finally, my deepest gratitude goes my dearest parents, who have given my life and brought me up the way I am. They offered me what they have and never asked for returns. For that, I am forever indebted. My last notes are dedicated to my girlfriend Yuan Liu, who has given me the most wonderful times in my life. Her unselfish love and forgiveness constantly touches my life. Her devoted support is essential to the completion of my dissertation.

Chapter 1 Introduction

1. What are Extracellular Enzymes (EE) and their ecological significance

Extracellular enzymes (EE) are the main study targets of this dissertation. Extracellular enzymes can be defined as enzymes that function outside of cell membranes of bacteria to decompose organic substrates into smaller pieces. The majority of EEs are excreted on purpose by organisms, while the other EEs may have different origins, such as the lysis of cells. The locations of extracellular enzymes can be varied. Though all extracellular, they may be free-dissolved, bound on cell-surface, periplasmic or adsorbed to surfaces other than those of its producer. In order to differentiate the locations of EEs, various terms have been introduced. For example, the terms ectoenzymes (Chrost 1991) or exoenzymes (Hoppe 1983) were created to represent cell-surface-bound or periplasmic enzymes, in contrast to the term 'extracellular enzymes' that specially represents free dissolved enzymes and enzymes adsorbed to other particles. In practical measurements, however, the differentiation between cell-surface-bound enzymes and particle-adsorbed enzymes are technically difficult. Besides, there is no evidence extracellular enzymes at different locations are structurally different. The use of multiple terms seems redundant and unnecessary. In most recent publications, the term extracellular enzyme has been widely accepted to represent all enzymes that function outside of cells and the terms free-dissolved and adsorbed EE are used to differentiate the locations of EE. According to the site of the organic matter that enzymes work on, extracellular enzymes can be categorized as endo or exo-acting enzymes. Endo-acting extracellular enzymes refer to enzymes that hydrolyze substrates mid-chain and exo-acting extracellular enzymes are enzymes that hydrolyze monomers from terminal ends of polymers.

2. The ecological role and significance of extracellular enzymes(EE)

Extracellular enzyme catalyzed polymer hydrolysis is the initial step in the microbial loop. For prokaryotes, only molecules smaller than 600 Da can be directly transported across cell membranes (Weiss et al. 1991). The majority of organic materials, which include all POC and the most DOC (>95%) (Chrost 1992) are above this limit so that must undergo a cleavage

step before being transported into cells(Amon & Benner 1994) , which is the function of extracellular enzymes. Extracellular enzymes cut small units, either monomers or oligomers, off from a diverse array of complex compounds. These small units have a MW <600 Da so they can be utilized by microbes. The EEs are also essential for eukaryotes. Eukaryotes, though they ingest big particles, these ingested particles are also hydrolyzed by extracellular enzymes in animals' digestion systems. That is to say, the decomposition of almost all polymeric molecules, despite their compositions and origins, are initiated by extracellular hydrolysis. Considering the essential role of EE together with the common existence of long-lived refractory organic particles, EE mediated hydrolysis is referred to as the rate-limiting step in organic matter degradation (Davey et al. 2001, Lehman & O'Connell 2002). Though recent studies have found this may not be the fact in all environments (Burdige & Gardner 1998, Arnosti 2011), there is no arguments that EE catalyzed hydrolysis, being an essential step, plays an extremely important role in elemental cycles.

3. Major groups of extracellular enzymes

To hydrolyze a diversified organic matter pool in nature necessarily requires a diversified group of EE. Despite a large number of different types of EE, with a few exceptions such as phenol oxidase and peroxidase, the majority of extracellular enzymes are hydrolytic enzymes. That is probably due to the limited energy support in extracellular environments that restrict the performance of other enzymes. The nomenclature of extracellular enzymes, according to associated Enzyme Commission Number (EC), is that most EEs belong to hydrolases category (EC 3). A relatively unofficial classification, which bases on the chemical bonds that EEs hydrolyze, separates EEs into 3 major groups: enzymes that hydrolyze C-O bond, enzymes that hydrolyze C-N bond and enzymes that hydrolyze O-P.

EEs that hydrolyze C-O bonds mainly include glycoside hydrolase (EC 3.2.1) and lipase (EC 3.1.1). This is a large group of EEs that hydrolyze the C-O bonds from a variety of carbohydrates and lipids. Some common poly-carbohydrates in natural environments include

starch, glycogen, cellulose, chitin, pullulan, laminarin, chondroitin sulfate, fucoidan and xylan etc (Arnosti 2000). Among glycoside hydrolases, β -glucosidase (BGA) is common and the most widely studied enzyme. It exhibits a relaxed substrate specificity hydrolyzing β -linked disaccharides of glucose. Many of the glycoside hydrolases comprise non-catalytic carbohydrate-binding modules (CBMs), which can be considered as a special expression of glycosylase. The role of CBMs is to promote the recognition and binding of enzymes to cognate polysaccharides as most of them are hydrophobic (Boraston et al. 2004). Some more details about glycoside hydrolase can be found reviews such as (Warren 1996, Davies et al. 2005).

Enzymes that hydrolyze C-N bonds (peptide bonds) are mainly aminopeptidase or proteinase (EC 3.2.4). They are exo and ecto-acting enzymes that initiate protein degradation in aquatic environments. In natural environments, the overall decomposition rate of proteins is a collaborate efforts of exo and ecto-acting enzymes. The ecto enzymes cut big chains into smaller peptides, providing more reactive terminals for exo-acting enzymes. Leucine-aminopeptidase (LAP) is the most widely studied aminopeptidase. LAP hydrolyzes a large number of peptides of the L-configuration but has the highest affinity with peptide bonds that have Leucine at the N side. Most aminopeptidases are metallozymes that have Zinc at their active centers.

Enzymes that hydrolyze O-P are within the group of esterase and mainly include phosphatases (PA) and phosphor-diesterases. Alkaline phosphatase is the most widely studied esterase in aquatic environments. In low pH environments, acid phosphatase takes the place of alkaline phosphatase in hydrolyzing organic phosphate. Almost all phosphatases are metalloenzymes (Coleman 1992).

The products of these three groups constitutes the major food and nutrients sources for: C, N and P respectively. The activity ratio between EEs therefore reflect the nutrient status and nutrient ratio demands of microbes. An explicit stoichiometry, however, is required when applying EEAs for these purposes. The product of peptidase hydrolysis (amino acid) is also an organic C source. Additionally, phosphatase conducted hydrolysis may be a prerequisite step for

the degradation of remnant organic C components, as suggested by studies which have found that C-limited bacteria in the deep strata produced phosphatase primarily targeting organic C compounds rather than phosphate (Hoppe & Ullrich 1999, Hoppe 2003).

4. Enzyme reaction kinetics.

In principle, extracellular enzyme conducted hydrolysis obeys Michaelis–Menten (MM) kinetics, with the kinetic equations being of the form:

$$v_0 = \frac{v_{\max} [S]}{K_m + [S]}$$

In this equation, $[S]$ is substrate concentration, v_0 is the instant reaction rate, v_{\max} is the maximum potential rate of reaction and K_m is the Michaelis-Menton saturation constant. The unit of enzyme activity is usually recorded as moles of substrate hydrolyzed per unit time per unit solution volume (or per unit weight in some case).

Enzyme activities are sensitive to environmental factors. Factors that impact any one of the three parameters on the right side of the above equation will consequently influence enzyme activity. Among the three parameters, v_{\max} and K_m are considered as the intrinsic properties of an extracellular enzyme. In a specially designed system with only one kind of EE and a single type of substrate exist, the K_m is constant and v_{\max} is proportional to enzyme concentration. K_m is a reflection of EE affinity with substrate. Its value is equal to the substrate concentration at which v_0 is equal to half v_{\max} . A high K_m represents a low affinity, which means slow activity increase at low concentration range. Enzymes with high affinities have better performance in low substrate environments, where a v_{\max} seem to be less important, whereas under substrate-rich conditions, a high potential is required.

The relationship between K_m and v_{\max} varies. High v_{\max} s correspond to low affinities (high K_m) and verse versa were often observed (Chrost 1992), which are considered as an adaptation of bacteria to nutrient conditions. However a decreased affinity together with a decreased v_{\max}

was also observed (Davey et al. 2001). Isoenzymes (enzymes that have the same functions but different structures) with disparate K_m and v_{max} may co-exist in some environments, especially those with inconstant organic supplies, resulting in a biphasic dynamic curve that has been observed in several environments (Richardot et al. 1999, Tholosan et al. 1999, Steen & Arnosti 2011).

5. Factors that control extracellular enzyme(EE) performance

Simply said, in natural environments, the activity of a group of extracellular enzyme (EE) is determined by the total number of enzyme molecules and the performance of each molecule. Both of the parts in natural environments are impacted by a variety of factors. In this section, our current understandings about the factors that influence the performance of one single enzyme molecule are briefly discussed. The subsequent section will focus on the mechanisms that determine the stocks of EE in environments.

5.1. The quantity of substrates

The Michaelis–Menten equation indicates that the EE performance is directly related to the quantity of substrates. In natural environments, such a quantity should refer to the available portion of substrate for enzymes rather than the absolute amount, as not all substrates are equally available to enzymatic digestion. Surface adsorption and association of substrates on minerals protect even labile OM from hydrolysis (Tietjen & Wetzel 2003, Ziervogel et al. 2007). The condensation, complexation and polymerization of OM degradation intermediate during different burial and deposit stages are also important factors that impede EEA (Boavida & Wetzel 1998, Rao & Gianfreda 2000). Current techniques have been able to quantify the total amount of organic C/N/P as well as some specific OM groups in samples. However, it is still difficult in many instances to get a reliable estimate of the available amount of substrate.

5.2. The quality of substrates.

Generally speaking, the quality of substrates refers to their reactivity or degradability, i.e. labile or refractory. From an enzyme perspective, as most EEs are able to work on a group of substrates, the quality of each substrate depends on the enzyme affinities and maximum potentials to process it. From the perspective of the whole organic pool, the quality of an organic pool mainly refers to the rate of which such a pool can be decomposed and to what extent it can be decomposed. Our inability to characterize the bulk of the particulate organic matter (Lee et al. 2004) has been the main obstacles to the evaluation of the overall degradability of organic pools. Elemental analysis can easily get the elemental compositions of organic materials. However, materials with the same element compositions might be quite different in their structures and chemical properties.

Most current techniques to measure EEA are not effective in reflecting the quality and quantity of *in situ* substrates, as all of them introduce additional substrates. Specifically designed experiments could provide more information. For example, measuring the degradation rates of not only one but a combination of fluorophore labeled polysaccharides more reliably reflects *in situ* OM qualities (Arnosti 1996, 2000). The introduction of both free dissolved substrate and the same substrate tethered to artificial particles (such as agarose beads) is a good tool to investigate the consequences of surface associations of substrates on hydrolytic activity (Ziervogel et al. 2007). As a whole, however, our knowledge regarding the quantity and quality of natural organic substrates is rather limited.

5.3. *The location of enzymes*

Extracellular enzymes are located at different places. They may be free dissolved or be associated with cells or particles. Such differences in the locations of enzymes influence enzyme performance. Studies have shown that attached enzymes have higher K_m (lower affinity) compared with their dissolved counterparts (Allison 2006, Ziervogel et al. 2007). The particle to which EE has attached blocks the accessibility of EE to substrates shielded by the particle. The association of enzymes may also block or interfere with the bonding sites of enzymes.

The locations of enzymes also make a difference to bacterial cells, as the bacteria benefit differently from enzymes with different states. This may well be part of the regulation strategy of bacteria to secrete cell-associated or dissolved EE. Such strategies might vary between free-lived and attached bacteria cells.

5.4. Temperature

As a common response of all enzymes, activities of EE are very sensitive to temperature changes. Three important parameters regarding temperature dependence of EEs are Temperature Optimum (*Topt*), Activation Energy (*Ea*) and Temperature Coefficient (*Q10*). Each enzyme has a temperature range in which a maximal rate of reaction is achieved. This maximum is known as the temperature optimum of the enzyme. The optimum temperature is usually significantly higher than the highest *in situ* environmental temperature where their producers live. Isoenzymes synthesized by different microbes may have varied optimum temperatures. Studies have found that EEs in Polar Regions have optimum temperatures much lower than those in temperate and tropical regions (Feller et al. 1996, Huston et al. 2000, Arnosti & Jorgensen 2003) at the expense of lower thermostability. This is considered as an adaptation of the microorganisms to their environments.

Both *Ea* and *Q10* reflect the temperature sensitivity of the enzyme. *Ea* is the energy barrier the enzyme needs to overcome in order for a reaction to occur. *Q10* is a measure of the rate of change of enzyme activity as a consequence of increasing the temperature by 10 °C. Both *Ea* and *Q10* can be calculated from EEA vs 1/T plots following the Arrhenius equation. Higher *Ea* and *Q10* represent a higher sensitivity to temperature. In natural environments, isoenzymes may have distinct *Eas*. The apparent *Ea* of an environment where multiple isoenzymes co-exist is the weighted average among isoenzymes. This apparent *Ea* may be different among different EE groups, resulting in a changed C: N: P production ratio with changed temperatures. How bacteria respond to such inconstant production ratios along with temperature change is an interesting topic and one of the major subjects of my dissertation.

5.5. *Other factors*

Many other factors including pH, salinity, dissolved oxygen and the presence and concentration of trace metals also influence EE performance.

Most enzymes are sensitive to pH. Each enzyme has its optimum pH range. For example, acid phosphatase has an optimum pH at low pH while alkaline phosphatase has better performance at basic pH. In marine aquatic zones, the pH is relatively stable so that pH is usually not important in controlling EE performance. In sediments, however, sharp pH gradients can occur within a few centimeter depths. Shifts in the dominating isoenzyme may occur within depth.

Dissolved oxygen, though it is a very dynamic parameter, is generally considered not to be an important parameter in determining EEA. That is mainly because hydrolysis doesn't involve redox reactions. Trace metals, on the contrary, may have great impacts on EEA. Research has found dissolved Mg and Ca stimulate BGA activity in sediment (Dell'Anno et al. 2003). In contrast, Cr may be an inhibitor of bacterial protein synthesis.

6. Mechanisms that control EE stocks in environments.

In the previous section, the factors that control enzyme performance were briefly discussed. This section will focus on the factors that control EE stocks in marine environments. In an idealized system that doesn't consider enzyme flux, the stocks of EE are determined by the production and the decay rates of enzymes. Factors that control these rates are discussed in the following part.

6.1. *The decay rate of EE.*

The decay rate of EE or a derived parameter such as the lifetime of EE describes how long an enzyme molecule remains functioning. Generally speaking, the decay rate of an enzyme is determined by both the enzyme structure as well as its surrounding environment. Studies have

shown that attached or absorbed EEs have resist to thermal and proteolytic degradation and have longer lifetimes than free dissolved EE (Allison 2006, Ziervogel et al. 2007). An accurate estimation of EE lifetime is still missing, it is generally estimated that EEs have lifetimes ranging from tens to hundreds of hours.

6.2. *Regulation of EE production.*

Small molecules produced from EE catalyzed hydrolysis are the main food source for bacteria. The production and excretion however, is at the cost of energy. It is estimated that about 5-20% of all incorporated C by bacteria is used to synthesize EE (Sochaczewski et al. 2008). To assure a profit from EE synthesis, a precise regulation mechanism is required for microbes. Such a mechanism should be able to control not only the total amounts produced but also a proper combination of enzymes. Such a mechanism should also be sensitive to environmental change. Furthermore, as bacteria species work as a community in most environments, the behavior of one bacteria cell is unavoidably influenced by surrounding organisms. How do bacteria regulate enzyme synthesis on a community level is also an interesting yet unclear question.

6.2.1. *Species level regulation*

Species level EE regulation mainly refers to the enzyme pool a certain species can produce, what signals induce enzyme production and what signals inhibit synthesis, and whether the synthesis of an enzyme is constitutive or induced. Through lab enrichment and starvation experiments, the strategies for regulation of enzyme synthesis are well known for specific prokaryotes. However these data are limited to cultivable species and don't explain the mechanism of regulation. In recent decades, the improvement in genomics and bioinformatics has made possible new promising achievements in understanding EE regulation. Whole genome sequencing has been proven to be a powerful tool to study the physiology of bacteria (Bauer et al. 2006, Lauro et al. 2009). From the sequences, not only the potential EE genes but also regulator genes can be

discovered. Judged by the genome localization of the respective genes, the possible mechanisms that control enzyme production can be further proposed (Bauer et al. 2006). The improvement in bioinformatics, has made it possible to predict the possible locations of EEs based on their gene sequences (Luo et al. 2009). It can be expected that many new discoveries regarding EE regulation will be reported in the foreseeable future.

6.2.2. *Community level regulation*

On community level, current studies mainly focus on: the constitution of isoenzymes in an environment; the response of bacteria as a community to environmental changes and also the inter-species relationships with respect to EE regulation: competitive or collaborative.

A number of techniques are able to examine enzyme constitutions. For example, with PCR, the potential EE genes can be amplified. With reverse transcriptase PCR (RT-PCR) that amplifies mRNA, both the gene potential and the gene regulation and transcription information can be acquired. A limitation to these techniques in contrast to whole genome sequencing is that PCR primes are required for amplification which relies on *a priori* knowledge of the target enzyme genes. The meta-proteomic approach also has great potential to elucidate the diversity and source of extracellular enzymes. Lastly but not least, zymography (Capillary Electrophoresis) has proved a powerful technique to detect isozymes. With zymography, different isoenzymes are separated and the activities of each isoenzyme are measured through electrophoresis.

The above techniques have provided promising prospects for our understanding of community potentials and EE regulation mechanisms. However, these techniques (except zymography) don't measure EEA directly. To quantitatively determine the extent to which bacteria communities respond to environmental change still relies on bulk incubations such as enrichment and starvation experiments. In the past decades, enrichment incubations (Boetius & Lochte 1994, Boetius 1995, Boschker & Cappenberg 1998, Pinhassi et al. 1999, Mallet & Debros 2001, Allison & Vitousek 2005, Souza et al. 2011) and starvation experiments

(Albertson et al. 1990) have been conducted in a variety of environments. From these experiments, we knew that bacteria communities respond rapidly to changes in conditions. Shifts in the dominant species of bacteria could strongly influence the rates and patterns of polymer and particle hydrolysis in seawater (Martinez et al. 1996). Some enzymes, for example peptidase, are more likely constitutive enzymes which are produced in constant amounts regardless of physiological demands of substrate concentration, while some enzymes are induced. The addition of substrates generally stimulates the synthesis of the relevant EEs and the addition of hydrolysis products inhibits EE production. At the same time, however, inconsistent or even contradictory patterns were also found between these studies indicating that a universal regulation mechanism may not exist in natural environments. For example, bulk incubation experiments have shown that expression of phosphatase in algae is generally regulated by the prevailing external concentration of inorganic phosphate (Boetius & Lochte 1994) although the internal N: P ratio may also play a role (Hoppe 2003). The addition of proteins stimulates glucosidase activities in some environments (Boschker & Cappenberg 1998) and was found to inhibit that glucosidase activities in others (Mallet & Debroas 2001). The community level regulation mechanisms may be very complicated and be closely related to surrounding environments. For example, the strategies between attached and free-living bacteria may vary. Free-dissolved enzymes may be more important for attached communities on aggregates (Ziervogel & Arnosti 2008, Ziervogel et al. 2010).

The strategy might also be different for different EEs. Phosphatase has been generally found with higher dissolved proportions (Hoppe 2003, Allison et al. 2012) than glucosidase and peptidase. This higher dissolved fraction because hydrolyzed phosphate has higher diffusion rate so that free-dissolved state may be more profitable to its producers. The elemental ratios of food sources, in other words, the stoichiometry, may have a greater influence than the absolute amount of OM in determining the regulation strategies for bacteria. In addition, other factors rather than substrate or hydrolysis products may be the critical factor in regulating EEs in some

environments. For example, in pelagic zones, dissolved Zinc may be the primary limiting factor for peptidase synthesis (as most peptidase contains Zinc) (Fukuda et al. 2000).

Inter-species relationships are another important topic that largely remains unknown. We know from genome sequence data and addition experiments (Sala & Gude 2004, Obayashi & Suzuki 2008) that each species is limited in the spectrum of substrates they can use. The absence of enzymes to hydrolyze a specific substrate has been observed in some environments (Arnosti 2000). The succession of EEs during polymer degradation has also been observed (Sala & Gude 2004). How do bacteria communicate with each other in the collaboration of organic matter degradation? Quorum sensing generally plays an important role in cell communications but details regarding interspecies enzyme production, expression, and degradation remain unclear. Besides collaboration, competition is also common in generally resources limited natural environments, which forces bacteria cells to carefully select their most competitive strategies. To secrete cell-attached or free dissolved EE may be an important part of this process. Cell-attached EE guarantees its producer to obtain most of the products, while free dissolved EE has increased opportunity to meet with substrates but the products may be taken up by other cells. Vetter et al. (1998) explored the circumstances under which free enzymes would be a profitable strategy for microbes. A model was proposed by Allison (2005) to evaluate the profits of EE producers and cheaters (don't produce EE but take advantage of EE producers) at varied conditions. The result showed that being a cheater might be the most economical strategy in some environments.

7. EEA in marine sediments

Compared with studies targeting water column environments, there are far fewer investigations of EEA in sediments (Arnosti 2011). The disparity is due mainly to the difficulties of collecting intact sediment samples, especially for open ocean deep water sediments. The complexities of sediment physical and chemical properties have also made the measurement process more complicated and thus more problematic.

Despite insufficient sedimentary EEA studies, it is clear that surface sediments are extremely important zones with respect to the global element cycle. The ocean seafloor, particularly in continental shelf/slope regions, can receive a large amount of organic matter. The EEA in sediments is typically two to three orders of magnitude higher than in the water column. Sediments are also the reservoir where the majority of refractory organic matter is decomposed. A clear understanding of the mechanisms controlling organic matter degradations and preservations is thus essential for estimating global element budgets.

Although our current studies are far from exhaustive, a considerable amount is known about sediment EEAs. For one, sedimentary EEA bacterial communities seem to be more versatile than EEA associated communities in the water column as recent studies found that sediment EEAs are able to hydrolyze a broader range of carbohydrates (Arnosti 2000). Attached enzymes seem to be the dominant enzyme states in most sediments. The activities of free dissolved extracellular enzymes in sediment interstitial or pore waters are commonly much lower than the activities of attached EEs. Strong adsorptions of organic matters on particles and humic substances (Ding & Henrichs 2002) have been reported, which were found greatly inhibiting EE activities (Keil et al. 1994, Ziervogel et al. 2007). Detailed mechanisms that link the relationship between OM adsorption and EE performances, however, remain to be uncovered. The exopolymeric substances (EPS) surrounding bacteria cells may play important roles in sediment organic matter degradation and preservation, however details about their functions haven't been fully studied (Ransom et al. 1997, Pacton et al. 2007). Sandy sediment generally has at least comparable EEAs with muddy sediments (Boer et al. 2009), despite their relatively low OM contents.

Surface sediments are very dynamic systems, characterized by sharp gradients of dissolved oxygen and successive electron acceptors. Significant vertical heterogeneities of surface sedimentary EEA have also been reported in many studies (Fabiano & Danovaro 1998). EEAs in most sediments decrease rapidly with increased depths. A maximum zone of EEA usually occurs at 0-2cm depth for both muddy and sandy sediments (Arnosti 1995). Because of

the high permeability of sandy sediments, however, constant subsurface maxima at 5-10 cm in sandy sediments was also reported (Arnosti 1995).

In bioturbated sediments, fresh sediments are brought into deep layers through bioadvection and bioirrigation processes induced by benthic faunas. To varying degrees, the faunal activities reduce vertical heterogeneities, but at the same time make sediments spatially more heterogeneous. Degradation hot spots or even subsurface EEA maximum can occur in bioturbated sediments. The introduction of fresh OM into barren layers may also trigger priming effects (the synthesis of EEs targeting refractory substrates owing to the energy support from fresh OMs) that further strengthen horizontal heterogeneities and the localization of organic aggregates. The observation and a quantitative evaluation of spatial heterogeneities, however, is more difficult compared with vertical heterogeneities. To trace such heterogeneity with traditional technique requires precise micro-sampling at different sites associated with bioturbated structures. Previous studies have reported enhanced EEAs surrounding burrow structures or resulting from faunal activities (Boetius 1995, Papaspyrou et al. 2006, Stief 2007). However, data reported in these studies had resolutions at mm to cm scale, which are way too coarse to be able to give a detailed description of small scale heterogeneities. New technologies with higher resolution to entirely resolve heterogeneity is urgently required.

8. Current techniques for EEA measurements.

As discussed in section 5 and 6, EEAs in natural environments are under complicated mechanistic controls. It is difficult to reliably predict EEA from other biogeochemical parameters. The EEA information still largely relies on lab measurements. In theory, the best technique to measure EEA is one that introduces no additional substrate yet is able to observe hydrolysis rate of natural polymers. Unfortunately, current techniques are not even capable of characterizing the majority of organic particles, no less to measure the natural hydrolysis rate of each of the organic constituent components. Available techniques all rely on the addition of pre-modified artificial enzyme substrates, which can be tracked after hydrolysis. The measured

signal is then used to calculate the hydrolysis rate. An inherent drawback of those addition techniques, however, is that they all measure EEA potential rather than *in situ* EEA. As the concentration of natural substrates is usually much lower than the enzyme saturating concentration, the measured maximum activity might be several times or even orders of magnitude higher than *in situ* EEA. Furthermore, these measured EEA maximum and affinity (K_m , if measured) are the parameters reflecting EE's ability to hydrolyze added substrates and may not equal to the EE working on natural substrates. Despite these drawbacks, however, this maximum EEA potential generally reflects the nutrients level and organic matter degradation rates within the study areas. The comparison of EEA with other biogeochemical parameters as well as the comparison of EEAs between areas provide important information for carbon cycle studies

A variety of substrates have been used for EEA measurements. The most widely used substrates are fluorophores 4-Methylumbelliferyl (MUF) and 7-coumarinylamide(MCA) based fluorogenic substrates that were firstly introduced by (Hoppe 1983, Somville & Billen 1983). These small substrate proxies consist of a monomer linked to a fluorophore unit. When the chemical bonds between monomer and fluorogenic unit are hydrolyzed, the fluorogenic units become fluorescent. Enzymes activities are measured as per time unit change of optical signals.

These small proxy techniques don't require a subsequent separation procedure after hydrolysis so that the measurements are relatively rapid and convenient. However, there are a few drawbacks associated with these techniques. Firstly, this method measures only exo-enzyme activities. Studies have shown that endo-acting glucanase doesn't work on or has at least much slower activity hydrolyzing MUF-cellobiose (Boschker & Cappenberg 1994). Secondly, the molecular weight of these small proxies are below 600Da that are possibly directly transportable into cells. Lastly, the fluorescence wavelength may conflict with natural fluorescence (Burdige et al. 2004).

To address the limitations of fluorogenic small proxies, fluorescently labeled high-molecular-weight substrates, including polysaccharides (Arnosti 1995) and peptides (Pantoja et al. 1997), have been used to measure extracellular enzymatic activities in sediments as well as in seawater (Pantoja & Lee 1999, Arnosti 2000, Mulholland et al. 2002, Mulholland et al. 2003, Arnosti et al. 2005). With this approach, the fluorescent units remain attached to the substrates when they are hydrolyzed. These substrates are true polymers so that they can not be directly used by bacteria and the activities of endo-acting enzymes can also be measured with this technique. The drawback of these techniques, however, is that an afterward separation process is needed to differentiate signals from different degradation intermediate.

Future directions for the development of EEA measurement technology, in my opinion, should involve three aspects. The first is the setup of a standardized and high throughput technique to measure EEA at high efficiency. The standardization relies on through studies of the factors that influence EEA measurements (German et al. 2011). To realize a high throughput, Flow Injection Analysis (FIA) (Gaas & Ammerman 2007), multiple Enzyme Analyzer (Jaeger et al. 2009) are promising techniques. Also, while applying plate reader method to measure soil EEA have been developed (Ammerman & Glover 2000, Marx et al. 2001, Popova & Deng 2010), no similar protocols have been reported for marine EEA measurements.

The second direction is the more in depth study of EEA with high-molecular-weight substrates. The high-molecular-weight substrate technique, while its widely application is limited by its low efficiency, more accurately reflects *in situ* EEA levels. If combined with molecular techniques, together they may be the best techniques to discover the regulation mechanisms of EEA.

The last direction is the development of high resolution methods that are able to accurately resolve and measure the EEA heterogeneities in dynamic sediment systems. This topic is the main subject of this dissertation.

9. The necessity of observing surface sediments in multiple dimensions and new appeared techniques designed for this need.

Quantifying the rates of biogeochemical processes is essential for understanding global elemental cycles and potential impacts of climate change for marine systems. As discussed previously, surface sediment, especially in coastal regions, received large amounts of organic material deposits from surface water column and therefore are very active layers in terms of organic matter degradation. Questions associated with the degradation, preservation or burial of organic matters in marine sediments however are thus inherently complex and interdisciplinary. Many coastal sediments display highly heterogeneous biogeochemistry because of complex biological and chemical interactions. The presence of benthic fauna can disrupt and reconstruct sediment, creating a complex, 3-dimensional mosaic of redox zones (Aller 1994). Biotic and abiotic processes are strongly altered in bioturbated sediments, resulting in changes to organic material decomposition rates and elemental cycles (Aller 1994, Kristensen 2000). Therefore, it is important to investigate the causes and effects of sediment heterogeneity and their influence on early diagenesis processes. The investigation of such heterogeneous systems requires measurement techniques with a range of characteristics to observe detailed distributions of sediment processes. Traditional measurement techniques, however, are limited in their ability to characterize high resolution distributions.

With the help of improved computing power, in the past decade, models to simulate surface sediment diagenesis, i.e. the Reaction-transport Models (RTM) have been greatly improved. However limited data sources have restricted model performance and extrapolation from one region to another. To improve model performance and reliability urgently requires high quality data on high resolutions.

To meet these requirement, in the past decades, several new techniques have been developed to investigate the lateral heterogeneity in surface sediments including microelectrodes, planar optode, and diffusional samplers (Glud et al. 1996, Wenzhofer & Glud 2004, Zhu et al.

2005, Glud et al. 2009) Tremendous interesting discoveries have been made from using these new techniques. For example, degradation hotspots, microniches, patchy and variable benthic distributions have been observed and found primarily due to temporal variations in fauna activity and photosynthesis(Wenzhofer & Glud 2004) . A more detailed review can be found in (Stockdale et al. 2009).

These techniques, however, all measure either the distribution of electron acceptors or the distribution of final metabolic products. A more desirable technique would be one that can measure directly a biological parameters that is directly linked to organic matter degradation. EEA sensor described in this dissertation is a great candidate for that.

10. Major objectives of this dissertation.

The main objects of my dissertation research are the development and the following application of a sensor system to measure 2-dimensional EEA (Leucine-aminopeptidase) profiles in surface sediments. Additionally explored was the bacteria response to rapid temperature change reflected in EEA levels. Chapter 2 will introduce in details the principles, the specifications of the enzyme sensor system. Tests of the properties and the performance of this sensor are also reported. This new sensor system had been applied to study the seasonal EEA patterns of two sub-tidal mud sites in Great Peconic Bay, an estuarine environment on eastern end Long Island, New York. The factors that determine annual sedimentary EEA in Great Peconic Bay are also discussed. In chapter 3, the bacteria response to rapid temperature change was studied with a lab incubation experiment series. The role of EE in bacteria adaptation to temperature change is discussed. Chapter 4 discusses patterns of seasonal EEA distributions, microscale EEA hotspots and their potential sources.

**Chapter 2 Development of fluorosensor for two-dimensional measurements of
extracellular enzyme activity in marine sediments**

1. Introduction

Traditional methods for measuring extracellular enzyme activity in sediments typically involve sectioning of sediment cores into centimeter scale slices, followed by homogenization, and in some cases dilution, and subsequent determination of enzyme activity after addition of a fluorogenic or otherwise labeled substrate (Hoppe 1983, Chrost 1991). Because of disturbance by manipulation, this approach has obvious potential for artifacts and at best results in an averaged, one-dimensional profile with relatively coarse resolution. Any natural heterogeneity in enzyme activity is obscured and the possible association of activity patterns with sedimentary structure particularly biogenic ones minimized.

Previous studies have shown enhanced extracellular enzyme activities in bioturbated (irrigated) sediments and near biogenic structures compared with non-bioturbated zones (Aller & Aller 1998, Stief 2007). As far as we are aware, however, only one attempt has been made to reveal high resolution spatial variation of extracellular enzyme activities in sediments. Rogers and Apte (2004) immobilized an insoluble enzyme substrate Naphthol AS in a filter membrane and used an azo dye as an indicator for mapping in situ esterase activity in sediments. In their approach, the membrane, attached to a plastic card, was deployed in sediment for 24 hrs and then removed. The color precipitate associated with enzyme activity was therefore developed in the dye solution for 24 hr and although they were able to demonstrate the heterogeneity of extracellular enzymes and the existence of enzyme activity hot spots, the slow enzyme reaction, slow and separate color development procedure, and millimeter scale resolution limited the method for real-time application. More importantly, the azo dye method does not respond to particle-bound enzymes, which dominate in sediments (Chrost 1991, Ziervogel et al. 2007), because the insoluble Naphthol AS substrate loaded on a filter membrane cannot diffuse into the surrounding environment.

Over the last decade, two-dimensional optical sensors of planar optodes have successfully been used to quantify sediment pore water O_2 , pH, and pCO_2 distributions with high spatial and

temporal resolution (Glud et al. 1996, Wenzhofer & Glud 2004, Zhu et al. 2005, 2006, Volkenborn et al. 2010, Zhu & Aller 2010). Here we describe the development of a thin-layer fluorogenic enzyme substrate delivery membrane that provides the basis for a new extracellular enzyme sensor and the ability to resolve heterogeneous patterns of microbial activities in sediments. The sensor membrane is deployed in a similar manner to other planar optodes: a thin foil with the enzyme substrate is inserted several centimeters into the sediment or onto a sediment surface and imaged perpendicularly to the plane of the film. The primary principles of the sensing system are the controlled release of a nonfluorescence substrate from a thin hydrogel layer into a contacting sediment surface and the time series monitoring of resulting fluorescence generated by enzyme hydrolysis. The sensor foils, which in this application utilize Leu-MCA as the substrate, reveal real-time proteolytic enzyme (Leucine-aminopeptidase) activity patterns across the planar surfaces at high spatial resolution (~50-100 μ m).

Leu-MCA was chosen for this first demonstration, because of the importance of proteolytic enzymes in organic matter decomposition in marine sediments and because the fluorescence response of the fluorophore MCA (7-Amino-4-methylcoumarin) is independent of pH within the range normally expected in marine deposits. Both MCA and MUF(methylumbelliferyl) based substrates fluoresce only after the target substrate is cleaved from the fluorophore, and thus may not accurately assay gross extracellular enzyme activity patterns, for example: endo-enzyme activities such as endopeptidases are not measured(Pantoja et al. 1997, Pantoja & Lee 1999, Arnosti 2000, Arnosti & Holmer 2003). Nevertheless, the simplicity and rapidity of MCA based substrate reactions, make them excellent probes for a subset of enzyme activities. In the present application, because the sensor foils are transparent, enzyme activity patterns can be related directly to visible physical and biological structures in bioturbated sediments, which optimizes our ability to interpret the relationship of bacterial activities, enzyme production, organic matter 'hot spots' and biogenic structures.

2. Materials and Methods

2.1. Reagents

The polyurethane hydrogel HydroMed D4 (D4) (Cardiotech, Wilmington, MA, US) was used as a substrate carrier and delivery source. A 10% (w/v) D4 stock solution was prepared by dissolving D4 in either 90% (9:1(v/v) ethanol/water) or 97% ethanol/water mixture. The enzyme substrate L-Leucine 7-amido-4-methylcoumarin hydrochloride (Leu-MCA) was purchased from Biosynth. A 100 mM stock solution was prepared in deionized distilled water and kept refrigerated (4°C). The stock solution was used for up to 30 days. Leucine aminopeptidase (Leu-AP) (microsomal from porcine kidney, type VI, ~25 unit/mg protein) and 7-Amino-4-methylcoumarin (MCA) were obtained from Sigma. A stock solution of Leu-AP was prepared in deionized distilled water with a final working activity of ~2.5 unit/ml and kept frozen at -20 °C. MCA standard solution was prepared in 100% ethanol with a concentration of 0.1 mM and stored at 4°C. Solvents were of analytical grade and obtained from Fisher Scientific except for ethanol which was purchased from Pharmco-AAPER.

All the experiments were performed at room temperature (22 °C) except when specifically stated.

2.2. Controlled-release sensor membrane fabrication

Here we describe the principles and fabrication of the substrate delivery membrane. Solutions were prepared in a 25-ml beaker using various proportions of D4 stock solution (10% in 97% ethanol), Leu-MCA stock solution (100 mM), ethanol, and if necessary deionized water. The relative volumes of Leu-MCA and D4 were calculated to achieve specific final concentrations of Leu-MCA and thicknesses of D4 as described subsequently. Ethanol and deionized water were added to make the final solution volume large enough to spread evenly on a polyester backing film. The D4 stock solution must be added last and slowly, with constant swirling of the beaker, to avoid precipitation during mixing. The final ethanol/water ratio in solution was between 92:8 and 96:4. The mixture was then cast with a micropipette onto a pre-cleaned, dry polyester Mylar film backing (~130 µm thickness). Typically, a total volume of 0.1

ml mixed solution per 1 cm² film was used with a final D4 proportion of 4.6% (w/v). This proportion ensured a smooth, transparent product. The thin solution layer on the Mylar film was evaporated at room temperature in a hood until completely dry (~ 24 hrs). For practical application, the polyester film measures 3 cm width by 9 cm length, but could vary depending on the specific use. In this report, sensor membranes were fabricated for use with natural samples with 5 mg/cm² D4 and 0.82 μmol/cm² Leu-MCA. The D4 and Leu-MCA load, however, can be varied between study areas, depending on the expected enzyme activities of each site. More details will be discussed subsequently.

Membrane thicknesses resulting from different D4 loadings were measured in representative sections using a microscope fitted with a micrometer scale. With a loading of 1 – 16 mg/cm² (weight of D4/cm² following evaporation), the sensor foil varied in total thickness between ~ 137 – 240 μm (7 – 110 μm D4 layer + 130 μm polyester backing).

2.3. Instrumentation

The properties of foil subsamples and solution extracts were examined using a Hitachi F-4500 fluorescence spectrophotometer. Sections of foils were inserted into a custom cuvette (1-cm²) that allowed excitation with light at an angle of incidence of ~30° and measurement of fluorescence spectra of the foil samples while maintaining contact of the membrane with small quantities of homogenized sediment or solutions (more details in Zhu et al., 2005). Wavelength shifts of both maximum excitation and emission light were observed when MCA is trapped in a D4 membrane. Fluorescence of trapped MCA was measured at 430 nm with excitation at 380 nm.

A two-dimensional fluorescence imaging system was used for examining the sides of sediment cores and microcosms into which the sensor foils were inserted (Figure 2.1, after Zhu et al, 2005). The excitation light source ($\lambda_{\text{ex}}=380$ nm) was a 150-W Xe-UV/vis arc lamp and monochromator controlled by a computer (Spectral Luminator, model 69050, Oriel Instruments). Emission was monitored using a commercial digital camera (Canon EOS 10D, resolution

2048×3072 pixels) controlled by Canon Remote capture 2.7 software. A Canon lens model EF-100 mm was used, with a 5 cm diameter emission filter ($\lambda_{em}= 430$ nm) mounted between the lens and target to minimize background interferences. To further avoid reflected light, the fluorescence image was recorded with excitation light at an angle of incidence of $\sim 30^\circ$ and emission at 90° to the target plane. Images were taken at 1 minute intervals. The ISO was set at 1600 and the exposure time was typically set at 10 seconds. Image analyses were performed with Image-Pro plus version 4.1 and Matlab 7.0.4 for Windows. For calculation, the blue band intensity was converted to 8-bit gray scale (0 – 255) for image series obtained over a 1 hour period.

2.4. Membrane characterization and optimization

Characterization of the diffusive release of substrate from foils and the optimization of D4 hydrogel thickness and substrate loading were done using subsamples of foils. A series of D4 thicknesses ranging from 1 – 16 mg D4/cm² (mass / area foil) with the same MCA load was used to evaluate substrate release rates from the foil into seawater. A one centimeter wide strip was cut from a larger section of foil and mounted in the custom cuvette. Seawater was then exchanged through the cuvette (10 ml/min; residence time 1.5 min) with a peristaltic pump and the residual fluorescence response of the membrane surface as a function of time during contact measured using the Hitachi F-4500.

In order to determine the optimal loading of Leu-MCA substrate in the carrier membrane, saturating concentrations of substrate were first determined in likely target sediments using the traditional slurry based method (Hollibaugh & Azam 1983, Hoppe et al. 2002). For these traditional measurements, ~ 1 g of wet sediment was added into a 15 ml centrifuge tube. Then 5 ml of 0.2 μ m pore size filtered sea water and 80 μ l of 100 mM Leu-MCA substrate were introduced, and the sample slurried using a vortexer. After one hour incubation in the dark at 22°C, 5 ml 30% acetone was added to stop the reaction (Belanger et al. 1997) and to extract MCA from sediment particles. The sample was centrifuged (4500 rpm, 15 mins), the supernatant

was filtered with a 0.2 μm pore size polysulfone filter, and fluorescence was measured at 440 nm with excitation 360 nm. Based on these slurry measurements, subsections of foils with Leu-MCA concentrations varied from 0.12 – 0.32 $\mu\text{mol}/\text{cm}^2$ foil were applied to fresh surface sediment from Long Island Sound to further determine the optimal membrane saturating load of Leu-MCA.

To test the response of the foil system and credibility of the measurements, different aliquots of standard Leu-AP enzyme solutions were added to homogenized surface sediments from Long Island Sound. The activities of each sample were measured in cuvettes with sensor film subsamples having the same load of Leu-MCA.

In order to evaluate the effect of possible variations in membrane fabrication (e.g., Leu-MCA loading uniformity, thickness) and incident light intensity, several foils with MCA were inserted into microcosms containing homogenized Long Island Sound sediment. The foils were imaged using the camera based system, and the standard deviations of pixel intensities within each foil area and between foils compared.

2.5. Transport and adsorption of the fluorophore in sediment

In addition to release from the carrier foil, the movement and adsorption reactions of MCA in sediment adjacent to the membrane are critical factors governing both the availability of substrate for enzymatic reaction and the interpretation of fluorescence response in images. An estimate of the diffusion coefficient of MCA in sediment was made by following the penetration of MCA into sediment from a well-mixed overlying water reservoir. A layer of seawater 5 cm thick with a MCA concentration of 5 $\mu\text{mol}/\text{L}$ was placed over an homogenized 10 cm thick sediment layer in a glass walled microcosm and the vertical penetration of MCA into the sediment imaged as a function of time.

As we observed strong adsorption of fluorophore MCA on sediment particles, a set of experiments was also designed to check the magnitude, time dependency, and reversibility of

MCA adsorption onto sediment. To determine the time required to reach adsorption equilibrium, homogenized sediment samples with similar weights (~10 g) were placed into 50-ml centrifuge tubes. MCA solutions made up in 8 ml of filtered seawater were introduced to reach a final concentration of 10.5 μ M, the sediment samples slurried, and the tubes sampled serially over time. Pore waters (~10 ml) were immediately separated by centrifuging (4500 rpm, 15 mins), and the percentage of MCA adsorbed on particles plotted over time.

Adsorption isotherms were determined by adding eight different concentrations (final concentrations: 4.5-14 μ M) of MCA to a set of sediment slurries. Adsorption isotherms were calculated according to the Freundlich equation (Coolen & Overmann 2000):

$$S = K \cdot C^n$$

Where S is the amount of MCA adsorbed (nmol/g dry weight) , K is the affinity coefficient (in ml/g dry weight), C is concentration of MCA remaining in solution(in nmol/ml) and n is a dimensionless exponent. S can be calculated from the total concentration of MCA added initially, measured C , and the dry weight content of the sediment. The values of K and n were determined by fitting the Freundlich equation to the data points after an incubation of 1hr and at apparent equilibrium (after 22hrs incubation). The estimation of K and n after 1hr incubation, though not at an equilibrium condition, best represent MCA adsorption behavior during sensor measurements.

The desorption of MCA from particles after adsorption was also estimated. at three separate times (1, 2, 16 hrs after the MCA solution was introduced). After each sampling time following a period of adsorption, the residual solution was removed, 10 ml of MCA-free filtered seawater was added back into the centrifuge tubes, mixed, the sample recentrifuged, and the solution immediately assayed for MCA.

2.6. Experimental applications

Two-dimensional enzyme activities were measured in both initially homogenized and

undisturbed natural sediment samples. Surface sediment to a depth of 5 cm was collected from Smithtown Bay, central Long Island Sound. The sediment was sieved through a 1 mm mesh screen with no added water, mixed and then carefully transferred into a rectangular glass-faced microcosm which had been previously fitted with a polyester film, slightly smaller than the side face of the microcosm, on the inside face of one side to serve as a placeholder for the sensor foil. The homogenized sediment tank was incubated in aerated sea water in the dark for 2 weeks. Prior to deployment, a sensor foil was first cut to a suitable size (usually 3×10 - 5×10 cm) and attached onto a polyester film holder using Teflon tape along the foil edges. The sensor foil surface was then gently rinsed with filtered seawater to wash off substrates loosely bound on the very surface of foil in an effort to avoid any uneven substrate distribution during deployment. The holder was then gently inserted between the placeholder film and the front face of the microcosm. The placeholder film was then carefully removed so that the sensing face of the membrane tightly contacted the sediment. A black plastic film was additionally inserted vertically in the overlying water near the rear of the tank to provide an opaque background to the sediment. The fluorescence generated on sensor foil side of the microcosm was imaged successively with time at 430 nm with excitation at 380 nm.

Natural sediment cores were collected from Flax Pond (intertidal, back barrier *Spartina* marsh on Long Island Sound) and Great Peconic Bay (subtidal, 8 m off the Atlantic Ocean), Long Island, NY using acrylic box corers. These box cores were transported to the laboratory and sub-sampled using rectangular glass-walled corers with sensor foils attached along one side. The fluorescence signal on the sensor foil side was then imaged at the excitation and emission wavelengths described previously.

3. Results

3.1 Diffusive release properties of the Leu-MCA carrier foil

The polyurethane type hydrogel D4 chosen as the substrate carrier matrix is a highly proton-permeable, uncharged polymer with equilibrium water contents approaching 50% (Stahl

et al 2006). D4 contains hydrophilic regions and hydrophobic blocks in which Leu-MCA is immobilized by physical entrapment. After deployment in seawater, the water content of D4 increases (swelling) allowing the diffusive escape of Leu-MCA into adjacent sediment pore water. A portion of the released Leu-MCA is adsorbed onto sediment particles directly contacting the surface of the D4 membrane.

MCA was chosen as a molecular tracer of diffusive release assuming that it has a similar behavior to Leu-MCA. A series of D4 thicknesses ranging from 1 – 16 mg D4/cm² (mass / area foil) with the same MCA load was used to evaluate substrate release rates from the foil into seawater. Depending on the thickness (loading) of the D4 membrane, a period of linear loss of MCA occurred, followed by exponentially decreasing rates consistent with diffusion (Figure 2.2A). Linear loss was sustained over a longer period as membrane thickness increased. This means that the D4 membrane thickness can be manipulated to achieve a rapid release of substrate into contacting sediment a few minutes after exposure (e.g., when measuring highly reactive coastal sediments), or a more sustained steady release over a period of a several hours (e.g., when measuring less reactive deep ocean sediments). The release rate (represented as %total MCA/min) for each foil plotted in Figure 2.2B, shows an exponential decrease with increased D4 load indicating that the thicker the D4 membrane, the slower the relative signal loss. For practical applications in our study, which was on coastal sediments, an optimized final D4 loading of 3-6 mg/cm² was selected. In these cases at least 60% of the total substrate load is released by diffusion from the carrier membrane in 15-30 min.

3.2. Adsorption behavior of MCA on sediment particles

As noted previously, after Leu-MCA is released from the carrier membrane it is subject to adsorption, diffusion, reaction with particle bound enzymes, and hydrolysis. The diffusive supply and/or adsorption of Leu-MCA substrate molecules on sediment particles are presumably factors in determining availability to particle bound enzymes (Ziervogel et al. 2007). On the other hand, the diffusion and adsorption of enzyme hydrolyzed fluorescent product MCA are also important

since the loss of MCA causes a change in fluorescence. Experiments were designed to study how environmental factors influence the adsorption behavior of MCA.

The results showed that due to its low hydrophilic nature, large amounts of MCA are adsorbed on sediment particles and the adsorption is time dependent. A typical adsorption pattern of MCA by sediment particles with time is shown in Figure 2.3A. Approximately 60% of MCA is adsorbed rapidly (< 1 hr), followed by a slower loss of up to a total of 70 - 80% occurring over 1 – 2 days. Concentration has a very small (i.e. <4%) influence on the fraction of MCA adsorption, at least within the practical MCA concentration range for the sensor system. Temperature substantially influenced the adsorption properties of MCA with more MCA adsorbed on sediment particles at lower temperatures. pH has very little influence on adsorption over a range of 5 to 9.5.

Adsorption isotherms were determined after 1 hr and 22 hrs incubation. The K and n values after 1hr incubation were 6.75 and 0.84, respectively. The K and n values after adsorption equilibrium (after 22hrs incubation) were 13.2 and 0.80, respectively (Fig 2.3B). The n value didn't change significantly during incubation. However, due to the time dependence of MCA adsorption, a substantial increase of K value occurred with time.

The reversibility of MCA adsorption was also tested. Reversibility was evaluated by exposing sediment with adsorbed MCA to MCA-free pore water after different incubation times. If MCA adsorption were completely reversible, adsorbed MCA should be partially released after the addition of MCA-free pore water and attain a new equilibrium consistent with the derived Freundlich equation. If the MCA adsorption were irreversible, no MCA should be removed from particles and the MCA signal in the supernatant should be due only to residual MCA in the pore water after centrifuging. The reversibility is represented as the percentage of adsorbed MCA on particles released back into pore water. In Figure 2.3C, the hollow circles show the percentage release of adsorbed MCA when the MCA adsorption is able to re-attain a Freundlich equation equilibrium. The values were estimated from Figure 2.3A (22°C). The solid dots show the

actual MCA percentage loss from particles. These patterns demonstrate that MCA desorption is approximately reversible initially and becomes progressively less reversible with time.

The above results combined with the fact that most Leu-AP was particle bound implied that the majority (e.g., 70 - 80%) of enzyme hydrolyzed product MCA molecules are adsorbed where they are formed. This phenomenon is beneficial to our sensor system, because the restriction of MCA movement following formation aids identification and spatial resolution of enzyme activities.

In order to determine the loss of fluorogenic MCA from the image plane during both diffusion and adsorption, the unsteady penetration of MCA from overlying water into sediment was followed experimentally, indicating a net penetration rate of ~ 1 mm/hr. Assuming no adsorption, this rate translates into an apparent whole sediment diffusion coefficient of ~ 0.06 cm²/d. Given the molecular weight of MCA (175), its free solution diffusion coefficient should be in the range of ~ 0.3 cm²/d in seawater and ~ 0.24 cm²/d in sediment with a porosity of 0.9 (Burdige et al. 1992, Hannides et al. 2005). A reversible adsorption coefficient (unitless) required to explain these differences in net diffusion coefficients would be ~ 3 , consistent with but somewhat less than the ~ 6.8 derived independently from the Freundlich relation.

3.3. Sensor response

To check the reliability of the sensing system, different quantities of standard Leu-AP solutions were added into homogenized surface sediment samples collected from Long Island Sound with the final enzyme load range from 0.10-0.38 μmol substrate per hour per gram wet sediment (labeled value). Natural enzymes present in the sediment were not deactivated, and standard additions were made immediately before measurements. Total Leu-AP activity of each sediment sample was measured using foil subsamples cut from the same large foil (0.5 μmol Leu-MCA/cm² foil) in the fluorescence spectrophotometer. Fluorescence signals of each sediment sample are plotted in Figure 2.4A. All treatments showed well defined linear fluorescence intensity increase over time after a short lag stage (< 5 mins, the time required to

wet the D4 layer), so that the slope of each curve can be used to represent potential Leu-AP activity of each sample. The slope of each line from Figure 2.4A (represented as net fluorescence increase/min) was then plotted against the various standard addition Leu-AP activities (Figure 2.4B). The excellent correlation ($r^2=0.97$) demonstrates that the foil system accurately reflects enzyme activity variations in sediment samples and is thus a reliable system for extracellular enzyme activity measurement. Additionally, the potential Leu-AP activity of natural sediment can be calculated to be $0.45\mu\text{mol sub}/(\text{hr}\cdot\text{g})$ (labeled value) based on extrapolation of the calibration curve in Figure 2.4B.

3.4. Membrane uniformity

The effect of layer evenness was tested by inserting foils (4×4 cm) with different MCA loads into homogenized sediment samples. The MCA foils were imaged by the camera system, and the gray scale fluorescence intensity difference between all pixels calculated. The average gray scale among all pixels (655×655 pixels for each foil) ranged from 136-172 for all 4 test foils. The average gray scale standard deviation was 1.4 ($n=4$) and an average RSD of $\sim 0.9\%$. Thus slight unevenness in foil thickness has an imperceptible influence on results. Additionally, these results demonstrated that the insertion procedure of foils into microcosms did not generate variability. In practical application, the substrate load was designed to deliver local concentrations much higher than the half saturation concentration, which further diminishes the influence of a minor difference of substrate concentration on the inferred enzyme activities.

4. Discussion

4.1. Leu-Aminopeptidase foil system design

Three strategies were considered when designing the enzyme foil system: covalent immobilization of enzyme substrates in foils and allowing enzymes to diffuse in; tethering substrates onto foil surfaces; and the substrate delivery strategy by physical entrapment into the polymer matrix that we describe here. Considering the fact that particle bound enzymes are the

dominant (>90%) enzyme form in sediment (Chrost 1991, Rogers & Apte 2004, Ziervogel et al. 2007) as well as indications that particle attached bacteria possess higher per cell enzyme activity (Lehman & O'Connell 2002), the strategy of binding substrates into a polymer sheet should greatly underestimate particle bound enzyme activity. Immobilizing substrates on polymer membrane surfaces by sorption or covalent bonding may be good for the free extracellular enzymes in pore water which can access the immobilized substrates by diffusion, but particle bound enzymes, even adjacent particle associated enzymes, can still not access the substrates. Furthermore, the required foil synthesis procedures are relatively laborious and determining proper saturation of enzymes potentially difficult.

In our present work, the enzyme substrate was initially physically trapped into an organic polymer layer (D4) and substrates were allowed to diffuse out of the polymer layer after deployment in an aquatic environment. This design has the following advantages: first, the diffusion of enzymes into polymer membranes is difficult (or impossible for particle bound enzyme), whereas the diffusion of small molecule substrates from the membrane into an aquatic environment is very easy and fast, and the response time (enzyme reaction) therefore more rapid; second, the free substrate that diffuses out of the polymer membrane is available to both free dissolved and particle bound enzymes in sediment; third, it easily allows a substrate load that is sufficient enough to locally saturate target enzymes. The disadvantage is that the substrate can be potentially lost into the contacting environment (e.g., water) and may diffuse out of the imaging plane. Thus, it is necessary to characterize both the diffusive release of substrate from the carrier membrane and its transport in the immediately contacting environment.

4.2. Determination of optimized Leu-MCA load

Enzyme catalyzed reactions follow Michaelis-Menten kinetics:

$$v_0 = \frac{v_{\max}[S]}{K_m + [S]}$$

Where: $[S]$ is the substrate concentration, v_0 is the initial reaction rate to the substrate concentration $[S]$, v_{\max} is the maximum rate of reaction and K_m is the Michaelis- Menton saturation constant representing substrate concentration at which the reaction rate reaches half of its maximum value.

When Leu-MCA concentration $[S]$ is much higher than the half saturation constant K_m the enzyme activity v_0 is very close to v_{\max} . In our foil membrane design, the Leu-MCA load is optimized to make sure that, after deployment, the concentration of Leu-MCA released into sediment near the foil surface (within 1mm distance) is high enough (in our study $>10K_m$) to saturate the ambient target enzyme for at least the experimental time period (usually 1hour). Thus, all reported measurements reflect maximum potential enzyme activity and any possible biphasic response is not resolved (Tholosan et al. 1999).

The likely load range was first estimated from traditional incubation results. A series of membrane foils with different loads was then used to measure extracellular enzyme activity in typical surface sediment from Long Island Sound. The results showed that a Leu-MCA load higher than $0.2 \mu\text{mol}/\text{cm}^2$ was enough to saturate enzymes in the experimental sediments (Figure 2.5). Considering varying enzyme activities at different sites and seasons, a final load of $0.5\text{-}1.0 \mu\text{mol}$ Leu-MCA per cm^2 foil was selected for the coastal sediments examined in the present study. The thickness of the D4 layer was then adjusted to generate a suitable release rate based on diffusive loss experiments in seawater filled cuvettes. A D4 load of $3 - 6 \text{ mg cm}^{-2}$ foil was typically selected.

4.3. Enzyme activities calculation and correction for diffusion and adsorption

Assuming a sufficient Leu-MCA supply, v_0 should be very close to v_{\max} for all pixels and should remain constant. Thus, the exact value of Leu-AP activity can be estimated as:

$$V_0 = \beta \frac{\Delta F}{\Delta T}$$

Where ΔF is the fluorescence increase per time increment ΔT , and β is the conversion constant from fluorescence to enzyme activity. The value of β can be estimated by adding a known concentration of enzyme into sediment or determined from a traditional incubation result. This latter approach effectively normalizes results to the traditional method.

The previous equation does not consider changes in the fluorescence signal due to adsorption and diffusion. To estimate fluorescence loss caused by MCA diffusion and adsorption during measurements, a MCA foil with the same D4 load as the substrate membrane was inserted next to the Leu-MCA foil. The fluorescence signal from the MCA loaded foil is determined by diffusion and adsorption of MCA and not by enzyme reaction. Thus the percentage MCA loss per unit time of contact was used to correct (amplify) the fluorescence signal of MCA generated by enzyme reaction at the same depth (porosity). The new equation then becomes:

$$V_0 = \beta \frac{\Delta F(1 + C\%)}{\Delta T}$$

Where C% is the percentage of MCA loss per minute in pixels from an equivalent depth interval with comparable porosity.

Sediment colors and particle size and shape can potentially influence the fluorescence background and reflection. However, no significant influence of sediment color on fluorescence intensities has been found to date, so correction for sediment color was not made. Particle size and shape might interfere with fluorescence due to their impact on solute diffusion. However, this effect was not studied in this work. Further research may be needed to determine circumstances when corrections other than the MCA diffusion – adsorption loss must be made.

4.4. Vertical enzyme activity profile in microcosm and comparison with traditional incubations

A foil deployed in a sediment core collected from Flax Pond was selected to illustrate the vertical enzyme activity profile measured by a foil sensor system. Figure 2.6A shows images captured during measurements. Panel A is a visible image under green light (550 nm) captured before actual measurements, panels B, C and D are fluorescence examples taken at 3 different

times, i.e. 6, 10, 28 min, respectively. The fluorescence emitted from the sensor is blue, but in the example fluorescence images, pseudo- colors (red) were applied to better demonstrate the contrast between pixels. The pseudo-colored pictures clearly show a fluorescence intensity increase over time and a relatively brighter area at the surface sediment.

To compare the enzyme activities measured using the foil system with traditional profiles, the horizontal enzyme activities across the whole membrane were averaged. The fluorescence increases during the first 10 – 40 minutes of incubation were used to calculate enzyme activities and the results are shown in Figure 2.6B. A clear surface enzyme activity maximum zone was found in the top 1 cm of sediment, and a sub-maximum zone occurred at a depth of ~2 cm. Compared with results from the traditional method (red triangles in Figure 2.6B), the two profiles matched quite well with the exception that in traditional method, the second subsurface maximum zone was not found. The difference may be the result of a loss of signal due to the low resolution of traditional volume slicing and simply the heterogeneity of sediment. Nevertheless, the comparison did show the sensor system not only produces comparable averaged profiles with the tradition incubation method, but most importantly has a much greater two-dimensional resolution.

4.5. Spatial heterogeneity of Leu-AP activity distribution in marine sediments

The spatial heterogeneity of remineralization in sediments has been revealed directly using specific solute planar optodes and by various sampling arrays (Wenzhofer & Glud 2004, Zhu et al. 2006, Stockdale et al. 2009, Bertics & Ziebis 2010). Hot spots of elevated remineralization are often associated with biogenic structures formed by meio- and macrobenthos. The enzyme sensor images from several sediment examples in this research also revealed considerable spatial heterogeneity and localized activity maxima. Figure 2.7, for example shows the enzyme activity distributions of a sediment microcosm collected from Great Peconic Bay, Long Island. Fluorescence image results from the initial 10-40 minutes of incubation were included in the calculation. The rates of increase in fluorescence intensity within

individual pixels, after corrections for diffusion and adsorption loss, were converted to enzyme activities by normalizing to the activity in a specific depth interval region measured in a traditional incubation. The conversion coefficients β , in this case, were estimated as the ratio of integrated gray scale from sensor images (horizontally averaged) to the integrated enzyme activities from traditional incubations (0-9cm). The calculated enzyme activities of all pixels were then plotted as a pseudo-color image shown in Figure 2.7A using Matlab. The images showed substantial heterogeneity both horizontally and vertically. A general maximum region was found between 0.5 – 1 cm depths. A high value zone was found at around 0.5 cm depth and separate hot spots with typical area $\sim 4 \text{ mm}^2$ were found at $\sim 1 \text{ cm}$. The patchy distribution of enzyme activity within the subsurface layer may result from earlier faunal activities, for example, excretions by meio and macrofauna, residual burrow structure, or other factors affecting small scale reactive organic matter patterns. It is also possible that microbial activity is generally enhanced due to coupled redox reactions near the primary subsurface oxic – anoxic boundary, which occurs at a few millimeters below the surficial sediment-water interface. The activities decrease sharply with depth and showed less, although still detectable, horizontal heterogeneity in sediments below 2 cm depth. The structure of the horizontally averaged, vertical profile (black line Figure 2.7B) from sensor images was also compared with traditional incubation results (gray dots). Both profiles showed a maximum enzyme activity in the top 1cm and decreasing activities with depth. However, the traditional incubation results showed relatively higher values within the top 1cm depth layer as well as layers below 7 cm. These mismatches may be caused in part by artifactual behavior during traditional incubations, error in the optical sensor corrections, or by sample heterogeneity not accounted for in a single image plane but otherwise incorporated into the homogenized interval used for the traditional incubation. When slicing sediment cores, for example, a small amount of compaction and pore water loss for the uppermost surface sediment layer is often unavoidable. For deeper sediment layers, trace amounts of oxygen may be introduced during slicing even though the cores were processed under nitrogen gas. These types of effects may result in differences in the estimation

of enzyme activities.

5. Summary and conclusions

Here we demonstrate the development and successful utilization of a new planarfluorosensor system for two-dimensional measurement and display of extracellular enzyme activities with submillimeter spatial resolution. The underlying principle of the new extracellular enzyme sensor is the incorporation of a fluorogenic enzyme substrate into a polymer carrier and the controlled release of that substrate into a contacting medium while transport and reactions are continuously monitored.

In addition to resolving average distributions comparable to those revealed by traditional methods, high spatial resolution and small hotspots of enzyme activity in the sediment were also documented, demonstrating microscale heterogeneity of hydrolytic processes. This technique can be utilized to measure other extracellular enzyme activities given suitable enzyme substrates. The technique can also be readily adapted for in situ applications, for example, using appropriately modified sediment profile imaging (SPI) cameras e.g.(Glud et al. 2001, Fan et al. 2011).

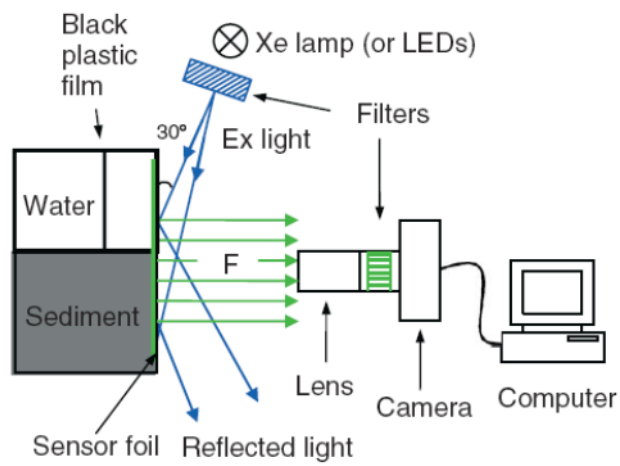


Fig.2.1. Imaging instrumentation used for two-dimensional Leucine-Aminopeptidase measurements (after Zhu et al., 2005).

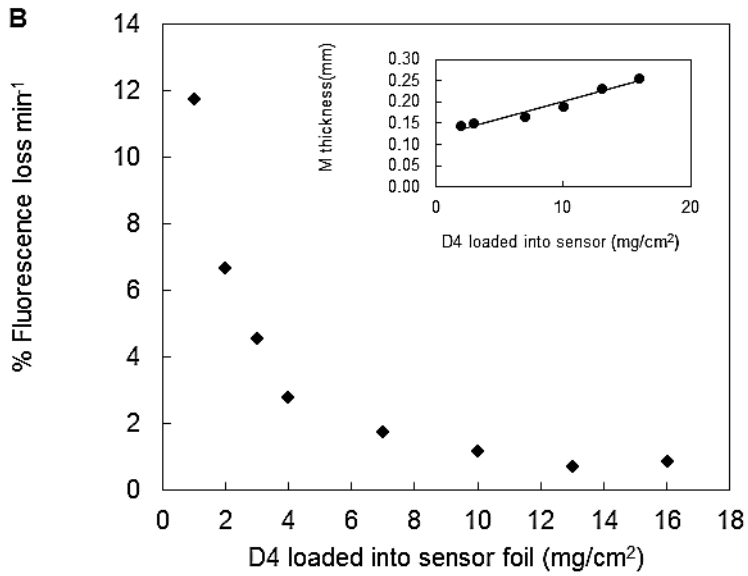
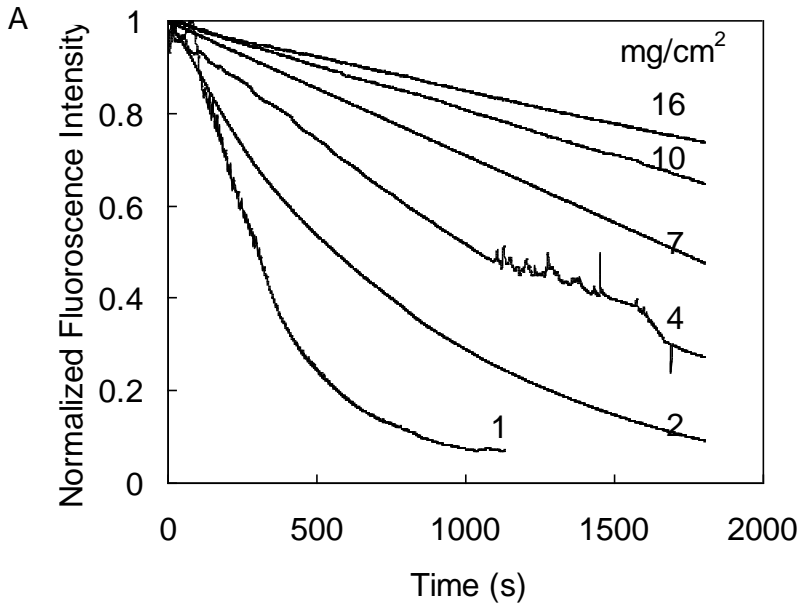


Fig. 2.2. (A) Release behavior of MCA membranes with different D4 loads. (B) Variation of unit time release rate of linear release period (represented as % total MCA/min) versus different D4 loads. Insert: relationship between D4 load and layer thickness.

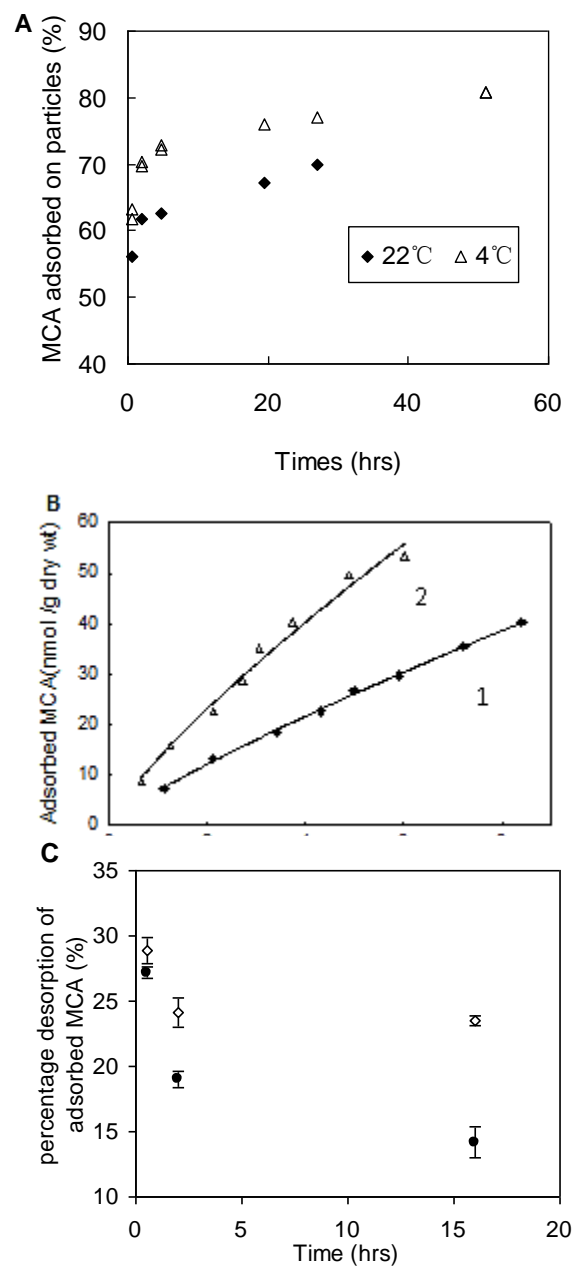


Fig. 2.3. (A) Adsorption behavior of MCA with time at 4 °C and room temperature 22 °C. MCA concentration: 10.5 μ M. (B) Adsorption isotherms of MCA fitted to Freundlich equations (lines). 1: after 1 hr incubation (Δ); 2: after 22 hrs incubation (\blacklozenge), (C) Desorption behavior of MCA in sediment shown as the percentage of adsorbed MCA released at a particular time after adsorption : (\circ) MCA adsorption behavior if the adsorption were completely reversible; (\bullet) measured

adsorption behavior of MCA in sediment.

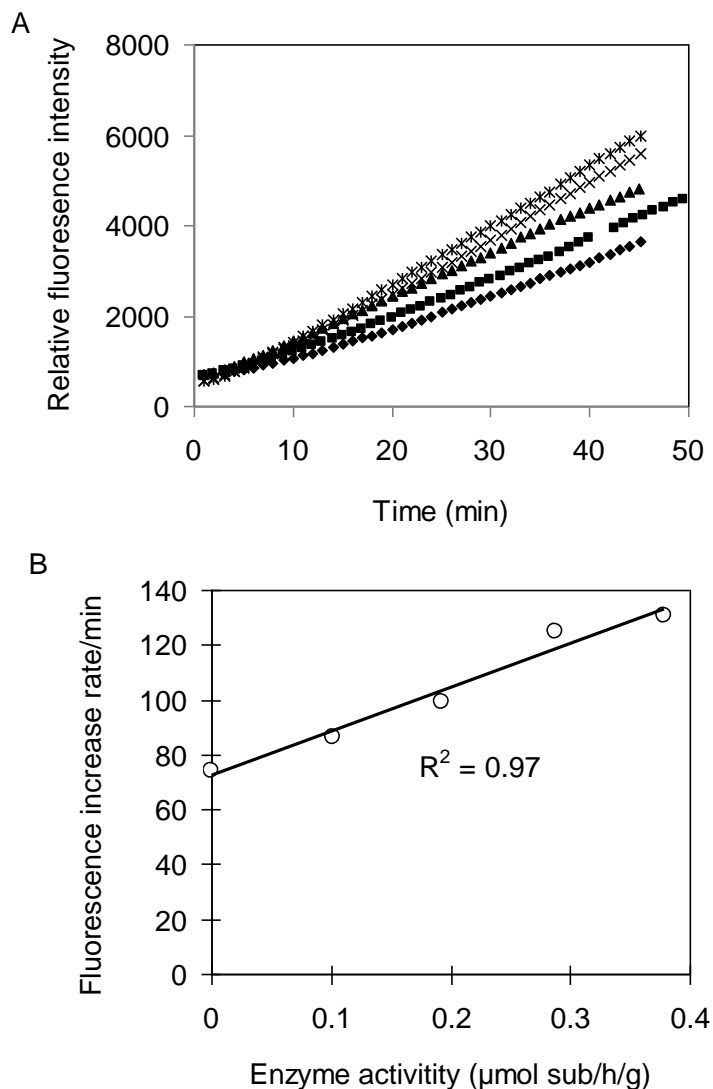


Fig. 2.4. (A) The response of the enzyme fluorosensor in the presence of various extracellular enzyme activities in marine sediments. The surface sediment (0 – 5 cm) collected from Long Island Sound was homogenized and sieved through a 1 mm mesh sieve before use. The relative fluorescence intensity increases with the incubation time. (B) Correlation between the rate of increase of fluorescence intensity and extracellular enzyme activity added into each sample. Substrate loaded: $0.5 \mu\text{mol Leu-MCA}/\text{cm}^2$. Extracellular enzyme activity: (◆) natural sediment; then added (■) 0.10, (▲) 0.19, (×) 0.29, and (*) 0.38 $\mu\text{mol sub}/\text{hr}/\text{g}$ standard Leu-AP enzyme

into the natural sediment.

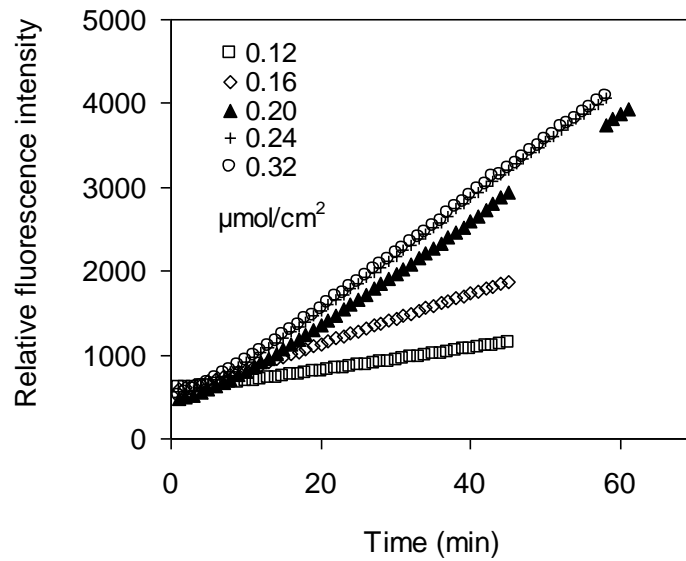


Fig. 2.5. The effect of substrate Leu-MCA load in the foil on sensor response. The homogenized surface marine sediment (0 – 5 cm) was obtained from Long Island Sound. The Leu-MCA amounts in each sensor foil are: (\square) 0.12, (\diamond) 0.16, (\blacktriangle) 0.20, (+) 0.24 and (\circ) 0.32 $\mu\text{mol}/\text{cm}^2$.

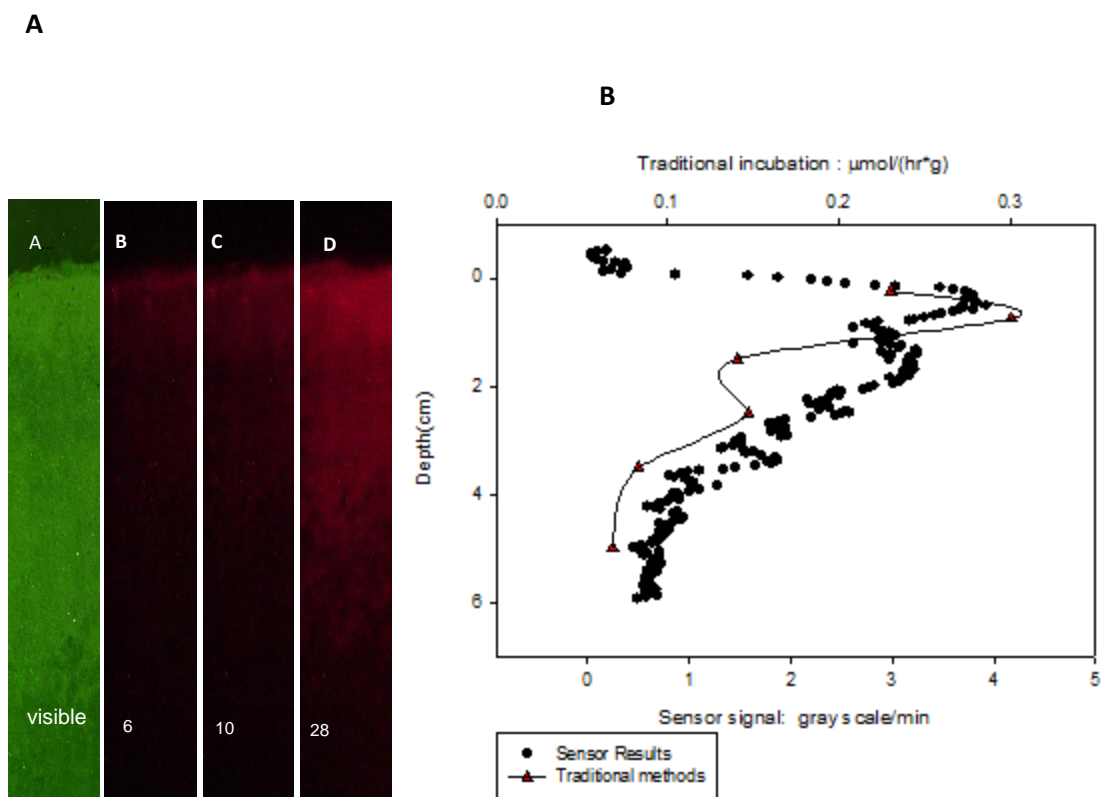


Fig. 2.6. (A) Visible and pseudo-color (red) fluorescence images of marine sediment at 6, 10 28 min after sensor foil deployment. The intact microcosm core was collected from Flax Pond, Long Island. (B) The comparison of enzyme activity profiles obtained from traditional methods and the fluorosensor technique. The fluorescence increase of the sensor during the first 10 – 40 minutes of incubation was used to calculate enzyme activities. The solid dots were horizontally averaged data extracted from 2-dimensional enzyme distribution.

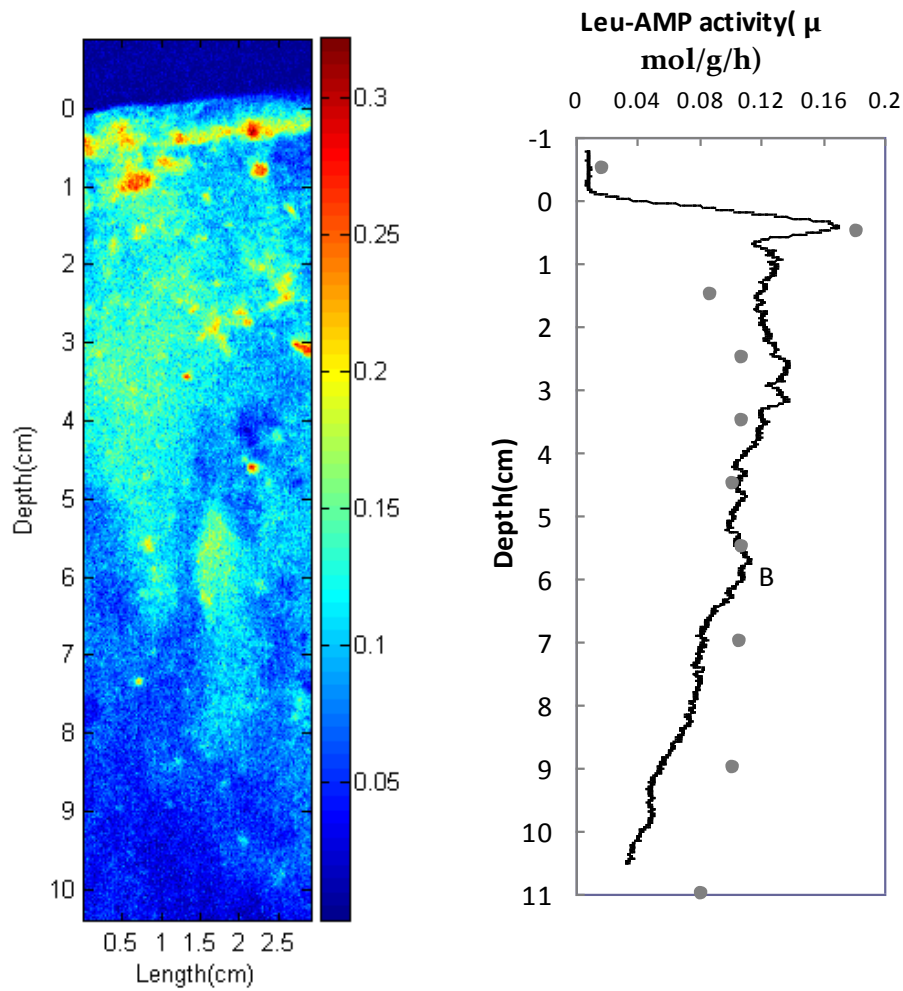


Fig. 2.7. Left: 2-dimensional extracellular enzyme distribution pattern in an intact marine sediment microcosm core collected from the Great Peconic Bay, Long Island. Right: Horizontally averaged enzyme activity vertical profile (black line) and its comparison with results from traditional incubations (gray dots).

Chapter 3 Temperature dependence of extracellular enzyme activities in temperate coastal sediments.

1. Introduction

Extracellular enzymes (EE) initiate the microbial loop. The rate of EE induced hydrolysis determines the amounts of polymeric organic matter that become available to bacteria. As an intrinsic character of enzyme, EEs are sensitive to temperature change. For most EEs an optimum temperature exists (King 1986). This optimum temperature is usually significantly higher than the *in situ* temperature range where the enzyme producers live. Isoenzymes (enzymes that have the same function but varied structures) synthesized by different microbes may have distinct optimum temperatures related to the environments in which they function. Studies have found that EEs in Polar Regions have optimum temperatures much lower than the isoenzymes found in temperate and tropical regions (Feller et al. 1996, Huston et al. 2000, Arnosti & Jorgensen 2003), which suggests that distinct bacterial phenotypes with distinct isoenzymes may exist in different oceans. In temperate regions, a shift of dominating isoenzymes may occur along with seasons as the adaption of bacteria communities to temperature change.

Aside from the distinction of isoenzymes with latitude and at different seasons, sudden temperature changes within a short time period (from intraday to a few days) also greatly influence enzyme activities. Different from the other factors that can influence EE performance; the variation of temperatures instantly changes EEA. For example, a sudden temperatures drop of 10 °C could result in an immediate decrease in food supplies to bacteria by about a half to 2/3. How bacteria respond to such a situation is a question that remains unclear and an interesting one to address. In addition, as different EEs have possible different sensitivities to temperature, the changes in temperature result in unsynchronized change in EEAs. To bacteria, this implies a changed proportion of nutrients. Previous studies have also found a different enzyme ratios among different latitudes(Christian & Karl 1995), indicating possible varied nutrient ratio requirements of bacteria at different temperatures. The bacteria's strategies to deal with this potential nutrient imbalance is another interesting question.

In this chapter, two questions are addressed with respect to temperature dependence of organic matter decomposition: a lab incubation experiment to study how microbes respond to sudden temperature change as reflected in extracellular enzyme activities; and a field study on seasonal basis to study the extent to which temperature determines the overall rate of organic polymer hydrolysis.

2. Methods

Sediment samples for incubations were collected in Flax Pond (Long Island, NY) in May, 2011 at intertidal salt marsh zone during low tide. The uppermost 5cm sediments were collected. Ambient temperature during sampling was around 17 °C. Collected samples were incubated at 18°C in lab for 2 days to allow a stable initial condition. Before incubation, sediments were sieved through 1mm sieve and then mixed. Well mixed samples were then filled in separate jars in full and sealed. The net weight of sediment in each jar is ~120 g. Sealed jars were then incubated anaerobically in either water bath (for incubation temperature >18 °C) or incubators (temperature <18 °C). Samples were incubated at 7 different temperatures (2, 7, 13, 19, 22, 26, 29 °C). Fluctuation of incubation temperature during is within ± 1 °C.

Three extracellular enzyme activities (EEA):Leucine-aminopeptidase (LAP), phosphatase (PA), β -glucosidase (BGA) as well as total dissolved CO₂ concentrations and pH were measured at 2 hrs, ~50 hrs and ~100 hrs after incubation started. Procedure for EEA measurements largely followed the one described in Chapter 2 with small modifications specifically designed for this experiment. The measurements were conducted in a N₂ filled hood, a small amount (~0.25 g) of mud from an opened jar was transferred into a 15 ml centrifuge tube. 3 ml of 0.2 μ m pore size pre-filtered pore water was then added into tube. After fully mixing, the tubes containing slurries were then put back into incubators/water bath for ~2 hrs to make the slurry temperature the same as incubator temperature. Fluorophore labeled substrates were then added into each tube and were counted as the start of the measurements. The temperature influence from substrate solution was neglected since its volume is small (<200 μ l) relative to the total solution volume. The

remaining procedures were the same as introduced in Chapter 2. Enzyme activities were measured in duplicate at each temperature. The remaining mud was transferred into a 50 ml centrifuge tube and then centrifuged. Supernatant pore water was collected for dissolved CO₂ measurements.

Field study sediment samples were collected from Great Peconic Bay during 6 cruises from 2009-2010 on a seasonal basis. More details about sampling dates, sites coordinates and sampling methods are described in Chapter 4. Sediments were sliced in the lab at 0.5~2 cm intervals. Activities of three EEs were measured in duplicate. Integrated EEA from surface to 14 cm depths were selected for temperature dependence study as integrated EEAs are a better reflection of overall EEA levels of surface sediments.

The effect of temperature on extracellular enzyme activities was modeled using the integrated form of the Arrhenius equation(Westrich & Berner 1988):

$$EEA = Ae^{-Ea/(RT)}$$

Where Ea is apparent activity energy, T is temperature in kelvin, A is the pre-exponential factor and R is the universal gas constant. Taking the natural logarithm of Arrhenius' equation yields:

$$\ln(EEA) = \frac{-Ea}{R} \frac{1}{T} + \ln(A)$$

The logarithm of EEA has a linear relationship with $1/T$, with slope $-Ea/R$. Activity energy (Ea) for extracellular catalyzed reactions can be calculated by plotting $\ln(EEA)$ versus $1/T$ and determining the slope using least squares regression method. The negative slope times R is equal to Ea .

It should be pointed out that the Ea measured in field studies is different from the definition of Ea in a strict biochemical sense, which by definition is a constant in a well-defined

enzymatic system. In natural bacterial communities, the overall enzymatic reactions are catalyzed by enzymes excreted by a complex consortium of bacteria targeting a variety of substrates. The E_a value calculated therefore is not the activation energy in the chemical sense but a measure of temperature response of the whole microbial community.

3. Results

3.1. *Behavior of LAP standard in pre-deactivated sediments.*

Commercial Leucine Aminopeptidase extracted from porcine kidney (Type IV, from Sigma Co.Ltd) was added in indigenous EEA deactivated mud samples to study the temperature response of single type LAP. Indigenous extracellular enzyme was deactivated by leaving sealed mud samples in boiled water for 20 mins. Pure commercial LAP were then added into deactivated cool sediments and its activity measured at above stated temperatures with results shown in Fig. 3.1 and 3.2. Optimum temperature of standard LAP in mud is around 22 °C but the activities didn't rapidly up to 33 °C. The activation energy (E_a) calculated from activities below 22 is 30.6 kJ/mol (Figure 3.2). The corresponding temperature coefficient Q_{10} is 1.63. These values can be used as references for environmental LAPs.

3.2. *Laboratory incubation*

Activities of three extracellular enzymes together with total CO_2 concentration during incubation are shown in Figure 3.3. Activities of LAP were the highest among three EEs throughout incubation, followed by activities of PA, both were about one magnitude higher than the activity of BGA. During incubation, LAP activities changed towards the opposite directions of BGA and PA changes at most temperatures. LAP activities decreased at temperatures >12 °C (Figure 3.3) but increased slightly at the two low temperatures (2 and 7 °C). In contrast, activities of BAG and PA at mid and high temperatures increased during the first 2 days and the activities at low temperatures decreased throughout incubation. Table 3.1 listed percentage change of activities at day 3 and day 5 compared with day 1. Higher percentage changes occurred at high

temperatures. For example, a decrease of 28-50 % of LAP activities were observed after 4 days' incubation. Activity of BGA at 29 °C increased by 34 % in 2 days and then decreased by 38 % after another 2 days.

Temperature sensitivity curves ($\ln(\text{EEA})$ vs $1/T$) of LAP, PA and BGA at the beginning of incubation (day 1) are plotted in Figure 3.4. Significant linear relationships were found between $\ln(\text{EEA})$ and reciprocal of temperatures ($1/K \cdot 10^3$) for all 3 enzymes. Activation energies (EA) of each EE were calculated from slopes of each curve. The value sequence of Ea is $\text{LAP} > \text{BGA} > \text{PA}$.

Temperature sensitivity curves of EEA at day 3 are plotted in Fig 3.5. $\ln(\text{EEA})$ and $1/T$ remained clear linear relationships for all three enzymes. However, the values of Ea changed significantly. A decrease of Ea for LAP and increases of EA for BGA and AP were observed (Table 3.2).

Temperature sensitivity curves at day 5 are shown in Fig 3.6. Different from the curves at day1 and day3, for all three enzymes, the curves at day 5 showed a two stages pattern: with stage 1, the 4 high temperatures and stage 2 the three low temperatures. Ea values calculated from each stage are also showed in Table 3.2. Ea values of stage 1 had the highest value over incubation for BGA and PA. . The Ea values calculated from all points were also calculated, which showed a continued decrease of Ea for LAP and an intermediate Ea for BGA and PA (Table 3.2).

3.3. *Seasonal temperature dependence of field sample EEA in great Peconic Bay*

The natural log of depth integrated (0-14 cm) surface sediment EEAs plotted versus sediment surface temperatures at sampling dates are shown in Fig 3.8. EEAs at two adjacent (sites map in Chapter 4, both sites are muddy sediments) are plotted together. For all three enzymes, activities at the lowest temperature (open circle) deviated from other seasons. If the EEA value obtained from that season is removed, integrated EEAs showed pretty good linear relationship with sampling temperatures. LAP has the best fit with temperature ($R^2=0.88$). The Ea values are 35.1 kJ/mol for LAP, 28.5 kJ/mol for PA, 25.5 kJ/mol for BGA respectively.

4. Discussion

4.1. *Temperature optimum*

The optimum temperature (T_{opt}) of commercial Leu-AMP standard (Sigma Co.Ltd) in pre-deactivated sediment is ~ 22 °C. This optimum temperature is significantly lower than the 37 °C claimed on the product sheet, which describes an activity at 25 °C to be ~ 60 % of that at 37 °C. This unexpected T_{opt} indicates that the optimum temperature of an enzyme may vary when functioning in different environments. Differing ion concentrations, pH, dissolved trace metals or adsorption of enzymes might be the reasons that cause T_{opt} to shift. This shifted T_{opt} may also imply that muddy sediment may play an important role in determining the rates and properties of enzyme reactions.

For indigenous EEs, no temperature optimum was observed within incubation temperature range, indicating a temperature optimum higher than 29 °C. This is consistent with the general observations that optimum temperatures of natural EEs were normally above *in situ* temperatures (King 1986, Christian & Karl 1995, Arnosti et al. 1998).

To put the results together, it is unexpected that the enzyme extracted from the kidney of a warm-blooded animal (37 °C) has a T_{opt} of 22 °C in sediment, whereas the sediment indigenous EEs, which never function at temperatures >30 °C, have T_{opts} apparently higher than that. Such results imply complex regulation mechanisms in natural environments. No specific properties should be assumed *a priori*.

4.2. *EEA change during short-term incubation at varied temperatures.*

As shown in Fig3.4, an interesting result of this experiment is that the activities of three EEs apparently changed along different directions during incubation. Activities of LAP decreased at high temperatures (> 12 °C) but increased at low temperatures (2 and 6 °C). In

contrast, activities of PA and BGA at high temperatures increased in the first 2 days of incubation, whereas activities at low temperatures decreased during incubation. Such varied patterns resulted in increased LAP/BGA (and LAP/PA) activity ratio at low temperatures and decreased LAP/BGA at high temperatures. It should also be pointed out that the BGA activity has been doubled just by increasing temperature from 19 °C to 29 °C, but an increase in BGA activity was still observed after 2 days incubation. To the contrary, though the BGA activities had decreased by >50% just by moving sediments from 19 °C to 2 and 6 °C, the BGA activities at these two temperatures kept on decreasing after incubation.

These observed patterns showed that bacteria respond rapidly to temperature change by changing the EE synthesis ratios. The general pattern is that, when temperature increases, the increase in organic carbon and phosphate demand of bacteria surpass the increments that BGA and PA activities could supply, even though the BGA and PA activities double from 19 to 29 °C, but the increase in N demand with increased temperature is within the capacity that LAP could accommodate. A study by (Christian & Karl 1995) observed a much higher LAP /BGA in polar regions than in temperate and equator regions. A likely explanation of such different organic C (or P) /N demands at different temperatures may be that, at high temperatures, microbes have higher respiratory and metabolism rates thereby consuming a higher proportion of organic carbon, while at low temperatures, microbes may have a relatively high amino acid demand to synthesize structural proteins to withstand low temperatures.

Another possible explanation is the artifact effects from sample processing. The sieving and mixing process redistributed organic matter and therefore increased organic matter availability for bacteria. The sieving process also removes benthic fauna and alleviate grazing pressures for bacteria. These effects all favor bacteria growth and can explain the rapid increases of (at temperatures >12 °C) in the first 2 days' incubations but then decreased as the benefits had been used up after 2 days. Similar patterns have also been used up after 2 days. Similar patterns had also been reported by (Boetius & Lochte 1994) in an organic carbon enrichment incubation.

However, this explanation doesn't work for LAP, as the LAP activities changed in the opposite direction as BAG and PA did.

The more rapid depletion of a labile protein pool might explain the LAP pattern. Even though the entire pool of protein may take a long time to degrade (Dell'Anno et al. 2000) because of strong irreversible adsorption of proteins (Ding & Henrichs 2002) (Borch & Kirchman 1999), the labile peptides are found being rapidly hydrolyzed (Pantoja & Lee 1999), with a turnover rate as small as an hour. Quick depletion of labile peptides and a relatively long lifetime of adsorbed proteins may force bacteria to look for alternative sources of amino acids. Bacteria are capable of synthesizing amino acids from ammonium and intermediate products of glycolytic pathways. Because the incubation was performed in sealed jars, the exchange of sediment with overlying water was shut off, resulting in accumulated ammonium. Flax pond sediment has also been reported to have a relatively high organic carbon content (Liu & Lee 2007). These effects altogether may stimulate *de novo* synthesis of amino acid by bacteria to alleviate the nitrogen demands. This hypothesis, though less robust, can also explain the varied enzyme ratios at different temperatures. At high temperatures, the labile peptide pool was depleted more rapidly so that bacteria are forced to produce additional BGA for amino acid synthesis from organic carbon compounds and ammonium. At low temperatures, the labile peptide pool may last longer so that bacteria still synthesize peptidase for N demands. The experiment design of this study is unable to differentiate which reason plays a central role, future studies are required to better explain the mechanisms.

4.3. *Activation energy change during short period incubation*

Activation energy (E_a) is a measure of the energy barrier that enzymes need to overcome in order to complete the hydrolysis reaction. It is thus also a measure of the temperature sensitivity of enzymes. A higher E_a indicates a more rapid activity change with temperature and represents a higher temperature sensitivity of the enzyme. According to the Arrhenius equation, values of E_a can be calculated by plotting EEA with temperature. Figure 3.4 showed the EEA

and temperature relationships at the start of incubation. At the start of an incubation bacteria were not left time to respond to temperature, these curves largely reflect the temperature sensitivity of *in situ* EEs. Curves of all three enzymes showed linearity. The values of E_a were calculated from curves and have the sequence of E_a LAP > BGA > AP. It is interesting that LAP had the highest E_a yet at the same time the highest activity, which may indicate a much higher standing stock of LAP than the other 2 enzymes. LAP has generally been considered as a constitutive EE because amino acids are the materials to synthesize all EEs. It is probably a fundamental strategy for bacteria to keep a considerable peptidase level though not necessarily at high efficiency.

After two days incubation, the E_a values changed significantly for all three enzymes (Figure 3.5). Compared with the E_a values at day 1, the E_a value of LAP decreased and that of BGA and PA increased, reflecting bacteria responses to temperature change in two days. Based on the definition of E_a , such a shift of E_a should be the consequence of enzyme composition change as different isoenzymes may have distinct E_a values. Such a conclusion is based on a prerequisite that the enzyme concentrations at each temperature are the same. In this study, however, the EE concentrations at different incubation temperatures were unlikely to remain the same after two days incubations, as the result of either different EE synthesis rate or bacteria growth rate or both. The change of E_a may also be caused by different enzyme concentration at different incubation temperatures.

Though both reasons might be possible, the perfect linearity of the curves at day 3 implies that an enzyme constitution shift might not be the reason for E_a change. If an isoenzyme shift occurred at either temperature or both, since different isoenzymes usually have different E_a values, it is unlikely the curve would still keep a good linearity, but should show a multi-stage pattern.

The E_a on day 5 (Fig. 3.6), however, the curves showed two stages patterns for all three enzymes. A hypothesis here is that 2 days after a temperature change, a shift of community

structure (or a shift of dominant isoenzymes at some temperatures) may lead to the curve deviating from a perfect linearity.

4.4. *A simplified model to estimate the cost for EE production at different temperatures.*

During incubation, the net change of EEA is the outcome of EEA of new synthesized enzymes minus lost EEA due to enzyme decay. The incubation results have shown that bacteria changed their enzyme production rate as a response to temperature change. A hypothetical model is proposed here to estimate the relative cost for EE production at different temperatures. The general equation of this model is as following:

$$\text{EEA change (in \% /d)} = \text{New EEA (\% /d)} - \text{Lost EEA (\% /d)}.$$

In this model, EEA change is the daily change of EEA during incubation, which can be calculated from measured EEAs at different days. The new EEA represents EEAs of new produced EEs during incubation and lost EEA represents the decrease of EEA due to enzyme decay. The rate of EEA loss at °C is estimated from literatures and the results of this experiment to be 30% per day. The decay rate at other temperatures was adjusted according to the LAP temperature dependence plot at day1 (Figure 3.4). The temperature dependence of LAP activity is used because peptidases are supposed to be the enzymes that decompose proteins. The new EEA is the net change of EEA plus EEA lost. To make the result comparable between temperatures, new EEA was calculated as percentage increase compared to the EEA at day 1.

The calculated rate results are shown in Fig 3.7. The 2-50 hrs curves (first 2 days incubation) showed a clear pattern that bacteria tend to increase peptidase production when they were put in temperatures lower than in *situ* temperature, the extent of increase is proportional to temperature decrease; but they tend to keep a relatively stable peptidase production when put in higher temperatures. In contrast, bacteria selected to keep their phosphatase and gluocosidase production at a stable level when put to lower temperatures but increase the production of these two enzymes at higher temperatures. Such results further confirm that bacteria respond

differently in the productivities of different extracellular enzymes, which indicate a varied C/N and N/P demands at different temperatures.

4.5. Seasonal EEA patterns from field sample measurements.

Despite a rapid short term response of EEA to temperature change, the seasonal patterns of all 3 EEA, when plotted with field temperatures, all had good linear relationships. The fit of integrated EEA from different seasons in the Ea curve demonstrated that temperature accounted for most of the annual variation in sediment EEA. In other words, after normalizing EEA of all seasons to the same temperature, EEA is at a stable level throughout the year. This may imply that microbes in temperate regions tend to keep a relatively stable EE level despite temperature variation. With the exception of the spring bloom pulse, the enzyme activity variation along with temperature changes seems to be enough to deal with the different OM supplies with season. This phenomenon also implies that high molecular weight organic matter hydrolysis is a rapid process in Peconic Bay sediments rather than being a limiting step in OC remineralization. During the spring bloom period (Feb – Mar), however, labile substrate deposition enhances EEA above that expected from T variation alone and lowers the estimated Ea derived from a simple plot of all EEA measurements versus $1/T$ over the annual period. The mechanism for net enhancement of EEA is either stimulated EE synthesis or a shift of EE to a low Ea isoenzyme or both.

5. Conclusion

The EEA patterns during incubation showed a rapid response of bacteria to temperature change. Bacteria synthesized varied amounts of EEs at different temperatures. At high temperatures, the microbes tend to require an increased organic carbon/phosphate demand but the increase in N demand is within the capacity that LAP could accommodate. At low temperatures, however, bacteria tend to produce more peptidase but require less phosphatase and gluocosidase.

Temperature sensitivity curves show that the initial response of the bacteria community to temperature change is always to alter their yield of EE. With longer exposure to a temperature change, community structure may alter or a succession of isoenzymes may occur shortly after a temperature shift.

The long time scale temperature dependence, as reflected the seasonal observations of EEA in Great Peconic Bay sediment, however, showed that bacteria communities seem to be insensitive to long time scale temperature changes. They chose to keep a relatively stable EE level that can apparently accommodate varied OM supplies in different seasons.

Table 3.1 pH and percentage activity changes of three EEs during incubation. The initial pH on day 1 is 7.10

Temperature	LAP		PA		BGA		pH	
	Day 3	Day 5	Day 3	Day 5	Day 3	Day 5	Day 3	Day 5
2	17.3	14.1	-6.9	-16.5	-9.1	-23.1	6.55	6.92
6.8	4.4	-4.2	0.3	-12.4	3.9	-10.2	6.49	6.91
12.7	-4.7	-28.0	2.3	-33.9	32.2	-7.1	6.49	6.80
19.2	-25.6	-38.0	8.7	-20.7	30.1	0.5	6.44	6.76
22.3	-26.2	-45.5	17.7	-9.5	6.9	-9.4	6.38	6.71
25.8	-18.3	-45.2	28.1	-6.2	10.5	-13.8	6.41	6.71
28.5	-22.1	-49.5	34.2	-7.0	33.9	-4.5	6.47	6.77

Table 3.2 Activation energies (Ea) of three EEs at different days. The Ea values at day 5 were calculated for all temperatures and two temperature stages (as shown in Fig. 3.6) respectively.

Activation Energy(Ea)	Day1	Day3	Day5	Day5	Day5
LAP	49.2	39.1	28.6	40.5	22.1
PA	26.7	36.7	30.6	45.6	21.5
BGA	40.0	47.3	44.2	56.0	40.3

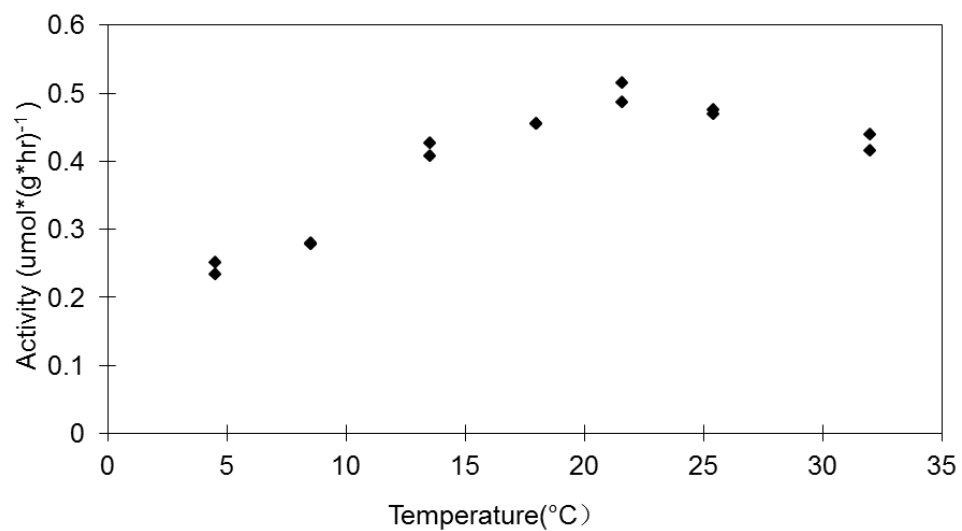


Figure 3.1. Temperature dependence of activities of LAP(Leucine-Aminopeptidase) standards added in deactivated sediments.

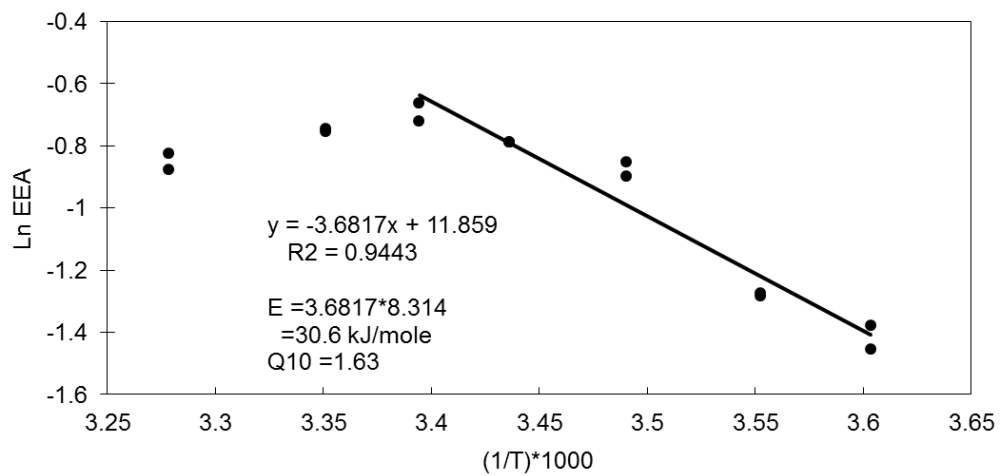


Figure 3.2. The Ln(EEA) vs 1/T curve of standard LAP added in deactivated sediments. Activation energy (Ea) and Q10 were calculated from the slope of the regression line.

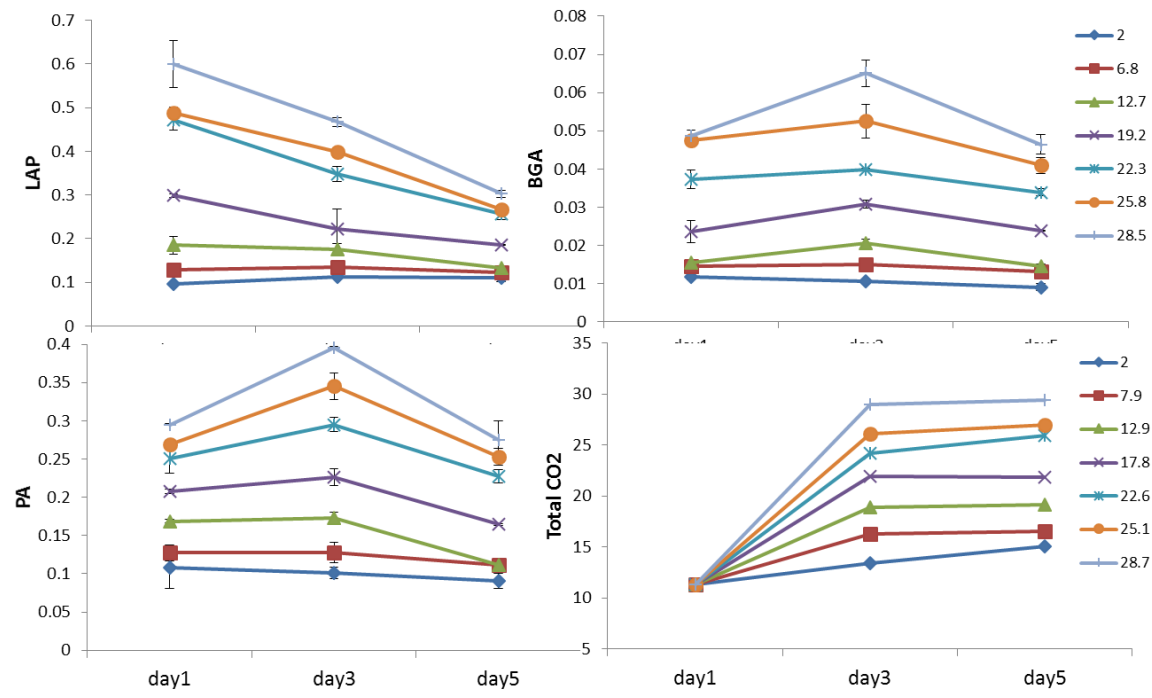


Figure 3.3. Change of activities of three EEs (LAP, PA and BGA) and Total CO₂ during 4 days incubation

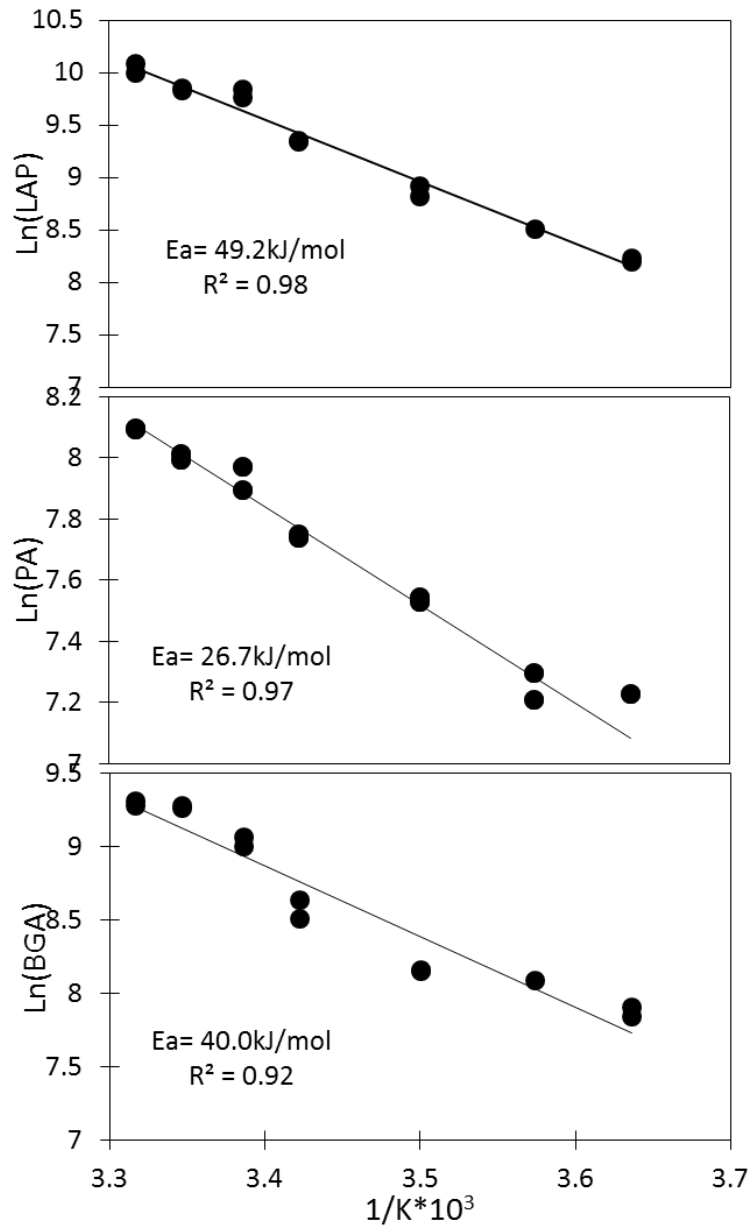


Figure 3.4. Temperature sensitivity curves of three EEs on Day 1

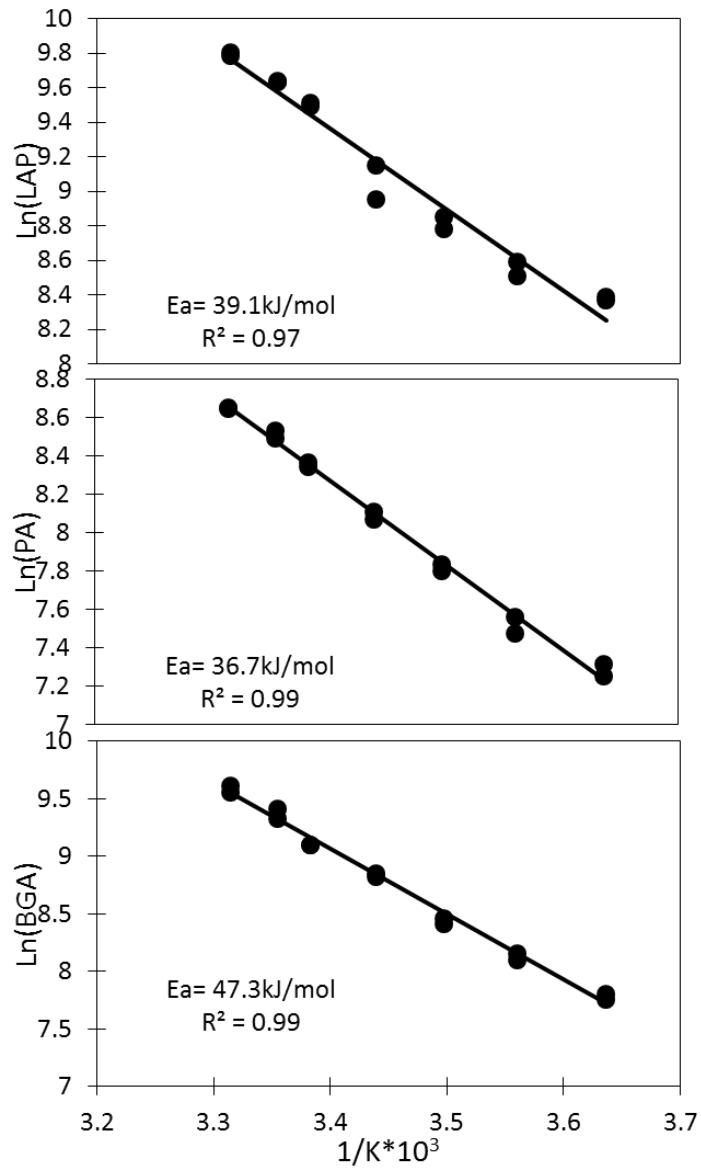


Figure 3.5. Temperature sensitivity curves of three EEs on Day 3

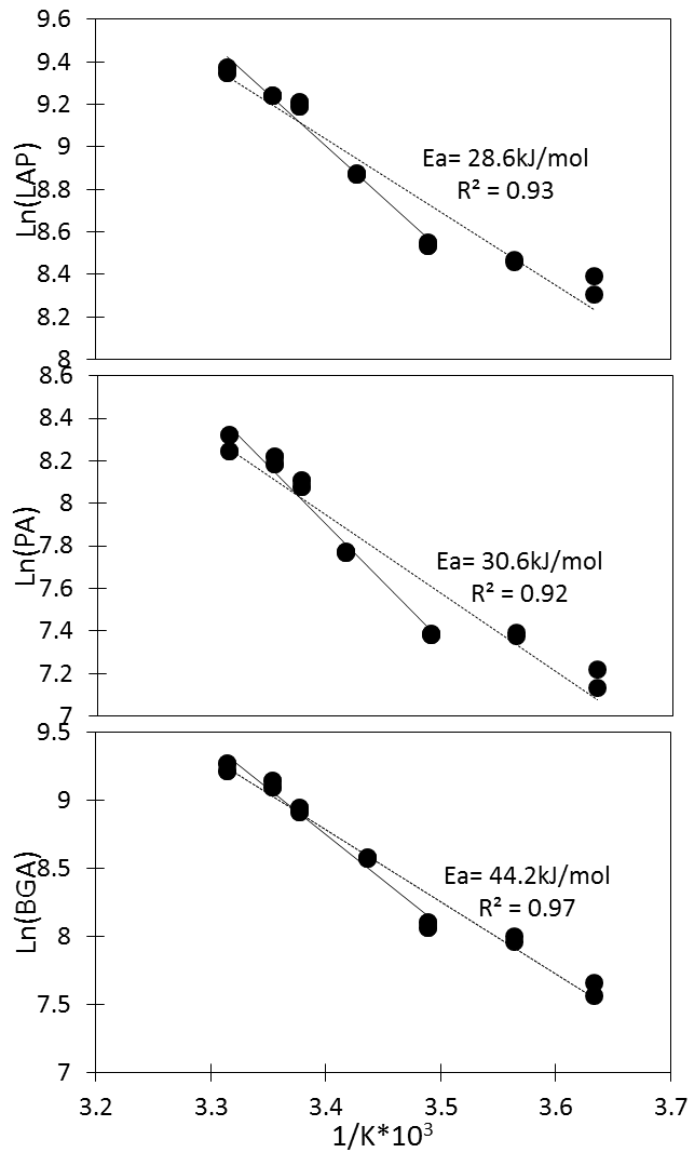


Figure 3.6. Temperature sensitivity curves of three EEs on Day 5

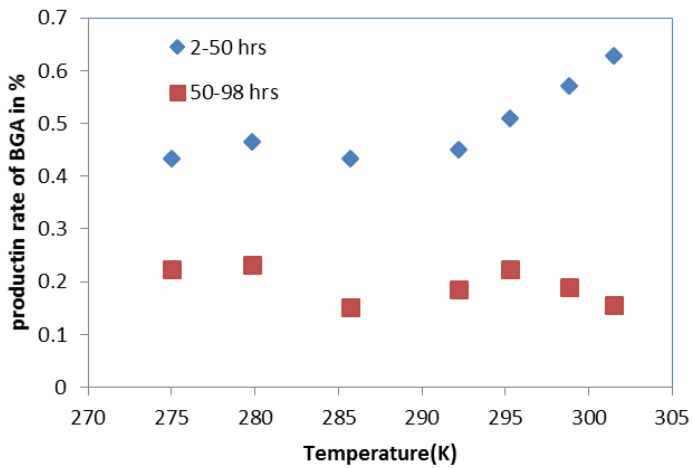
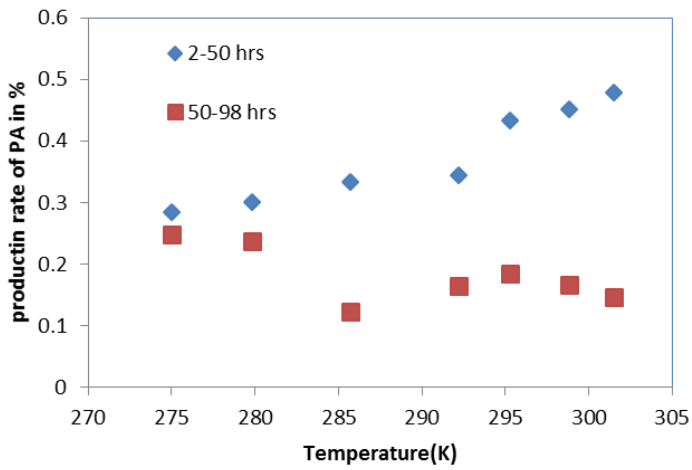
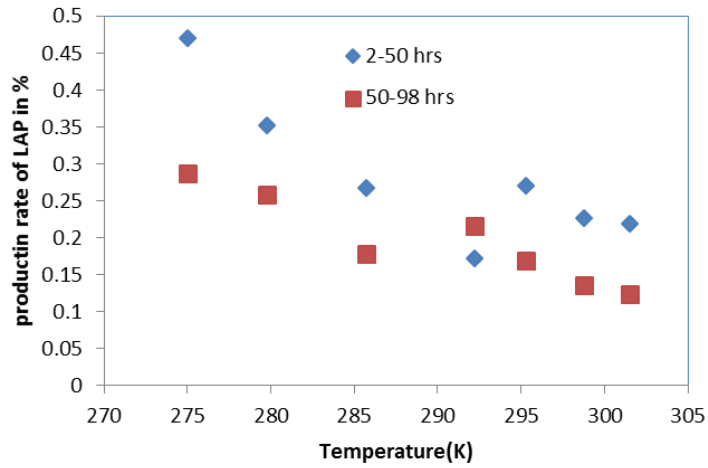


Figure 3.7. Percentage new produced (%*d⁻¹) of three EEs at different temperatures compared to the respective activities on day 1 during incubation

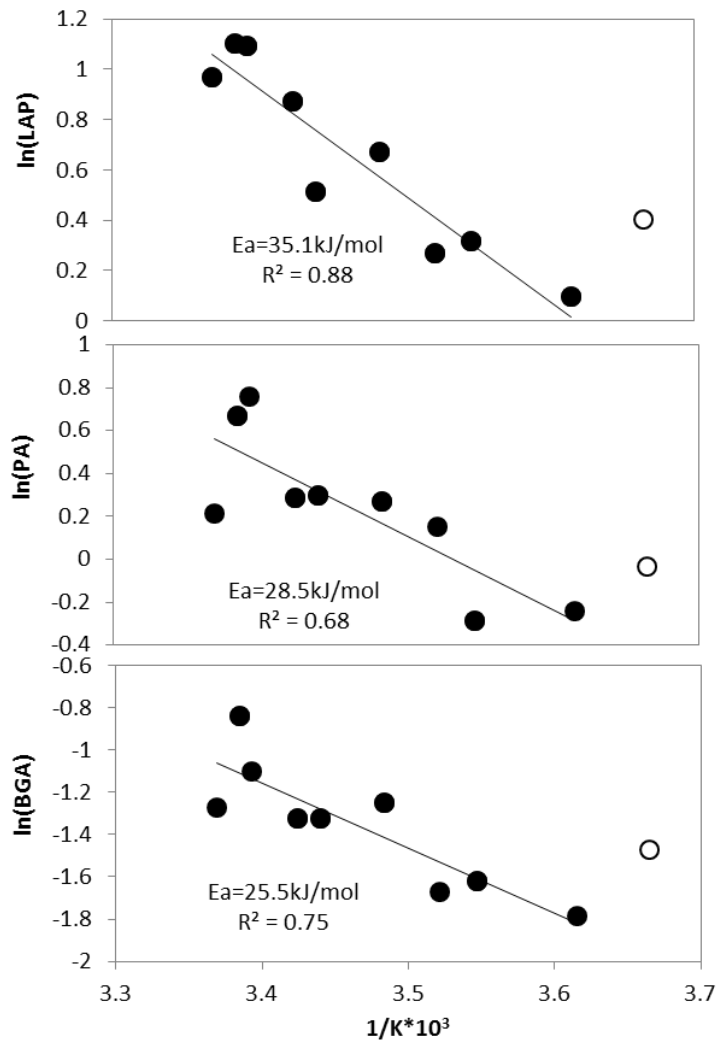


Figure 3.8 Temperature sensitivity curves of three EEAs of Peconic Bay sediments. EEAs were 0-12 cm integrated activities. Temperatures are *in situ* temperatures.

Chapter 4 Seasonal, 2-D sedimentary extracellular enzyme activities and controlling processes in Great Peconic Bay, Long Island

1. Introduction

In most marine ecosystems, a large portion of the energy and nutrient flow is channeled through the microbial community. The recycling of organic matter starts with the consumption and degradation of detrital organic carbon by a diverse community of heterotrophic microorganisms. Due to the limitation in transport, however, microbes cannot assimilate molecules larger than ~600 Da (Weiss et al. 1991). High molecular weight organic materials must be fragmented by extracellular enzymes (EE) before being incorporated into the cell. EE catalyzed hydrolysis is thus a crucial initial step in organic matter remineralization (Arnosti et al. 1994, Burdige & Gardner 1998). Understanding rates of extracellular enzymatic activity (EEA) as well as the factors that control enzyme production, performance and distribution are essential to carbon cycling budgeting in marine ecosystems (Boetius & Lochte 1994, Arnosti 2011). As such, a number of studies of EEA and controlling mechanisms have been conducted over the past decades in a wide range of marine environments from tropical to polar regions (Chrost 1991, Hoppe et al. 2002, Arnosti 2011), and the water columns (Huston & Deming 2002, Hoppe 2003, Baltar et al. 2009) and sediments (Meyer-Reil 1986, Mayer 1989, Boetius & Lochte 1994). Compared to the water column, there are far fewer investigations of EEA in sediments (Arnosti 2011), despite the fact that EEA in sediments is typically two to three orders of magnitude higher than in the water column (Hoppe et al. 2002). This disparity is mainly due to the physical and chemical complexity of the sediment matrix, making the EEA measurement process more complicated and thus more problematic. Traditional methods typically involve dilution of sediment with seawater into slurries which destroys the physical structure of the sediment and leads to potential overestimation of EEA. New techniques with fewer artifacts are required for accurate sediment EEA studies (Arnosti 1995).

In addition, surface sediments, especially those underlying oxygenated waters, normally display greater small scale (mm to cm) spatial and temporal heterogeneity. Organic rich, surface sediment typically possesses sharp vertical gradients of O₂, pCO₂, labile organic substrates and other biogeochemical properties as the consequence of early diagenetic reactions. Furthermore,

the activities of benthic organisms create a complex, three-dimensional mosaic of redox zones and labile substrates that make sediment heterogeneity much greater than in seawater (Aller 1994, Hulthe et al. 1998, Papaspyrou et al. 2006). Understanding the influence of such small scale heterogeneity on organic matter distribution and decomposition is fundamental for the more accurate estimation carbon flux through surface sediments. Traditional EEA measurement techniques, however, are incapable of characterizing the distributions of reactions at high resolution.

Over the past ten years, planar optical sensors have been applied to quantify chemical distributions in marine sediment with high spatial and temporal resolution, and have documented significant small-scale heterogeneities (Glud et al. 1996, Glud et al. 2001, Wenzhofer & Glud 2004, Zhu et al. 2005, 2006, Glud 2008, Glud et al. 2009). For example, Zhu et al. (2006) used a two-dimensional planar fluorosensor to study sediment $p\text{CO}_2$ distributions in bioturbated sediment, revealing heterogeneity at the submillimeter scale. Glud (2008) applied continuous O_2 imaging showing that short-lived anoxic microniches developed during the degradation of 1-2 mm size diatom aggregates within zones of oxic sediment. Such small scale patterns and events are normally impossible to capture by traditional measurements, but were revealed by planar sensors. A novel thin-layer foil for a planar optical sensor was also recently developed to resolve heterogeneous patterns of EEA in sediments (Cao et al. 2011). This new system is capable of imaging two dimensional distribution of sediment EEA with fewer artifacts than traditional techniques. The output of this planar sensor reveals real-time proteolytic enzyme activity patterns at high resolutions (~50-100 μm). Substantial heterogeneity and millimeter scale “hot spots” of EEA have been observed using this sensor system. In the present study, this 2-D enzyme sensor system was used to investigate seasonal EEA patterns of Leucine aminopeptidase at two subtidal muddy sediment sites in Great Peconic Bay, an estuarine environment on the eastern end of Long Island, New York. EEAs (aminopeptidase, β -glucosidase, and phosphatase) were also measured by traditional incubation techniques for comparison. The underlying hypothesis was that EEA distributions would track seasonal patterns in temperature (general

metabolic activity), substrate supply (nutrient remineralization rates), and macrofaunal activity (particle reworking patterns); measurements of which were made at the same sites and time.

2. Materials and Methods

2.1. Study site and sampling

Sediment samples were collected seasonally at two sites in Great Peconic Bay (Figure 4.1) during 7 cruises spanning the period from spring 2009 to fall 2010. Great Peconic Bay is part of the Peconic estuary system, which is situated between the North and South Fork at the east end of Long Island, NY (USA). It is a shallow (<9 m), well-mixed tidal estuarine basin with little or no seasonal stratification. Circulation is dominated by tidal effects which are much greater than freshwater inputs. Salinities are in the range of 25 ‰ 28 and temperature varies seasonally from -1 to 28 °C. Site 1 (40° 56.055'N, 72° 29.887'W) is located at the center of the Bay and had a water depth of (~7 m). Site 2 (40°57.298'N, 72°29.983'W) is to the north of site 1 and had the same water depth (~7 m). Both sites are characterized by fine grain muddy bottoms (Katuna 1974). Samples from sites 1 and 2 were collected each season during the period from July 2009 to June 2010. Sediment samples were collected using acrylic box corers (dimensions = 30 × 12.5 × 30 cm) by scuba divers. Cores were stored in containers filled with unfiltered sea water from the sampling site, both on board and during transportation to the laboratory. After reaching the laboratory, cores were immediately stored in a cold room at in situ temperature. EEA analysis and supporting measurements were conducted within 24 hours after sampling. Pore water depth profiles of NH_4^+ , NO_3^- , ΣCO_2 , PO_4^{3-} were measured and anoxic incubations were set-up in the laboratory to estimate respective solute production or consumption rates within 24 hours of sampling. Sediment bacterial abundances were documented during two seasons (fall 2009 and winter 2009-2010) at both sites.

2.2. Pore water analyses and bacteria counts

Sediment cores were sectioned rapidly at 1 – 3 cm vertical intervals. The sampled intervals were transferred with minimal exposure to air (seconds) into centrifuge bottles continuously purged with N₂. The sediment was centrifuged under N₂, and the supernatant pore water was sucked into syringes (no gas head space) and filtered through 0.2 μm polysulfone inline filters. We have found this procedure, when carried out rapidly, to produce analytical results indistinguishable from cores handled exclusively within a N₂-filled glove bag. Pore water was analyzed for ΣCO₂ within 24 hours of collection by the flow injection analysis with conductivity detection (Aller & Mackin 1989, Hall & Aller 1992). Pore water samples for NH₄⁺ and NO₃⁻ analyses were frozen immediately after filtering, and samples for reactive PO₄³⁻ analysis were acidified before later measurements. Nutrients were analyzed by colorimetric methods modified for a 96-well microplate reader (NH₄⁺ (Solorzano 1969); NO₃⁻/NO₂⁻ (Miranda et al. 2001, Doane & Horwath 2003); PO₄³⁻ (Presley 1971)). Sediment porosity was estimated from wet – dry weights assuming a solid phase density of 2.6 g cm⁻³. Production estimates for ΣCO₂ and NH₄⁺ were derived from serial anoxic incubations of 18 cm long whole cores that were incubated in sealed glass tubes and kept in oxygen-free, impermeable bags over 1 - 4 weeks (Aller & Mackin 1989); (Waugh, et al., in prep.). Epifluorescence direct counts of bacteria were made following staining with acridine orange after Hobbie et al. (1977) and Watson et al. (1977).

2.3. EEA measured by traditional incubation methods

The activities of three extracellular enzymes were measured in homogenized intervals of sediment: β-glucosidase (BG), Leucine-aminopeptidase (LAP), and phosphatase (PA), corresponding to the decomposition of organic C, N, P substrates respectively. The procedure generally followed Hoppe (1983) with minor modifications (Aller & Aller 1998). Briefly, sediment cores were subcored using a small butyrate tube (O.D. = 7.5 cm). The subcored sediment was extruded and sliced at 0.5 ± 2 cm intervals, with thinner intervals near the top of the core. Sediment layers were quickly transferred into 50-ml centrifuge tubes filled with N₂ gas. Tubes were then transferred to a N₂ filled anaerobic chamber, where the sediment in each tube was well mixed by hand and after which about 0.6 g of sediment was transferred into 15-ml

centrifuge tubes. The sediment in each 15-ml centrifuge tube was slurried by adding 5.0 ml of 0.2 μm pore size filtered deoxygenated sea water. Specific fluorogenic substrates were then added, and the tubes were incubated for one hour with continuous shaking in the dark at the temperatures of core collection ($T = 0$ to 24). The extracellular enzyme kinetic parameters (V_{max} and K_m) were measured in two summer seasons that had relatively high activity levels. The final concentration of each fluorogenic substrate added to slurries was determined based on V_{max} and K_m , respectively. These final concentrations are: L-leucine 7-amido-4- methylcoumarin hydrochloride (Leu-MCA) 1.6 mM, 4-methylumbelliferyl glucoside (MUF-G) 1.0 mM and 4-methylumbelliferyl phosphate (MUF-P) 1.8 mM. Incubations were stopped by adding 5.0 ml pH 10.5 glycine buffer for MUF based substrates or 5.0 ml of 30% acetone for MCA based substrates (Belanger et al. 1997). Mixtures were then centrifuged at 4500 rpm for 15 min, and the supernatants were then filtered through 0.2 μm pore size polysulfone filters. Fluorescence was measured at 450 nm (with excitation 365 nm) for MUF or at 440 nm (with excitation 360 nm) for MCA using a Hitachi F-4500 fluorescence spectrophotometer. All samples were measured in duplicate, and one control (boiled sediment) was also incubated to correct for background fluorescence and for abiotic cleavage of the artificial substrates. Potential background interference by organic detritus in sediment as discussed by Arnosti (2011) was found to be negligible after filtration. Control measurements showed very low fluorescent signals at all times for BG and LAP. For PA, however, substrate MUF-P was found to undergo slow but steady hydrolyzation even in enzyme deactivated sediment (boiled or microwaved). To our knowledge, no similar phenomenon has been reported previously, and the exact mechanism that causes such abiotic hydrolysis remains unclear, but it is certainly worthy of attention for those utilizing MUF-P in sediment. In our current study, fluorescence signals from MUF-P were corrected by subtraction of background rates measured in boiled sediment controls. Photobleaching of MUF is not a problem in our sensing system.

2.4. EEA Controlled-release foil sensing system

Our planar sensing system is based on the controlled release of a fluorogenic substrate from a thin hydrogel membrane (hydromed D4) into contacting sediment interface, while the resulting fluorescence generated by enzyme hydrolysis is monitored over time. The sensor foils, which in this application utilize Leu-MCA as substrate, reveal in situ, real-time proteolytic enzyme (Leucine-aminopeptidase) activity patterns across the planar surface at high spatial resolution (~50–100 μm). Leu-MCA was chosen because of the importance of proteolytic enzymes in organic matter decomposition and because the fluorescence response of the fluorophore MCA is independent of pH within the range normally expected in marine sediments. Because the sensor foils are transparent, enzyme activity patterns can be related directly to visible physical and biological structures in bioturbated sediments, optimizing our ability to interpret the relationship of bacterial activities to sedimentary structure. Details about membrane preparation and performance are described in Cao et al. (2011).

2.5. Instrumentation and deployment

A schematic drawing of the optical system for 2-D Leucine-Aminopeptidase (LAP) activity measurements is shown in Figure 4.2. The sensor membrane is deployed in a manner similar to other planar sensors: a thin foil with the enzyme substrate is inserted vertically several centimeters (usually ~ 10 cm) into sediment or placed horizontally onto a sediment surface. In both cases images were taken perpendicularly to the plane of the sensor foil. A companion foil that is prepared the same as sensor foil but contains fluorophore MCA instead of substrate (Leu-MCA) was used to correct for diffusive loss of fluorescence signal out of the image plane (Cao et al. 2011). Images were obtained with a theoretical pixel resolution of $50 \times 50 \mu\text{m}$. To further avoid reflected light, the fluorescence image was recorded with excitation light at an angle of incidence of ~ 30° and emission at 90° to the target plane. Images were taken at one minute intervals over a 45-90 minute period. Captured images were analyzed with Image-Pro Plus (version 4.1) and Matlab (version 7.0.4). More details about sensor deployment and calculations are described elsewhere (Cao et al. 2011).

3. Results

3.1. Nutrients and Environmental parameters

Depth integrated nutrient inventories over the top 15 cm as well as depth integrated production rates of ΣCO_2 and NH_4^+ at each season for both sampling sites, are shown in Table 4.1 (detailed data from Waugh et al., in preparation). The net NH_4^+ production rates measured with incubations were corrected for reversible adsorption assuming an adsorption coefficient of 1.3 (Mackin & Aller 1984). Nutrient concentrations are of the same magnitude at the two sampling sites and have similar patterns of seasonal variation. For both sites, lower nutrient concentrations occurred in winter and higher concentrations in summer and fall. Dissolved N/P ratios ranged from 1.7 to 16.3, lower than the canonical Redfield ratio of 16/1 in most seasons (assuming quasi-steady state at sampling time). Ratios of N/P were lower in summer and spring for both sites (1.6-3.2), compared with significantly higher ratios (5.1-16.3) in fall and winter. Production rates of ΣCO_2 and NH_4^+ also showed varied organic carbon and nitrogen decomposition rates over seasons. Production rates were higher in spring and summer ($> 5\%$) than in fall and winter.

3.2. Seasonal patterns of EEA

Activities of three extracellular enzymes β -glucosidase (BG), leucine aminopeptidase (LAP) and phosphatase (PA) were measured by traditional incubation techniques (slurries). Vertically integrated activities (0-12 cm) are shown as bar graphs in Figure 4.3. Also plotted is the percentage of EEA in the top 2 cm for depth integrated values. The relative magnitudes of activities of the three enzymes is $\text{LAP} > \text{PA} > \text{BG}$, consistent with most previous studies of coastal sediment EEA (Poremba & Hoppe 1995). All three enzymes showed similar seasonal patterns with EEA lowest in winter, beginning to increase during early spring, peaking in summer, and then gradually decreasing. Site 1 has higher enzyme activities than site 2 among all series except in May 2010, when EEA of all three enzymes was higher at site 2. BG has a higher proportion of its activity in the top 2 cm of sediment than the other 2 enzymes.

3.3. Bacterial abundance

Bacterial abundances were several times higher in winter than in the fall, in spite of much lower nutrient concentrations, decomposition rates, and EEA during that season (Figure 4.4, Table 4.1). While bacterial abundances generally decreased with increased depth in the sediment, in winter a subsurface (3-6 cm) maximum region was found at both sites.

3.4. 2-D Enzyme activity distribution patterns

Seasonal enzyme activity distributions of surface sediment at site 1 are shown in Figure 4.5. Enzyme activities in individual pixels were converted to pseudo-color images which readily show both horizontal and vertical heterogeneities of enzyme activities.

A clear seasonal variation can be observed in the seasonal LAP profiles at site 1, between April 2009 and May 2010 (Figure 4.5). Late spring and summer (May – July) had much higher overall EEA than fall - winter and early spring at all depths. In April, 2009, maximum values were generally found between 0.5-1 cm depths. A relatively continuous layer with high values was apparent at around 0.5 cm depth and isolated microzones of elevated activity, termed hot spots, were found at about 1 cm depth. The activities decreased rapidly with depth and showed less horizontal heterogeneity in deeper sediment layers. EEA was generally higher EEA at all sampled depths in July than in April, although the zone of maximal activity still occurred within the top 2 cm. Fluorescence signals on the left bottom part of the sensor foil were blocked by sediment particles accidentally penetrating the space between the membrane and core wall, and this area was excluded from calculations. In the fall, the overall EEA magnitudes are comparable with those in April, however, the spatial distribution is quite different. The 2-D EEA image in the fall (October) lacks a downward gradient and thus shows more vertical homogeneity. The surface EEA in the fall is lower than in April, while EEA in deeper sediment is higher than in April. From fall to late winter, vertical gradients became more distinctive as the EEA at the sediment surface increased and the EEA in the deeper regions decreased. The maximum EEA in surface sediment during February corresponded to deposition of planktonic debris from the late

winter - spring bloom. From winter to late spring (Feb to May), EEA gradually increased throughout the upper ~ 10 cm of the deposit. The EEA in deeper sediment during May, though much lower than that in surface maximum zone, is much higher than that at the same depth in February.

Seasonal enzyme activity distributions at site 2 are shown in Figure 4.6. Generally site 2 and 1 showed similar seasonal EEA distribution patterns. In addition, two burrow structures were captured in summer and fall samples at site 2. EEA was low in the water-filled burrow centers but was enhanced in immediately surrounding sediment. An early spring bloom occurred during late winter sampling (March). Phytoplankton detritus deposited from the late winter - spring bloom formed a fluffy layer with a thickness of ~2 cm on surface sediment. EEA was greatly enhanced in this layer. Below the fluff layer, EEA remained at the low activity more typical of winter. The EEA profile in May at site 2 is similar to that at site 1, with a difference in the position of the maximum EEA layer. Site 1 has the highest EEA on the very surface, while at site 2, a maximum activity occurred within a subsurface layer at 1~2 cm.

4. Discussion

4.1. Comparison of enzyme activity profiles determined by fluorosensor and traditional incubations

The EEA distributions obtained by 2D planar imaging can be compared with EEA determined using traditional techniques by horizontally averaging the 2-D images to derive equivalent vertical EEA profiles. Vertical profiles derived from the two techniques showed similar general features with maximum EEA at or just below the sediment surface and a decrease with depth during most seasons (Figure 4.7, four site 1 measurements were shown). However, profiles from traditional incubations have relatively higher activity at the sediment surface as well as sharper downward gradients. While such differences may come from natural heterogeneities between cores, the consistency in the relative differences implies methodological artifacts in one or both techniques.

We believe that the most likely basis for these differences is the manipulation of sediment during the traditional EEA method. The traditional method involves slicing sediment cores, followed by slurrying and serial incubation of the slurry. Both steps may introduce artifacts. When slicing sediment cores, the process of drawing off the overlying water to expose the sediment surface typically causes a small degree of dewatering and compaction of the uppermost sediment layer, which could result in an over estimation of the per wet weight sediment EEA. When sediment is slurried, additional pore water is added and the combined material well mixed. During this process the micro-structure of the sediment is largely destroyed. The porosity is thus increased, and tortuosity decreased. These changes influence the adsorption equivalence of both enzyme and substrate as well their mobility in pore water. Desorption of enzyme and substrate from attached forms plus enhanced diffusion rate in water increases the chances of enzyme meeting a target substrate molecule (Arnosti 1996), leading to an overestimation of EEA (Hansen et al. 2000). Considering the relative higher organic matter content, bacteria abundance and EEA in the top sediments (Figure 4.4) are higher than deeper layers, if a similar proportion of EEA increase over depth due to slurrying is assumed, the top layers will have a larger increase of EEA in absolute amount because of their higher initial levels.

4.2. Annual pattern of EEA in Great Peconic Bay

As far as we are aware, this study is the first to examine seasonal 2-D EEA distributions in sediments, and dynamic coastal deposits in particular. The results demonstrate significant seasonal variations in both the average magnitude of EEA and its distribution in surface sediment. Average EEA calculated from sensor images profiles (Figures 4.5, 4.6) showed lower values in fall and winter ($\sim 0.09 - 0.1 \mu\text{mol}\cdot\text{cm}^{-2}\cdot\text{h}^{-1}$). The deposition of spring bloom detritus during late winter – spring results in enhanced EEA focused into the surface most sediment layer. As temperature rises and reactive substrates penetrate into deeper layers by biogenic reworking, the average EEA (0-12cm) increases and reaches an annual maximum during summer ($0.15 - 0.2 \mu\text{mol}\cdot\text{cm}^{-2}\cdot\text{h}^{-1}$). The activity subsequently decreases again during fall.

Distributions of EEA in surface sediment also showed significant seasonal patterns. In winter and early spring, benthic infauna are depleted in number and relatively inactive. During these seasons, the surface sediment showed generally less lateral heterogeneity in EEA. In summer and fall, however, enhanced heterogeneity at multiple spatial scales was observed mostly due to elevated particle reworking and bioirrigation by benthic faunas. A sharp contrast is apparent in EEA profiles between spring and fall (Fig. 4.5; Apr., Oct.). The two seasons have comparable magnitude of average EEA, but the distributions are different. In spring, primary production increases rapidly resulting in pulsed deposition of reactive organic matter (OM) and stimulation of bacterial growth at the sediment surface; however, the activity of the benthic fauna clearly lags the deposition of the bloom detritus as illustrated by the very presence of a distinct layer. The late winter EEA showed obvious decreases with depth (an almost two layer structure) but not much horizontal heterogeneity. In fall, the primary production drops (Lonsdale et al. 2006), causing decreased OM supply relative to summer. However, the benthic fauna are still surviving?, reworking and irrigating sediment, forming burrow structures and redistributing organic matter that brings reactive substrate into deeper layers.

4.3. Surface sediment heterogeneity and decomposition “hot spots” discriminated by EEA imaging

The 2-D EEA sensor allows the discrimination of small scale heterogeneities, which appeared to be common during certain seasons. Previous studies applying 2-D optical sensors in surface sediment have also revealed various scales of heterogeneity. For example, CO₂ patterns reflect macrofaunal burrow structures at the millimeter – centimeter scale (Zhu et al. 2006), and O₂ images exhibit microsites of preferential consumption, that is, hot spots of remineralization activity (Glud 2008).

The information derived from the EEA sensor system differs from other optical sensors such as O₂, pH, or pCO₂ planar sensors, in that, firstly, it directly measures reaction rates in contrast to concentrations. Secondly, as shown by previous studies, EEA is dominantly

associated with solid particles and is not directly subject to solute transport processes such as molecular diffusion and bioirrigation (Arnosti 2011, Cao et al. 2011). Thus, EEA imaging directly and uniquely reflects biosubstrate properties of sediment particles, including the size, density and activity level of reactive organic aggregates. EEA imaging also reveals reaction heterogeneity under completely anoxic in addition to oxic conditions, which is incapable for O₂ sensors.

These specific properties can cause EEA images to look different from 2-D patterns obtained by pH or *p*CO₂ fluorescence sensors (Zhu et al. 2005, 2006). One of the most obvious differences is that most 2-D EEA distributions (Figure 4.5& 4.6) showed a granular pattern at the millimeter scale rather than the relatively smooth patterns obtained by the solute concentration sensors at micrometer scales. Conversion of solute concentration gradients such as H⁺ (pH) into net reaction rates can also produce more granular patterns but unlike the more direct EEA measurements these may be due in part to calculation artifacts (noise amplification) (Zhu et al. 2006). In spite of the recognition and ubiquity of heterogeneity associated with organic aggregates in sediments, the significance of aggregates during early diagenesis has not been well studied, particularly under anoxic conditions where O₂ sensors do not reveal reactivity patterns (Jorgensen 1977). We examined the effect of microniche heterogeneity on local statistical distributions of EEA during different seasons. In most seasons, when EEA data of all pixels from a specified depth interval (Figure 4.8, top figure; an example of May 2010 site 1 sample 0-2 cm layer) are plotted as a histogram, the resulting distribution shows a typical symmetrical, normal distribution pattern, with a skewness of -0.03. This symmetry suggests that aggregates and reactive substrate are relatively uniformly mixed by physical and chemical processes. In those seasons, although there are microsites of high EEA levels, they appear randomly and approximately normally distributed about a mean value and are compensated by equivalent sites of low EEA activities.

There are seasons and zones within the sediment, however, where relatively high EEA microniches are larger and distinctly skew EEA distributions in a non-random fashion. For

example, when EEA data from the top 2 cm during spring 2009 site 1 were plotted (Figure 4.8 bottom), the distribution is skewed to higher values (white + black bar), with a skewness of 0.77. This skewed distribution implies that additional highly reactive organic sources were introduced. These additional high EEA spots are a distinct departure from a symmetrical random distribution. The comparison between these two samples also shows higher relative standard deviation (RSD %) in EEA distributions during April than in May (34.7% vs 10.1%), consistent with these differences in the distribution patterns.

It is clear that the microscale distribution of EEA can change seasonally and that distinct microniches of elevated activity are more or less obvious. How such phenomena are best defined and quantified? We identified microniches by both size and relative activity. Firstly, we set an EEA threshold of 1.34* the mean value within a depth interval (that is, EEA positively exceeds 1 standard deviation). Secondly, the imaged area of the enhanced EEA pixel group had to exceed 1 mm² in order to differentiate the region from the regular background EEA grain scale. In the case of the April distributions, hot spots defined in this manner accounted for 9.9% of the image area and contributed 15.7% of overall EEA activity (black regions, Figure 4.8 bottom). If these hot spots are excluded from the distribution, the skewness drops to 0.27 (white bar), indicating a more symmetrical compared to May. It should be pointed out that the contribution of functional hot spots in this example may still be underestimated as smaller high EEA zones (<1 mm²) are excluded in calculation. The positive value of skewness (0.27) after hot spot subtraction may be a sign of this underestimation.

Based on these definitions, three sediments samples were found to have zones of significant hot spots accounting for a substantial portion of total decomposition activity. Two of these cases were in regions surrounding burrow structures; the other is the previously discussed example which we believe reflects initial stages of the penetration and mixing of phytoplankton debris into the deposit following the spring bloom (Figure 4.5a& Figure 4.6a,b, the hot spots zones in figure 4.6b is not intuitive from figure because of the scale setting). This observation

may lead to a conclusion that hot spots are not naturally and universally present in sediments, but are closely related to animal behaviors and bloom events in overlying water.

4.4. Hot spots associated with burrow structures

Benthic fauna significantly change surface sediment structure. Through processes including particle manipulation, grazing, excretion/secretion, nutrient release, irrigation and particle transport (Aller & Aller 1998), macrobenthos greatly influence pathways, rates, and extents of organic matter remineralization and associated reactions, causing a complex transport of particles (sediment reworking) and fluids (bioirrigation), and creating a three dimensional zonation pattern of geochemical processes (Ziebis et al. 1996, Glud 2008). Furthermore, abandoned tubes or burrows are often surprisingly stable and can last for months to years after being vacated, acting as traps for labile organic material (Aller & Aller 1986); (Zhu et al. 2006). Previous studies have shown elevated EEA activities around both recently infilled as well as actively irrigated macrofaunal burrows (Boetius 1995, Aller & Aller 1998, Wenzhofer & Glud 2004). In the present study, we also found elevated EEA associated with burrows (Figure 4.6; July, Nov.), but regions of enhanced EEA were characterized by relatively abundant hot spots rather than continuously elevated EEA distributions. These patterns may reflect burrow properties of particular species or may be a more accurate general indication of enhanced EEA around burrows. Fecal material and excretion of mucus may also promote the formation of hot spots. In any case, there are insufficient data on in situ burrow structures at this point to determine the possible generality of the distributions. More examples and the best a 3D observation of distributions will be needed. Nevertheless, the results from this study have provided intuitive and valuable information on EEA and organic matter distributions around burrow structures

4.5. Impacts of algal blooms and pulse deposition of detritus

Site 2 sediment collected in March 2010 had a fluff layer with a thickness of ~2 cm at the surface (Figures 4.6& 4.9). This fluff layer largely consisted of phytoplankton detritus deposited

from an early spring bloom that presumably occurred a few days to weeks before sampling. A clear boundary can be found between the fluff layer and deeper sediments. Within this layer, LAP activity reached an abnormally high level for that season. The average value even exceeded the surface EEA in summer. Below this fluffy layer, however, EEA remained at the low activity more typical for winter. The integrity and distinctive nature of the surface fluff layer shows that surface sediment had not yet been reworked or extensively irrigated by benthos. The lack of substrate dispersion from particle bioturbation and minimal bioirrigation, results in a close correspondence between EEA and remineralized metabolites, as demonstrated by $p\text{CO}_2$ patterns obtained at the same site (more details about the principle and deployment of the $p\text{CO}_2$ sensor can be found in Zhu and Aller (2010)). High $p\text{CO}_2$ is clearly superimposed with high EEA in the fluff layer (Figure 4.9). This superposition demonstrates that EEA directly reflects metabolic activity. As discussed previously, as biogenic transport processes such as bioirrigation become more intense, and reactive substrates penetrate and are dispersed into the deposit, solute concentrations and metabolite build up patterns may not readily reflect local remineralization activity. Another very interesting fact is that in contrast with the highly elevated aminopeptidase activity in the surface-most fluff layer, the glucosidase activity within the top 2 cm layer remains at a low level (Figure 4.3). Such decoupling between GA and LAP is a very good example of the regulated response of bacteria to the characteristics or the “quality” of the polymeric organic material pool. While directly bioavailable carbohydrate monomers may be abundant in the fresh phytoplankton debris layer as a result of cell lysis, bacteria tend not to expend much energy on glucosidase excretion but rather on stimulating proteinase excretions to satisfy their N demand.

The late winter – spring – late spring EEA distributions in Great Peconic Bay provide an illustration of the non-steady state seasonal remineralization processes previously documented in estuarine surface sediments (e.g., (Bruno et al. 1980, Hunt 1983, Graf 1992, Gerino et al. 1998, Breuer et al. 1999) . As spring bloom material is deposited on the seabed and reworked into the underlying deposit by meio- and macroinfauna, microniche hot spots develop as seen during April in our samples. The low temperatures and relatively low infaunal activity at the time both

hinder the complete decomposition and enhance temporary preservation of the phytoplankton detritus.

4.6. Factors controlling EEA in Great Peconic Bay sediments.

Our results show that sedimentary EEA activity varies significantly seasonally due in part to temperature and in part to substrate availability (Figures 4.4-4.6, 4.10). At a fixed substrate composition, the temperature dependence of LAP in slurried sediment follows an Arrhenius rate law with an apparent activation energy (E_a) of ~30.6 kJ/mol (Cao, et al., in prep.). When the natural log of the depth integrated EEAs measured in all cores either by traditional or optical sensor methods is plotted versus $1/T$ (T = absolute temperature of collection), the apparent activation energy derived from the slopes is much smaller: 18.9 kJ/mol (Figure 4.10, all points included). However, if the EEA value obtained during the winter – spring transition is removed, the apparent activation energy is ~35.7 kJ/mol (Figure 4.10, open circle excluded), and more comparable to experimental measurements. The fit of integrated EEA from different seasons in the E_a curve demonstrated that temperature accounted for most of the annual variation in sediment EEA. In other words, after normalizing EEA for each season to the temperature, EEA is stable during most of the year. This phenomenon implies that the hydrolysis of the labile portion of organic polymers is a rapid process in Peconic Bay surface sediments rather than being a limiting step in OC remineralization. The level of LAP present is sufficient to accommodate the range of substrate variation over most of the year. During the spring bloom period (Feb – Mar), however, labile substrate deposition enhances EEA above that expected from T variation alone. The mechanism for net enhancement of EEA is either stimulated LAP synthesis or a shift of dominant LAP to a low E_a isoenzyme or both.

The activities of the three classes of enzymes measured correlated with each other, suggesting coupled controlling factors in general (Figure 4.11). When EEAs versus their respective end member nutrient product concentrations were plotted: LAP vs. DIN, BG vs. ΣCO_2 and PA vs. PO_4^{3-} among all seasons from all depth intervals, no significant relationships were

found (data not shown). In contrast, EEA and direct measurements of metabolite production such as depth integrated NH_4^+ and $\sum\text{CO}_2$ production rates, clearly correlate (Figure 4.12 A, B). The results indicated that the metabolism of microbes in GPB sediment is closely coupled with polymer hydrolysis. Small organic units cut from polymers are fast assimilated and utilized by microbes. Previous studies have found inorganic P is the dominant regulating factor of phosphatase activity (Hoppe 2003). However, the pattern is not obvious in this study, probably because bacteria may also produce PA targeting the organic part (C) of P containing polymers, rather than P requirements per se, especially in C-limited subsurface sediments (Hoppe & Ullrich 1999).

Even though the suite of EEA in Great Peconic Bay seems to be co-regulated in general, the ratios between enzymes may still reflect a nutrient limitation regime shift among seasons. It has been suggested that the EEA ratios between enzyme groups can be potential nutrient limitation indicators (Hill et al. 2010). In this study, when enzyme ratios (LAP/PA) were plotted against ratios of inorganic nutrients (N/P derived from inventories 0 – 15 cm) (Figure 4.12C), we found that during warm seasons (April – mid Oct), the N/P ratio is low compared with that in cold seasons (late Oct – March). In these two periods, no clear relationship was found between LAP/PA and N/P. In the cold seasons, the N/P is much higher, probably due to lower biological activity and relatively enhanced chemical sinks for P; a weak but significant correlation ($P < 0.01$) was found between LAP/PA vs. N/P indicating a decreased P supply and potential P deficiency.

As noted previously, a major reason that EEA correlates with metabolite production rate but not product solute concentrations is the different transport processes affecting particles and solutes. EEA measures the instantaneous potential rate of substrate hydrolysis associated with reactive particle distributions. Reactive particle transport occurs on slower time scales than solute transport and by different mechanisms, for example, particle reworking and sedimentation.. Solute concentrations are strongly affected by diffusion and bioirrigation in addition to production – consumption reactions. The sediment-water interface region demonstrates these differences directly: the most reactive substrate is present and decomposition

rates are often highest, but metabolite levels (e.g., ΣCO_2) are usually minimal due to diffusive losses into contacting overlying water.

Another interesting relationship between metabolite production rates and EEA is that the regression intercepts suggest measurable EEA in the absence of net metabolite production into pore water (Figure 4.12A, B). These intercepts may reflect the level of EEA required to support biomass synthesis (e.g., incorporation of NH_4^+ into biomass rather than release to solution), or may be artifacts of the measurement methods since the current techniques measure EEA maximum potential.

5. Conclusions

Sedimentary extracellular enzyme activity (EEA) varies seasonally in estuarine sediments of Great Peconic Bay: highest during the spring bloom and summer, and lowest during the fall and early winter. Seasonal variation is determined by both temperature and the availability of reactive organic substrates, with EEA varying directly with both. Although traditional EEA measurements document these overall seasonal patterns, high resolution, 2-D EEA distributions, obtained using a novel optical sensor that preserves sedimentary structure, reveal controlling factors, substrate transport patterns, and metabolic phenomena more accurately and in ways not possible using traditional slurry techniques. A high degree of horizontal heterogeneity in EEA was present, particularly during warm seasons. Hot spots of metabolic activity associated with aggregates of reactive organic material can be discriminated statistically. These microniches of enhanced EEA were most obvious during initial penetration of reactive detritus into underlying sediment following the spring bloom, and around burrow structures during other times. EEA is closely associated with metabolites ($p\text{CO}_2$) when bioturbation is minimal, for example, in the highly reactive fluff layer deposited as a pulse during the spring bloom. However, EEA and solute build up patterns are decoupled during much of the year because of the different transport mechanisms and rates of transport affecting reactive particle substrates and solutes in bioturbated

deposits. EEA correlates directly with depth integrated remineralization rates (ΣCO_2 , NH_4^+ production). The 2-D EEA methodology provides a unique means to directly and independently measure the complex, unsteady processes affecting reactive organic matter substrate distributions in both oxic and anoxic zones of sedimentary deposits.

Table 4.1. Integrated (0-15cm) nutrient inventories and depth integrated (0 – 15 cm) production rates in different seasons*

Seasons	Temperature (°C)		NH ₄ ⁺ (mmol/m ²)		PO ₄ ³⁻ (mmol/m ²)		ΣCO ₂ Production (mmol/m ² /d)		NH ₄ ⁺ Production (mmol/m ² /d)	
	Site 1	Site 2	Site 1	Site 2	Site 1	Site 2	Site 1	Site 2	Site 1	Site 2
Summer2009	22.3	23.7	5.3	8.0	1.4	2.6	16.6	18.8	1.8	6.4
Fall 2009	17.5	11.1	15.9	8.9	1.0	1.9	8.7	4.2	0.2	0.5
Winter2010	-0.29	3.4	3.03	7.4	0.7	1.3	1.2	3.3	0.2	0.2
Spring 2010	15.1	22.1	4.9	5.2	3.8	2.3	10.1	37.7	1.8	6.7

*Original data from Waugh, et al (in preparation)

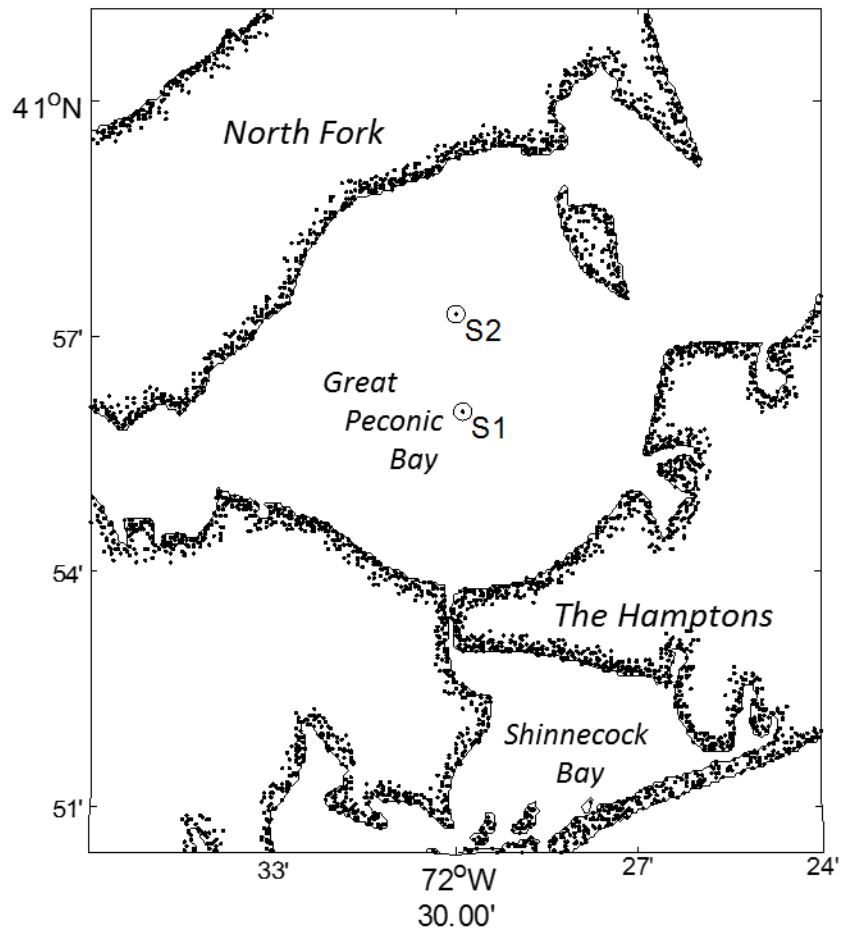


Figure 4.1. Location of sampling sites in Great Peconic Bay, at the eastern end of Long Island, New York, USA.

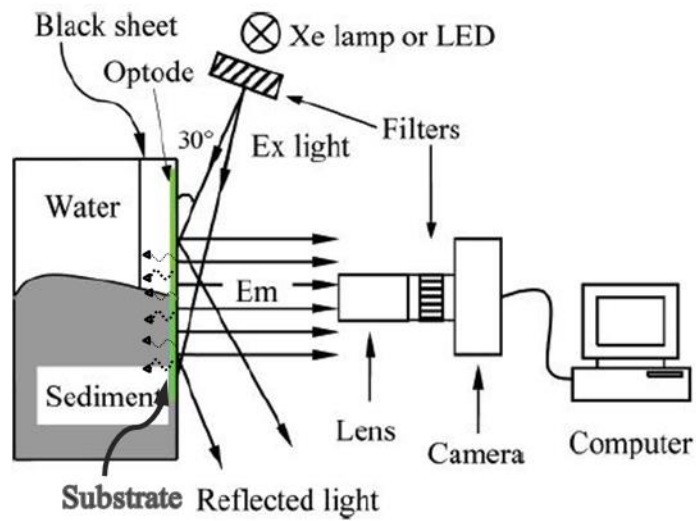


Figure 4.2. Imaging instrumentation used for two-dimensional Leucine-aminopeptidase measurements (modified after (Zhu et al. 2005) showing position of enzyme substrate (green) against the sediment.

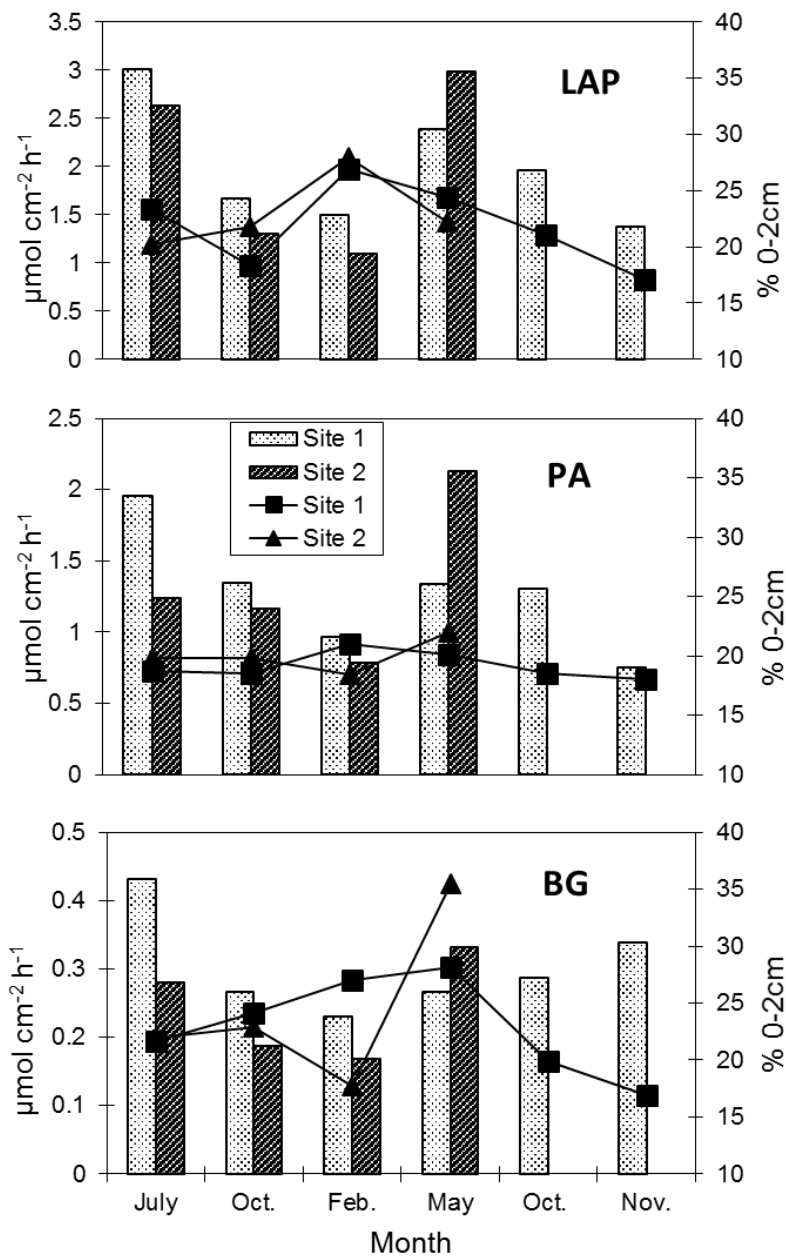


Figure 4.3. Vertically integrated activities (as bars) over the top 12 cm of A: leucine aminopeptidase (LAP) B: phosphatase (PA), and C: β -glucosidase (BG) in different sampling seasons overlain by the percentage of EEA in the top 2 cm for depth integrated values. While LAP activity overall was greater than PA activity followed by BG activity all three enzymes showed similar seasonal patterns activities lowest in winter, highest in the summer and Site 1 more active than Site 2.

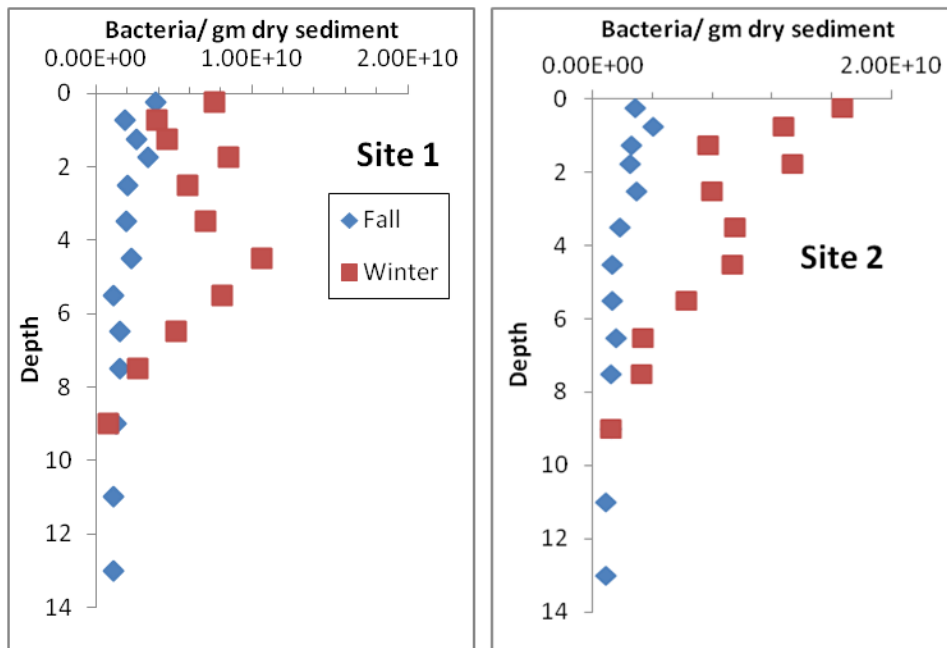


Figure 4.4. Comparison of bacterial abundances during fall and winter 2009 at Sites 1 and 2. Overall higher concentrations and elevated concentrations at the surface during winter are consistent with lower grazing rates.

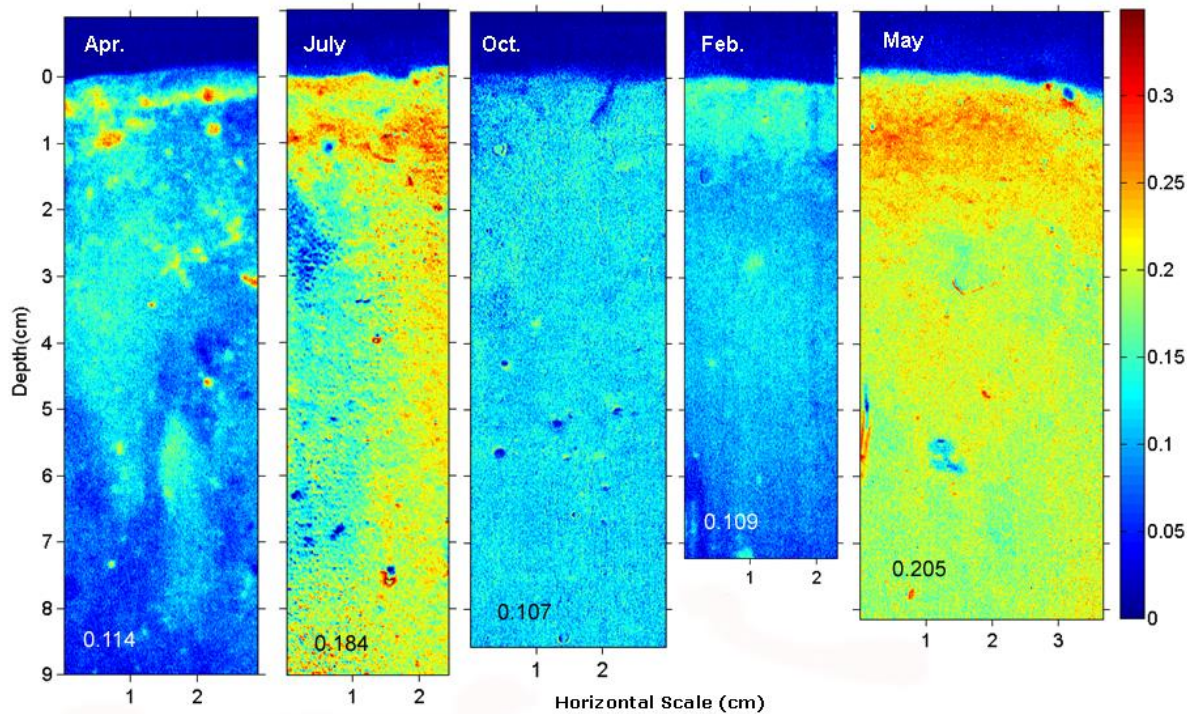


Figure 4.5. 2-Dimensional extracellular leucine aminopeptidase (LAP) distribution patterns plotted as pseudo-color images in cores collected in different seasons of Site 1. From left to right: April 2009, July 2009, Oct.2009, Feb. 2010, May 2010. X and Y axes are actual length scale within the sediment. Point 0 on the Y axis indicates the position of the water-sediment interface. Because the sediment surface is seldom level, the exact position of the interface is estimated. Color bar reflects EEA(in $\mu\text{mol}\cdot\text{h}^{-1}\cdot\text{g}^{-1}$). The average EEA over the image area is indicated at the lower left in each panel

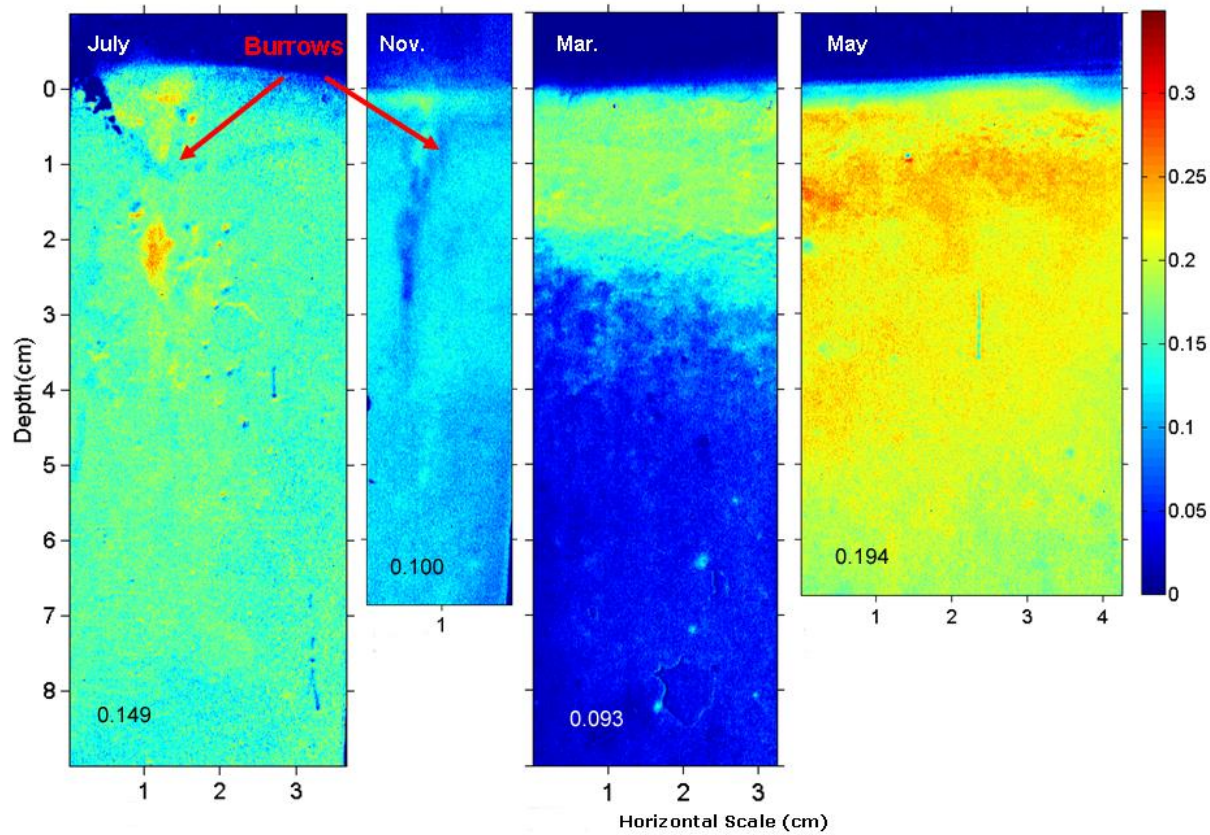


Figure 4.6. 2-Dimensional extracellular leucine aminopeptidase (LAP) distribution patterns plotted as pseudo-color images in cores collected in different seasons of Site 2. From left to right: July 2009, Nov.2009, Mar. 2010, May 2010. X and Y axes are actual length scale within the sediment. Point 0 on the Y axis indicates the position of the water-sediment interface. Color bar reflects EEA. The average EEA over the image area is indicated at the lower left of each panel.

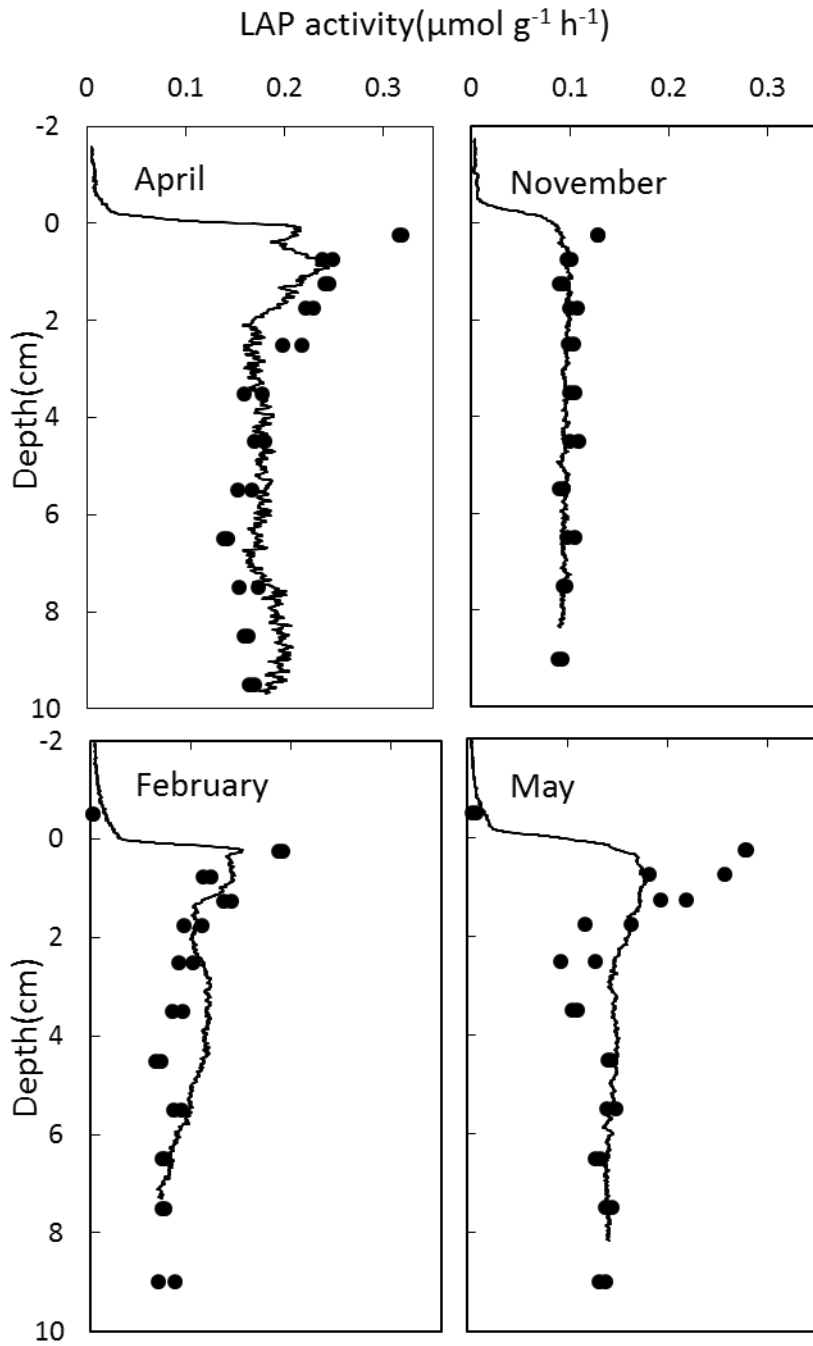


Figure 4.7. Vertical profiles of horizontally averaged enzyme activity obtained from 2-D sensor images (black line) compared with results from traditional incubations (black dots).

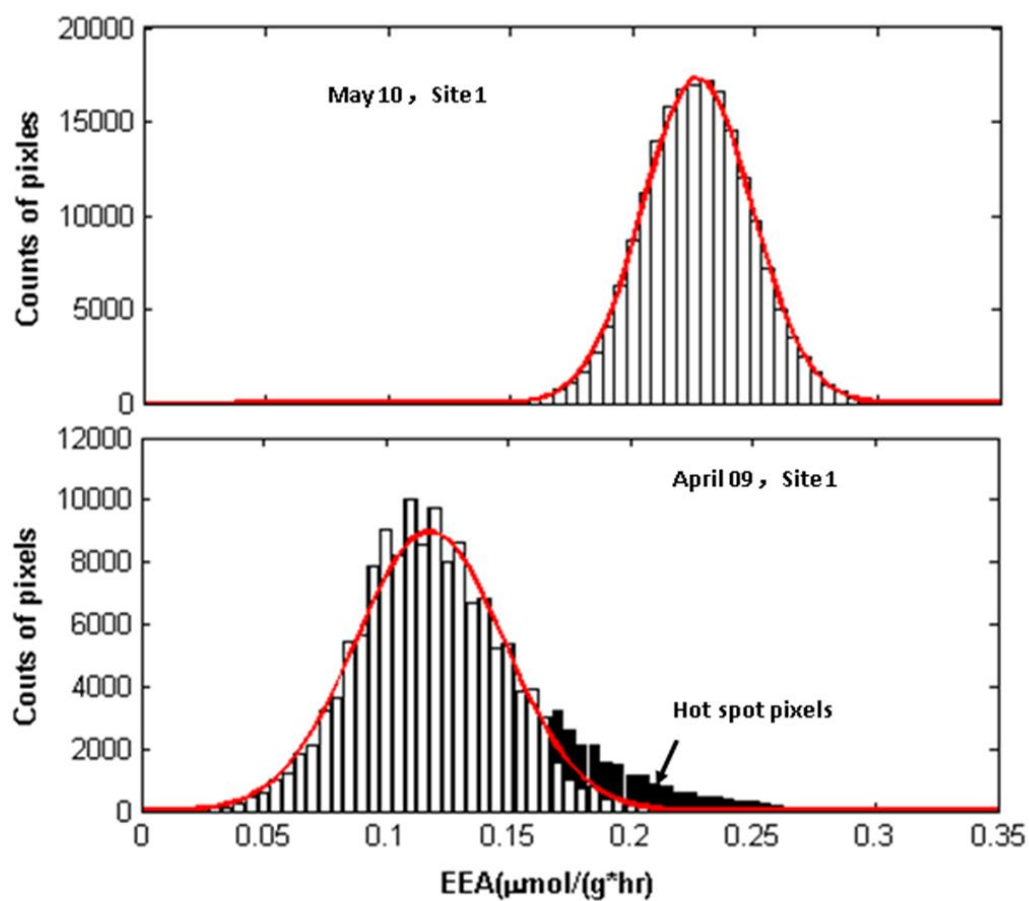


Figure 4.8. Histograms showing surface sediment (0-2 cm) EEA distributions without (top) and with (bottom) hot spots. The x axis is the range of EEA and the y axis represents the number of pixels that are within each EEA interval. Red lines in each figure are normal distribution simulations based on sample mean and variance.

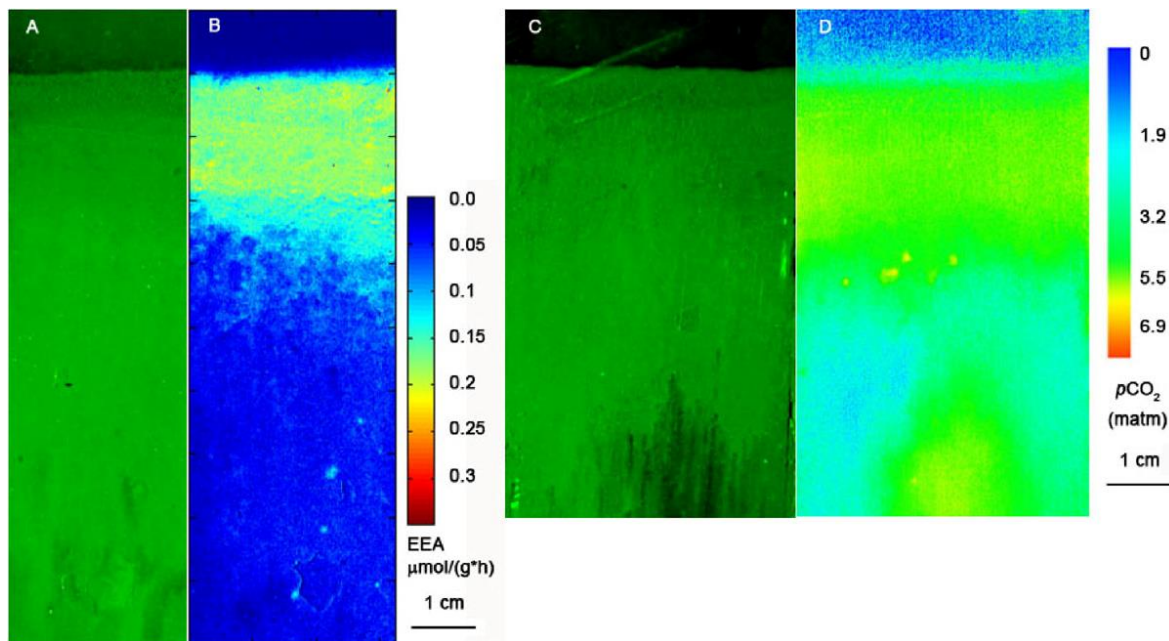


Figure. 4.9. Aminopeptidase activity (LAP) (Image B) and $p\text{CO}_2$ (Image D) in vertical sections from two cores taken during the spring bloom (late Feb – Mar 2010) in Great Peconic Bay at Site 1. Image A and C are raw visible images under green light corresponding to each sensor image respectively (black color in visible images is Fe-sulfide). Note that the vertical and horizontal scales are in cm. The depositional focusing of reactive particles and the relative lack of bioirrigation results in the close correspondence of reactive particle and metabolite distributions near the sediment-water interface (red rectangle outlines).

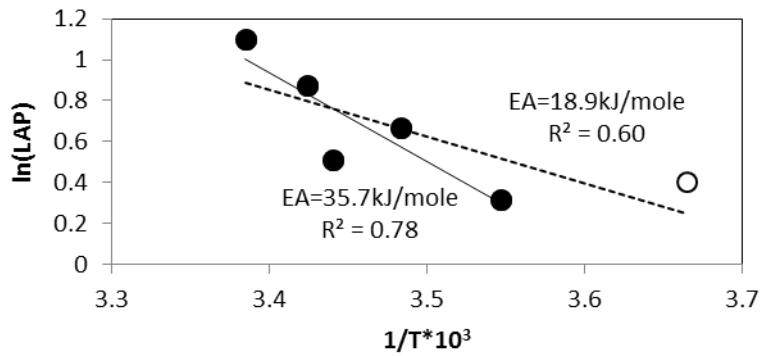


Figure 4.10. Natural log of the depth integrated EEAs plotted against $1/T$. T is absolute temperature. The hollow circle is the Feb 10 EEA while the filled circles are EEAs from the other 5 seasons as shown in Fig. 4.3. The solid line is a linear regression of the solid circles. The dashed line is the regression of all points.

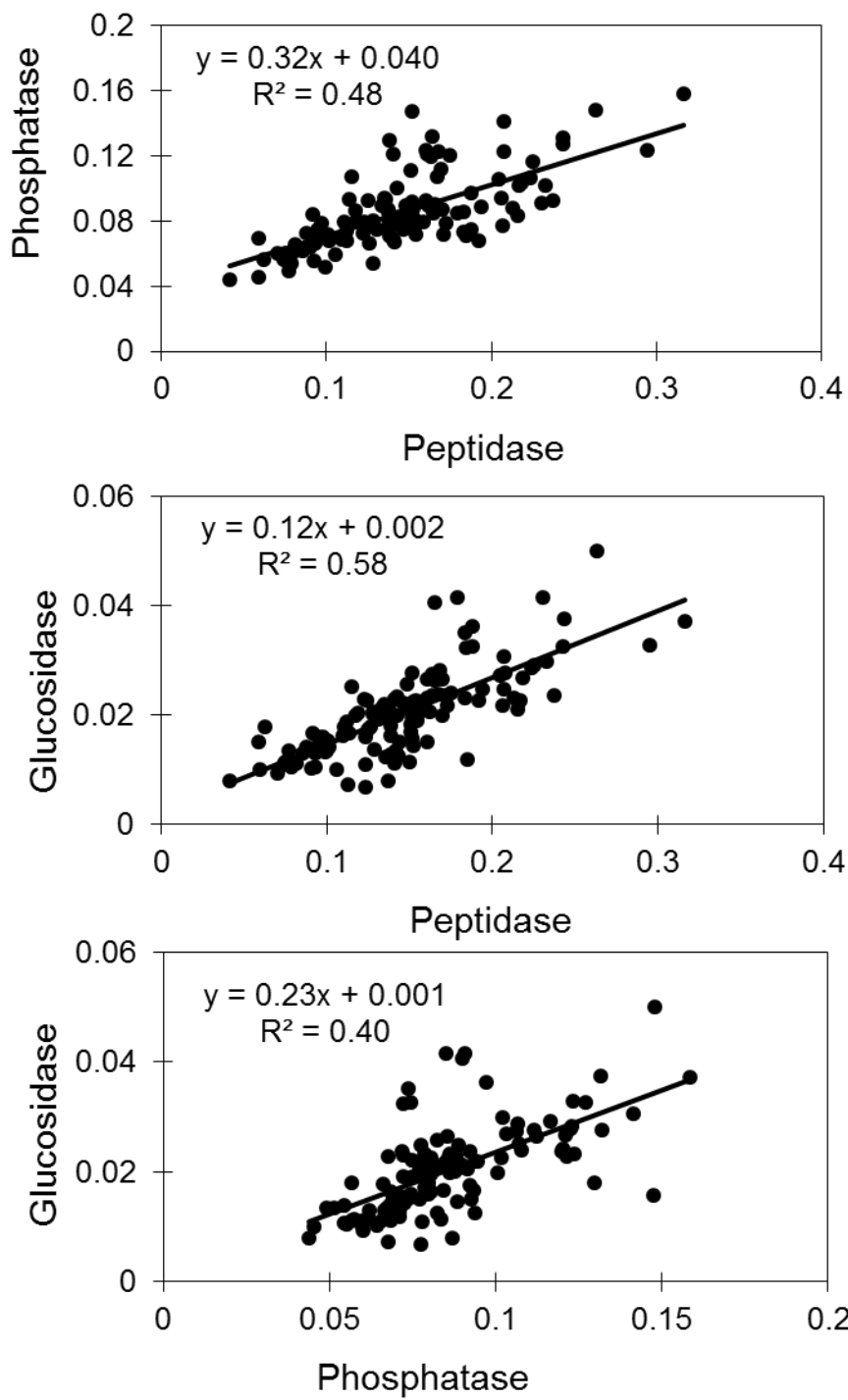


Figure 4.11. Comparison of the activities of the three classes of enzymes with each other during all sampling seasons demonstrating correlations and suggesting coupled controlling factors.

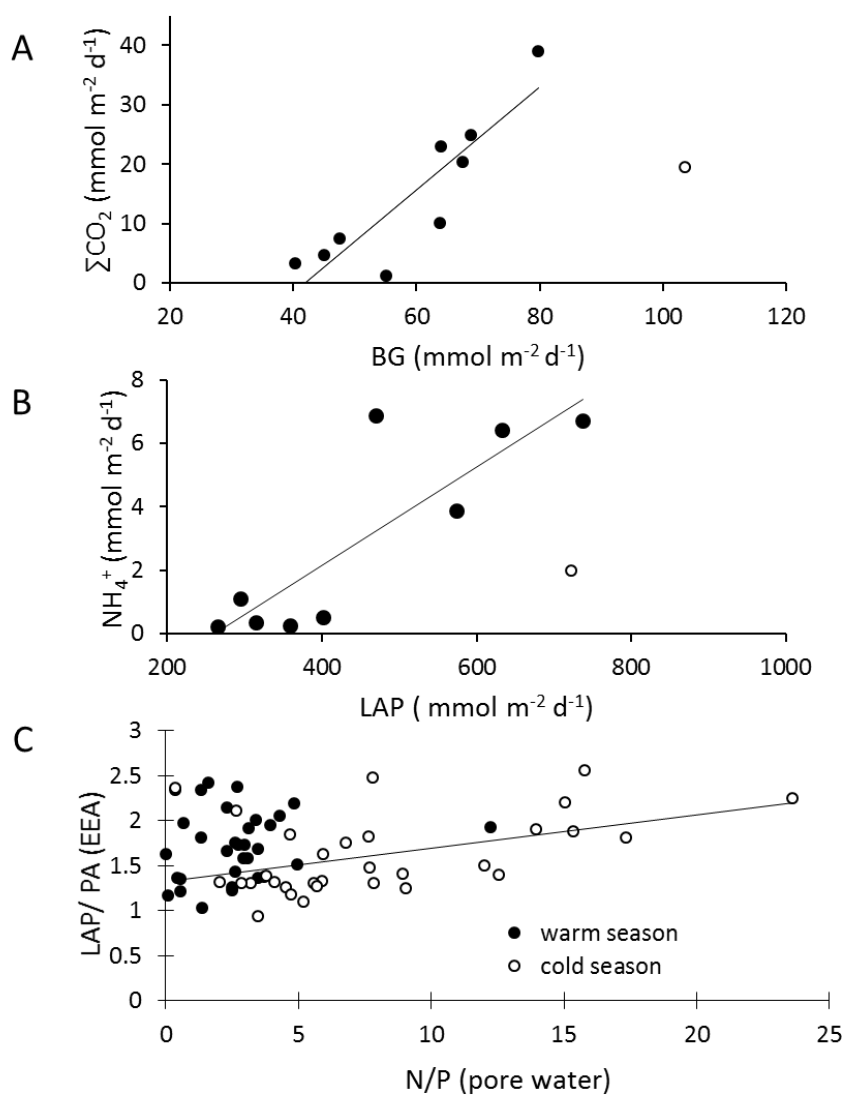


Figure 4.12. EEAs versus their respective end member nutrient production rates : The relationship between BG and ΣCO_2 production (integrated as equivalent flux) (A) and between LAP and NH_4^+ production (B) show clear correlations, whereas there is no clear relationship between N/P and LAP/PA (C) although the N/P is lower during the warmer seasons compared with that in colder seasons. The lines plotted in (A) and (B) are the type 2 (geometric mean) regressions (ΣCO_2 flux = $0.87(\text{BG}) - 36.2$; $r^2 = 0.79$; NH_4^+ flux = $0.0068(\text{LAP}) - 1.76$; $r^2 = 0.73$).

Chapter 5. Summary and future perspectives

1. Summary of major findings

The development of a new sensor system

A novel planar sensor system to measure two-dimensional EEA in marine sediments was developed. The underlying principle of the new extracellular enzyme sensor is the incorporation of a fluorogenic enzyme substrate into a polymer carrier and the controlled release of that substrate into a contacting medium while transport and reactions are continuously monitored. The sensor foils, which in this application utilize Leu-MCA as the substrate, reveal real-time proteolytic enzyme (Leucine-aminopeptidase) activity patterns across the planar surfaces at high spatial resolution (~50-100 μm)

Seasonal EEAs and controlling processes in Great Peconic Bay

Sedimentary extracellular enzyme activities (EEA) were measured seasonally by both the new sensor systems and the traditional incubation methods. Results showed that EEA varies seasonally in estuarine sediments of Great Peconic Bay: highest during the spring bloom and summer, and lowest during the fall and early winter. Seasonal variation is determined by both temperature and the availability of reactive organic substrates, with EEA varying directly with both. Spatial heterogeneity was less obvious in cold seasons mainly due to low bio-activities. In warm seasons, however, higher degree of horizontal heterogeneity was observed as the result of increased organic deposits and active macrobenthos. Hot spots of metabolic activity associated with aggregates of reactive organic material can be discriminated statistically. These microniches of enhanced EEA were most obvious during initial penetration of reactive detritus into underlying sediment following the spring bloom, and around burrow structures during other times. EEA is closely associated with metabolites ($p\text{CO}_2$) when bioturbation is minimal, for example, in the highly reactive fluff layer deposited as a pulse during the spring bloom. However, EEA and solute build up patterns are decoupled during much of the year because of the different transport mechanisms and rates of transport affecting reactive particle substrates and solutes in bioturbated deposits. EEA correlates directly with depth integrated remineralization rates (ΣCO_2 , NH_4^+ production).

Change of extracellular enzyme activities as a response of bacteria to temperature variation

An incubation experiment was conducted to study the EEA change as a response of bacteria communities to rapid variation in temperature. The results showed that bacteria responded quickly to temperature changes. Bacteria tend to synthesize a higher portion of LAP at low temperatures and a greater portion of Glucosidase and Phosphatase at temperatures higher than the *in situ* temperature they live. Temperature sensitivity curves showed that the initial response of the bacteria community to temperature change is always to alter their yield of EE. With longer exposure to a temperature change, community structure may alter or a succession of isoenzymes may occur shortly after a temperature shift.

The long time scale temperature dependence as reflected seasonal observations of EEA in Great Peconic Bay sediment, however, showed that bacteria communities seem to be insensitive to long time scale (monthly to seasonal) temperature changes. They chose to keep a stable EE level to accommodate varied OM supplies in different seasons. .

2. Future perspectives

Future works may focus on the development of new sensors to measure activities of other extracellular enzymes such as phosphatase and gluocosidase. The potential new sensors can also apply the controlled release membrane as the substrate release. The difficulty in new sensor design, however, is to look for the suitable substrates. Most current fluorogenic substrates have pH sensitive fluorophore subunits, which make them unreliable to measure EEA in sediments pH insensitive fluorogenic substrates for phosphatase and glucosidase activity measurements have been reported (Sun et al. 1997, Sun et al. 1998). These substrates are perfect for the enzyme sensor system. Their prices, however, are currently too high for practical applications. To synthesizing these substrates in house would be the best solution.

In this study, the new sensor system was applied to study the annual EEA distributions in Great Peconic Bay. Future works should utilize this new sensor to measure EEA in other surface sediments under varied conditions. More EEA profiles will help to the further understanding of the sources and properties of degradation hot spots. The EEA profiles should also be compared with profiles measured by other sensors such as dissolved CO₂ and O₂ sensors to better uncover the coupling of different links in OM degradation

The incubation experiments to study the temperature response of sediment bacteria should also be continued. The experiment reported in this dissertation has been an excellent pioneer work. Future experiments should include more parameters such as bacterial abundances and molecular biological measures to better explain the mechanism that determine the response of bacteria to temperature changes.

References

- Albertson NH, Nystrom T, Kjelleberg S (1990) Exoprotease activity of two marine bacteria during starvation. *Appl Environ Microbiol* 56:218-223
- Aller JY, Aller RC (1986) Evidence for localized enhancement of biological activity associated with tube and burrow structures in deep-sea sediments at the HEBBLE site, Western North Atlantic. *Deep-Sea Res* 33:755-790
- Aller RC (1994) Bioturbation and Remineralization of Sedimentary Organic-Matter - Effects of Redox Oscillation. *Chem Geol* 114:331-345
- Aller RC, Aller JY (1998) The effect of biogenic irrigation intensity and solute exchange on diagenetic reaction rates in marine sediments. *Journal of Marine Research* 56:905-936
- Aller RC, Mackin JE (1989) Open-incubation, diffusion methods for measuring solute reaction-rates in sediments. *J Mar Res* 47:411-440
- Allison SD (2005) Cheaters, diffusion and nutrients constrain decomposition by microbial enzymes in spatially structured environments. *Ecol Lett* 8:626-635
- Allison SD (2006) Soil minerals and humic acids alter enzyme stability: implications for ecosystem processes. *Biogeochemistry* 81:361-373
- Allison SD, Chao Y, Farrara JD, Hatosy S, Martiny AC (2012) Fine-scale temporal variation in marine extracellular enzymes of coastal southern California. *Frontiers in microbiology* 3:301
- Allison SD, Vitousek PM (2005) Responses of extracellular enzymes to simple and complex nutrient inputs. *Soil Biol Biochem* 37:937-944
- Ammerman JW, Glover WB (2000) Continuous underway measurement of microbial ectoenzyme activities in aquatic ecosystems. *Mar Ecol-Prog Ser* 201:1-12
- Amon RMW, Benner R (1994) Rapid cycling of high-molecular-weight dissolved organic matter in the ocean. *Nature* 369:549-552
- Arnosti C (1995) Measurement of Depth-Related and Site-Related Differences in Polysaccharide Hydrolysis Rates in Marine-Sediments. *Geochim Cosmochim Acta* 59:4247-4257
- Arnosti C (1996) A new method for measuring polysaccharide hydrolysis rates in marine environments. *Org Geochem* 25:105-115
- Arnosti C (2000) Substrate specificity in polysaccharide hydrolysis: Contrasts between bottom water and sediments. *Limnology and Oceanography* 45:1112-1119

- Arnosti C (2011) Microbial Extracellular Enzymes and the Marine Carbon Cycle. In: Carlson CA, Giovannoni SJ (eds) Annual Review of Marine Science, Vol 3, Book 3. Annual Reviews, Palo Alto
- Arnosti C, Durkin S, Jeffrey WH (2005) Patterns of extracellular enzyme activities among pelagic marine microbial communities: implications for cycling of dissolved organic carbon. *Aquat Microb Ecol* 38:135-145
- Arnosti C, Holmer M (2003) Carbon cycling in a continental margin sediment: contrasts between organic matter characteristics and remineralization rates and pathways. *Estuarine Coastal and Shelf Science* 58:197-208
- Arnosti C, Jorgensen BB (2003) High activity and low temperature optima of extracellular enzymes in Arctic sediments: implications for carbon cycling by heterotrophic microbial communities. *Mar Ecol-Prog Ser* 249:15-24
- Arnosti C, Jorgensen BB, Sagemann J, Thamdrup B (1998) Temperature dependence of microbial degradation of organic matter in marine sediments: polysaccharide hydrolysis, oxygen consumption, and sulfate reduction. *Marine Ecology Progress Series* 165:59-70
- Arnosti C, Repeta DJ, Blough NV (1994) Rapid bacterial-degradation of polysaccharides in anoxic marine systems. *Geochim Cosmochim Acta* 58:2639-2652
- Baltar F, Aristegui J, Sintès E, van Aken HM, Gasol JM, Herndl GJ (2009) Prokaryotic extracellular enzymatic activity in relation to biomass production and respiration in the meso- and bathypelagic waters of the (sub)tropical Atlantic. *Environmental Microbiology* 11:1998-2014
- Bauer M, Kube M, Teeling H, Richter M, Lombardot T, Allers E, Wurdemann CA, Quast C, Kuhl H, Knaust F, Woebken D, Bischof K, Mussmann M, Choudhuri JV, Meyer F, Reinhardt R, Amann RI, Glockner FO (2006) Whole genome analysis of the marine Bacteroidetes 'Gramella forsetii' reveals adaptations to degradation of polymeric organic matter. *Environmental Microbiology* 8:2201-2213
- Belanger C, Desrosiers B, Lee K (1997) Microbial extracellular enzyme activity in marine sediments: extreme pH to terminate reaction and sample storage. *Aquat Microb Ecol* 13:187-196
- Bertics VJ, Ziebis W (2010) Bioturbation and the role of microniches for sulfate reduction in coastal marine sediments. *Environmental Microbiology* 12:3022-3034
- Boavida MJ, Wetzel RG (1998) Inhibition of phosphatase activity by dissolved humic substances and hydrolytic reactivation by natural ultraviolet light. *Freshw Biol* 40:285-293
- Boer SI, Arnosti C, van Beusekom JEE, Boetius A (2009) Temporal variations in microbial activities and carbon turnover in subtidal sandy sediments. *Biogeosciences* 6:1149-1165

- Boetius A (1995) Microbial hydrolytic enzyme activities in deep-sea sediments. *Helgol Meeresunters* 49:177-187
- Boetius A, Lochte K (1994) Regulation of microbial enzymatic degradation of organic matter in deep-sea sediments. *Marine Ecology Progress Series* 104:299-307
- Boraston AB, Bolam DN, Gilbert HJ, Davies GJ (2004) Carbohydrate-binding modules: fine-tuning polysaccharide recognition. *Biochem J* 382:769-781
- Borch NH, Kirchman DL (1999) Protection of protein from bacterial degradation by submicron particles. *Aquat Microb Ecol* 16:265-272
- Boschker HTS, Cappenberg TE (1994) A sensitive method using 4-methylumbelliferyl-beta-cellobiose as a substrate to measure (1,4)-beta-glucanase activity in sediments. *Applied and Environmental Microbiology* 60:3592-3596
- Boschker HTS, Cappenberg TE (1998) Patterns of extracellular enzyme activities in littoral sediments of Lake Gooimeer, The Netherlands. *Fems Microbiology Ecology* 25:79-86
- Breuer E, Sanudo-Wilhelmy SA, Aller RC (1999) Trace metals and dissolved organic carbon in an estuary with restricted river flow and a brown tide bloom. *Estuaries* 22:603-615
- Bruno SF, Staker RD, Sharma GM (1980) Dynamics of phytoplankton productivity in the Peconic Bay Estuary, Long Island. *Estuar Coast Mar Sci* 10:247-263
- Burdige DJ, Dhakar SP, Nealson KH (1992) Effects of manganese oxide mineralogy on microbial and chemical manganese reduction. *Geomicrobiology Journal* 10:27-48
- Burdige DJ, Gardner KG (1998) Molecular weight distribution of dissolved organic carbon in marine sediment pore waters. *Mar Chem* 62:45-64
- Burdige DJ, Kline SW, Chen WH (2004) Fluorescent dissolved organic matter in marine sediment pore waters. *Mar Chem* 89:289-311
- Cao ZR, Zhu QZ, Aller RC, Aller JY (2011) A fluorosensor for two-dimensional measurements of extracellular enzyme activity in marine sediments. *Mar Chem* 123:23-31
- Christian JR, Karl DM (1995) Bacterial ectoenzymes in marine waters - activity ratios and temperature responses in 3 oceanographic provinces. *Limnology and Oceanography* 40:1042-1049
- Chrost RJ (1991) Environmental control of the synthesis and activity of aquatic microbial ectoenzymes. In: Chrost RJ (ed) *Microbial enzymes in aquatic environments*. Springer-Verlag, New York
- Chrost RJ (1992) Significance of bacterial ectoenzymes in aquatic environments. *Hydrobiologia* 243:61-70

- Coleman JE (1992) Structure and mechanism of alkaline phosphatase. *Annu Rev Biophys Biomol Struct* 21:441-483
- Coolen MJL, Overmann J (2000) Functional exoenzymes as indicators of metabolically active bacteria in 124,000-year-old sapropel layers of the eastern Mediterranean Sea. *Applied and Environmental Microbiology* 66:2589-2598
- Davey KE, Kirby RR, Turley CM, Weightman AJ, Fry JC (2001) Depth variation of bacterial extracellular enzyme activity and population diversity in the northeastern North Atlantic Ocean. *Deep-Sea Res Part II-Top Stud Oceanogr* 48:1003-1017
- Davies GJ, Gloster TM, Henrissat B (2005) Recent structural insights into the expanding world of carbohydrate-active enzymes. *Curr Opin Struct Biol* 15:637-645
- Dell'Anno A, Fabiano M, Mei ML, Danovaro R (2000) Enzymatically hydrolysed protein and carbohydrate pools in deep-sea sediments: estimates of the potentially bioavailable fraction and methodological considerations. *Mar Ecol-Prog Ser* 196:15-23
- Dell'Anno A, Mei ML, Ianni C, Danovaro R (2003) Impact of bioavailable heavy metals on bacterial activities in coastal marine sediments. *World J Microbiol Biotechnol* 19:93-100
- Ding XL, Henrichs SM (2002) Adsorption and desorption of proteins and polyamino acids by clay minerals and marine sediments. *Mar Chem* 77:225-237
- Doane TA, Horwath WR (2003) Spectrophotometric determination of nitrate with a single reagent. *Anal Lett* 36:2713-2722
- Fabiano M, Danovaro R (1998) Enzymatic activity, bacterial distribution, and organic matter composition in sediments of the Ross Sea (Antarctica). *Applied and Environmental Microbiology* 64:3838-3845
- Fan YZ, Zhu QZ, Aller RC, Rhoads DC (2011) An in situ multispectral imaging system for planar optodes in sediments: Examples of high-resolution seasonal patterns of pH. *Aquat Geochem* 17:457-471
- Feller G, Narinx E, Arpigny JL, Aittaleb M, Baise E, Genicot S, Gerday C (1996) Enzymes from psychrophilic organisms. *Fems Microbiol Rev* 18:189-202
- Fukuda R, Sohrin Y, Saotome N, Fukuda H, Nagata T, Koike I (2000) East-west gradient in ectoenzyme activities in the subarctic Pacific: Possible regulation by zinc. *Limnology and Oceanography* 45:930-939
- Gaas BM, Ammerman JW (2007) Automated high resolution ectoenzyme measurements: instrument development and deployment in three trophic regimes. *Limnology and Oceanography-Methods* 5:463-473

- Gerino M, Aller RC, Lee C, Cochran JK, Aller JY, Green MA, Hirschberg D (1998) Comparison of different tracers and methods used to quantify bioturbation during a spring bloom: 234-thorium, luminophores and chlorophyll a. *Estuar Coast Shelf S* 46:531-547
- German DP, Weintraub MN, Grandy AS, Lauber CL, Rinkes ZL, Allison SD (2011) Optimization of hydrolytic and oxidative enzyme methods for ecosystem studies. *Soil Biol Biochem* 43:1387-1397
- Glud RN (2008) Oxygen dynamics of marine sediments. *Mar Biol Res* 4:243-289
- Glud RN, Ramsing NB, Gundersen JK, Klimant I (1996) Planar optodes: A new tool for fine scale measurements of two-dimensional O₂ distribution in benthic communities. *Marine Ecology Progress Series* 140:217-226
- Glud RN, Stahl H, Berg P, Wenzhofer F, Oguri K, Kitazato H (2009) In situ microscale variation in distribution and consumption of O₂: A case study from a deep ocean margin sediment (Sagami Bay, Japan). *Limnology and Oceanography* 54:1-12
- Glud RN, Tengberg A, Kuhl M, Hall POJ, Klimant I, Host G (2001) An in situ instrument for planar O₂ optode measurements at benthic interfaces. *Limnology and Oceanography* 46:2073-2080
- Graf G (1992) Benthic-Pelagic Coupling-A benthic view. *Oceanogr Mar Biol* 30:149-190
- Hall PO, Aller RC (1992) Rapid, small-volume, flow-injection analysis for $\Sigma\text{-CO}_2$ and NH_4^+ in marine and fresh-waters. *Limnol Oceanogr* 37:1113-1119
- Hannides AK, Dunn SM, Aller RC (2005) Diffusion of organic and inorganic solutes through macrofaunal mucus secretions and tube linings in marine sediments. *Journal of Marine Research* 63:957-981
- Hansen JW, Thamdrup B, Jorgensen BB (2000) Anoxic incubation of sediment in gas-tight plastic bags: a method for biogeochemical process studies. *Marine Ecology Progress Series* 208:273-282
- Hill BH, Elonen CM, Jicha TM, Bolgrien DW, Moffett MF (2010) Sediment microbial enzyme activity as an indicator of nutrient limitation in the great rivers of the Upper Mississippi River basin. *Biogeochemistry* 97:195-209
- Hobbie JE, Daley RJ, Jasper S (1977) Use of nuclepore filters for counting bacteria by fluorescence microscopy. *Appl Environ Microb* 33:1225-1228
- Hollibaugh JT, Azam F (1983) Microbial-degradation of dissolved proteins in seawater. *Limnology and Oceanography* 28:1104-1116
- Hoppe HG (1983) Significance of exoenzymatic activities in the ecology of brackish water: measurements by means of methylumbelliferyl-substrates. *Marine Ecology Progress Series* 11:299-308

- Hoppe HG (2003) Phosphatase activity in the sea. *Hydrobiologia* 493:187-200
- Hoppe HG, Arnosti C, Herndl GJ (2002) Ecological significance of bacterial enzymes in the marine environment. . In: R.G. B, Dick RP (eds) *Enzymes in the environment*. Dekker, New York
- Hoppe HG, Ullrich S (1999) Profiles of ectoenzymes in the Indian Ocean: phenomena of phosphatase activity in the mesopelagic zone. *Aquat Microb Ecol* 19:139-148
- Hulthe G, Hulth S, Hall POJ (1998) Effect of oxygen on degradation rate of refractory and labile organic matter in continental margin sediments. *Geochim Cosmochim Acta* 62:1319-1328
- Hunt CD (1983) Variability in the benthic Mn flux in coastal marine ecosystems resulting from temperature and primary production. *Limnol Oceanogr* 28:913-923
- Huston AL, Deming JW (2002) Relationships between microbial extracellular enzymatic activity and suspended and sinking particulate organic matter: seasonal transformations in the North Water. *Deep-Sea Res Part II-Top Stud Oceanogr* 49:5211-5225
- Huston AL, Krieger-Brockett BB, Deming JW (2000) Remarkably low temperature optima for extracellular enzyme activity from Arctic bacteria and sea ice. *Environmental Microbiology* 2:383-388
- Jaeger SA, Gaas BM, Klinkhammer GP, Ammerman JW (2009) Multiple Enzyme Analyzer (MEA): Steps toward the in situ detection of microbial community ectoenzyme activities. *Limnology and Oceanography-Methods* 7:716-729
- Jorgensen BB (1977) Bacterial sulfate reduction within reduced microniches of oxidized marine-sediments. *Mar Biol* 41:7-17
- Katuna MP (1974) *The Sedimentology of Great Peconic Bay and Flanders Bay, L.I., N.Y.*, Vol
- Keil RG, Montluçon DB, Prahl FG, Hedges JI (1994) Sorptive preservation of labile organic-matter in marine-sediments. *Nature* 370:549-552
- King GM (1986) Characterization of beta-Glucosidase Activity in Intertidal Marine Sediments. *Appl Environ Microbiol* 51:373-380
- Kristensen E (2000) Organic matter diagenesis at the oxic/anoxic interface in coastal marine sediments, with emphasis on the role of burrowing animals. *Hydrobiologia* 426:1-24
- Lauro FM, McDougald D, Thomas T, Williams TJ, Egan S, Rice S, DeMaere MZ, Ting L, Ertan H, Johnson J, Ferriera S, Lapidus A, Anderson I, Kyrpides N, Munk AC, Detter C, Han CS, Brown MV, Robb FT, Kjelleberg S, Cavicchioli R (2009) The genomic basis of trophic strategy in marine bacteria. *Proceedings of the National Academy of Sciences of the United States of America* 106:15527-15533

- Lee C, Wakeham S, Arnosti C (2004) Particulate organic matter in the sea: The composition conundrum. *Ambio* 33:565-575
- Lehman RM, O'Connell SP (2002) Comparison of extracellular enzyme activities and community composition of attached and free-living bacteria in porous medium columns. *Applied and Environmental Microbiology* 68:1569-1575
- Liu ZF, Lee C (2007) The role of organic matter in the sorption capacity of marine sediments. *Mar Chem* 105:240-257
- Lonsdale DJ, Greenfield DI, Hillebrand EM, Nuzzi R, Taylor GT (2006) Contrasting microplanktonic composition and food web structure in two coastal embayments (Long Island, NY, USA). *Journal of Plankton Research* 28:891-905
- Luo HW, Benner R, Long RA, Hu JJ (2009) Subcellular localization of marine bacterial alkaline phosphatases. *Proceedings of the National Academy of Sciences of the United States of America* 106:21219-21223
- Mackin JE, Aller RC (1984) Ammonium adsorption in marine-sediments. *Limnology and Oceanography* 29:250-257
- Mallet C, Debros D (2001) Regulation of beta- and alpha-glycolytic activities in the sediments of a eutrophic lake. *Microbial Ecology* 41:106-113
- Martinez J, Smith DC, Steward GF, Azam F (1996) Variability in ectohydrolytic enzyme activities of pelagic marine bacteria and its significance for substrate processing in the sea. *Aquat Microb Ecol* 10:223-230
- Marx MC, Wood M, Jarvis SC (2001) A microplate fluorimetric assay for the study of enzyme diversity in soils. *Soil Biol Biochem* 33:1633-1640
- Mayer LM (1989) Extracellular proteolytic-enzyme activity in sediments of an intertidal mudflat. *Limnology and Oceanography* 34:973-981
- Meyer-Reil LL (1986) Measurement of hydrolytic activity and incorporation of dissolved organic substrates by microorganisms in marine sediments. *Marine Ecology Progress Series* 31:143-149
- Miranda KM, Espey MG, Wink DA (2001) A rapid, simple spectrophotometric method for simultaneous detection of nitrate and nitrite. *Nitric Oxide-Biology and Chemistry* 5:62-71
- Mulholland MR, Gobler CJ, Lee C (2002) Peptide hydrolysis, amino acid oxidation, and nitrogen uptake in communities seasonally dominated by *Aureococcus anophagefferens*. *Limnology and Oceanography* 47:1094-1108
- Mulholland MR, Lee C, Glibert PM (2003) Extracellular enzyme activity and uptake of carbon and nitrogen along an estuarine salinity and nutrient gradient. *Mar Ecol-Prog Ser* 258:3-17

- Obayashi Y, Suzuki S (2008) Occurrence of exo- and endopeptidases in dissolved and particulate fractions of coastal seawater. *Aquat Microb Ecol* 50:231-237
- Pacton M, Fiet N, Gorin GE (2007) Bacterial activity and preservation of sedimentary organic matter: The role of exopolymeric substances. *Geomicrobiology Journal* 24:571-581
- Pantoja S, Lee C (1999) Peptide decomposition by extracellular hydrolysis in coastal seawater and salt marsh sediment. *Mar Chem* 63:273-291
- Pantoja S, Lee C, Marecek JF (1997) Hydrolysis of peptides in seawater and sediment. *Mar Chem* 57:25-40
- Papaspyrou S, Gregersen T, Kristensen E, Christensen B, Cox RP (2006) Microbial reaction rates and bacterial communities in sediment surrounding burrows of two nereidid polychaetes (*Nereis diversicolor* and *N-virens*). *Marine Biology* 148:541-550
- Pinhassi J, Azam F, Hemphala J, Long RA, Martinez J, Zweifel UL, Hagstrom A (1999) Coupling between bacterioplankton species composition, population dynamics, and organic matter degradation. *Aquat Microb Ecol* 17:13-26
- Popova IE, Deng SP (2010) A high-throughput microplate assay for simultaneous colorimetric quantification of multiple enzyme activities in soil. *Appl Soil Ecol* 45:315-318
- Poremba K, Hoppe HG (1995) Spatial variation of benthic microbial production and hydrolytic enzymatic activity down the continental slope of the Celtic Sea. *Mar Ecol-Prog Ser* 118:237-245
- Presley BJ (1971) Determination of selected minor and major inorganic constituents. In: Initial reports of the Deep Sea Drilling Project, Book 7. U.S. GPO.
- Ransom B, Bennett RH, Baerwald R, Shea K (1997) TEM study of in situ organic matter on continental margins: Occurrence and the "monolayer" hypothesis. *Mar Geol* 138:1-9
- Rao MA, Gianfreda L (2000) Properties of acid phosphatase-tannic acid complexes formed in the presence of Fe and Mn. *Soil Biol Biochem* 32:1921-1926
- Richardot M, Debroas D, Thouvenot A, Romagoux JC, Berthon JL, Devaux J (1999) Proteolytic and glycolytic activities in size-fractionated surface water samples from an oligotrophic reservoir in relation to plankton communities. *Aquat Sci* 61:279-292
- Rogers NJ, Apte SC (2004) Azo dye method for mapping relative sediment enzyme activity in situ at precise spatial locations. *Environ Sci Technol* 38:5134-5140
- Sala MM, Gude H (2004) Ectoenzymatic activities and heterotrophic bacteria decomposing detritus. *Arch Hydrobiol* 160:289-303

- Sochaczewski L, Stockdale A, Davison W, Tych W, Zhang H (2008) A three-dimensional reactive transport model for sediments, incorporating microniches. *Environ Chem* 5:218-225
- Solorzano L (1969) Determination of ammonia in natural waters by phenolhypochlorite method. *Limnol Oceanogr* 14:799-&
- Somville M, Billen G (1983) A method for determining exoproteolytic activity in natural-waters. *Limnology and Oceanography* 28:190-193
- Souza AC, Pease TK, Gardner WS (2011) The direct role of enzyme hydrolysis on ammonium regeneration rates in estuarine sediments. *Aquat Microb Ecol* 65:159-168
- Steen AD, Arnosti C (2011) Long lifetimes of beta-glucosidase, leucine aminopeptidase, and phosphatase in Arctic seawater. *Mar Chem* 123:127-132
- Stief P (2007) Enhanced exoenzyme activities in sediments in the presence of deposit-feeding *Chironomus riparius* larvae. *Freshw Biol* 52:1807-1819
- Stockdale A, Davison W, Zhang H (2009) Micro-scale biogeochemical heterogeneity in sediments: A review of available technology and observed evidence. *Earth-Sci Rev* 92:81-97
- Sun WC, Gee KR, Haugland RP (1998) Synthesis of novel fluorinated coumarins: Excellent UV-light excitable fluorescent dyes. *Bioorg Med Chem Lett* 8:3107-3110
- Sun WC, Gee KR, Klaubert DH, Haugland RP (1997) Synthesis of fluorinated fluoresceins. *J Org Chem* 62:6469-6475
- Tholosan O, Lamy F, Garcin J, Polychronaki T, Bianchi A (1999) Biphaseic extracellular proteolytic enzyme activity in benthic water and sediment in the northwestern Mediterranean Sea. *Applied and Environmental Microbiology* 65:1619-1626
- Tietjen T, Wetzel RG (2003) Extracellular enzyme-clay mineral complexes: Enzyme adsorption, alteration of enzyme activity, and protection from photodegradation. *Aquat Ecol* 37:331-339
- Vetter YA, Deming JW, Jumars PA, Krieger-Brockett BB (1998) A predictive model of bacterial foraging by means of freely released extracellular enzymes. *Microbial Ecology* 36:75-92
- Volkenborn N, Polerecky L, Wetthey DS, Woodin SA (2010) Oscillatory porewater bioadvection in marine sediments induced by hydraulic activities of *Arenicola marina*. *Limnology and Oceanography* 55:1231-1247
- Warren RAJ (1996) Microbial hydrolysis of polysaccharides. *Annu Rev Microbiol* 50:183-212
- Watson SW, Novitsky TJ, Quinby HL, Valois FW (1977) Determination of bacterial number and biomass in marine environment. *Appl Environ Microb* 33:940-946

- Weiss MS, Abele U, Weckesser J, Welte W, Schiltz E, Schulz GE (1991) Molecular architecture and electrostatic properties of a bacterial porin. *Science* 254:1627-1630
- Wenzhofer F, Glud RN (2004) Small-scale spatial and temporal variability in coastal benthic O₂ dynamics: Effects of fauna activity. *Limnology and Oceanography* 49:1471-1481
- Westrich JT, Berner RA (1988) The effect of temperature on rates of sulfate reduction in marine-sediments. *Geomicrobiology Journal* 6:99-117
- Zhu QZ, Aller RC (2010) A rapid response, planar fluorosensor for measuring two-dimensional pCO₂ distributions and dynamics in marine sediments. *Limnology and Oceanography-Methods* 8:326-336
- Zhu QZ, Aller RC, Fan YZ (2005) High-performance planar pH fluorosensor for two-dimensional pH measurements in marine sediment and water. *Environ Sci Technol* 39:8906-8911
- Zhu QZ, Aller RC, Fan YZ (2006) Two-dimensional pH distributions and dynamics in bioturbated marine sediments. *Geochim Cosmochim Acta* 70:4933-4949
- Ziebis W, Huettel M, Forster S (1996) Impact of biogenic sediment topography on oxygen fluxes in permeable seabeds. *Mar Ecol-Prog Ser* 140:227-237
- Ziervogel K, Arnosti C (2008) Polysaccharide hydrolysis in aggregates and free enzyme activity in aggregate-free seawater from the north-eastern Gulf of Mexico. *Environ Microbiol* 10:289-299
- Ziervogel K, Karlsson E, Arnosti C (2007) Surface associations of enzymes and of organic matter: Consequences for hydrolytic activity and organic matter remineralization in marine systems. *Mar Chem* 104:241-252
- Ziervogel K, Steen AD, Arnosti C (2010) Changes in the spectrum and rates of extracellular enzyme activities in seawater following aggregate formation. *Biogeosciences* 7:1007-1015